

See discussions, stats, and author profiles for this publication at: <https://www.researchgate.net/publication/258953439>

Uptake of Engineered Gold Nanoparticles into Mammalian Cells

ARTICLE *in* CHEMICAL REVIEWS · JANUARY 2014

Impact Factor: 46.57 · DOI: 10.1021/cr300441a · Source: PubMed

CITATIONS

53

READS

298

2 AUTHORS:



Lev Dykman

Saratov State University

105 PUBLICATIONS 2,269 CITATIONS

[SEE PROFILE](#)



Nikolai G. Khlebtsov

Institute of Biochemistry and Physiology of...

229 PUBLICATIONS 4,659 CITATIONS

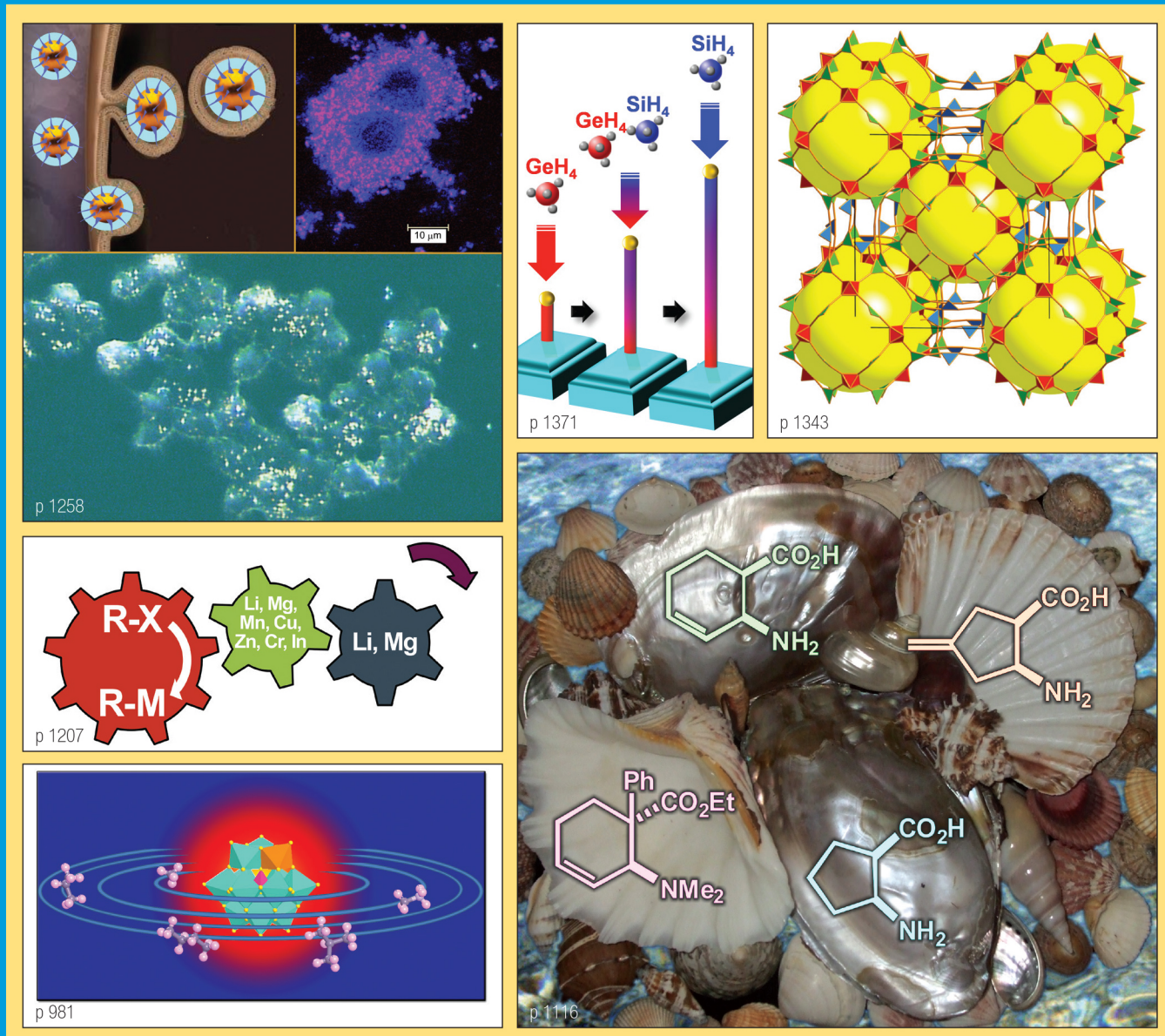
[SEE PROFILE](#)

CHEMICAL REVIEWS

JANUARY 22, 2014

VOLUME 114 NUMBER 2

pubs.acs.org/CR



ACS Publications

MOST TRUSTED. MOST CITED. MOST READ.

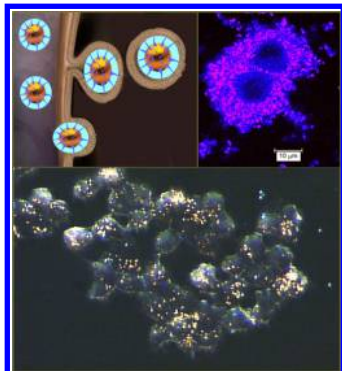
www.acs.org

Uptake of Engineered Gold Nanoparticles into Mammalian Cells

Lev A. Dykman[†] and Nikolai G. Khlebtsov*,^{†,‡}

[†]Institute of Biochemistry and Physiology of Plants and Microorganisms, Russian Academy of Sciences (IBPPM RAS), 13 Prospekt Entuziastov, Saratov 410049, Russia

[‡]Saratov State University, 83 Ulitsa Astrakhanskaya, Saratov 410012, Russia



CONTENTS

1. Introduction	1258
2. Dependence of Intracellular Uptake on GNP Size and Shape	1259
2.1. Effects of GNP Size	1259
2.2. Effects of GNP Shape	1262
2.3. Experimental Methods and Theoretical Models	1264
3. Effect of GNP Functionalization on Intracellular Uptake	1266
3.1. Basic Methods for GNP Functionalization	1266
3.2. Formation of a GNP–Protein Corona in a Biological Environment	1267
3.3. Intracellular Uptake of PEGylated GNPs	1268
3.4. Uptake of GNPs Functionalized with Other Synthetic Polymers and Proteins	1270
3.5. Uptake of GNPs Conjugated with Antibodies	1273
4. Use of Penetrating Peptides for the Delivery of GNPs into Cells	1274
5. Intracellular Uptake of Oligonucleotide-Coated GNPs	1276
6. Selective Internalization of Engineered GNPs into Cancer Cells	1276
7. Interaction of GNPs with Immune Cells	1278
7.1. Immunostimulation Effects of GNPs	1278
7.2. Immune Cell Receptors Involved in the Interaction with GNPs	1280
8. Concluding Remarks	1280
Author Information	1282
Corresponding Author	1282
Notes	1282
Biographies	1282
Acknowledgments	1282
References	1282

1. INTRODUCTION

In the past decade, mammalian cells have increasingly encountered gold nanoparticles (GNPs), owing to the active development of nanomedicine.^{1–3} GNPs have been more and more applied to diagnostics *in vivo*,⁴ photothermal therapy,⁵ and targeted delivery of drugs,^{6–8} genetic material,⁹ and antigens,¹⁰ as well as being used as a therapeutic agent *per se*, e.g., in the treatment of tumors^{11,12} or rheumatoid arthritis.¹³

Theranostics, a new trend in the biomedical use of GNPs,¹⁴ is closely related to the fabrication and application of multifunctional nanoparticles, which combine therapeutic and diagnostic possibilities within a single structure.^{15,16} The first time that the term “theranostics” appeared in the literature was in 2002.^{17,18} The use of GNPs of various sizes and shapes in theranostic nanomedicine was first demonstrated by Loo et al.¹⁹ (for gold nanoshells), Lapotko et al.²⁰ (for gold nanospheres), and Hleb et al.²¹ (for gold nanorods). In 2010, Lukianova-Hleb et al.²² presented a complete concept of theranostics.

Researchers employing GNPs *in vivo* inevitably have to deal with particle biodistribution over animal organs and tissues, pharmacokinetics, and assessment of possible particle cytotoxicity.^{23–27} In view of this, one of the hottest areas in current research is the interaction of GNPs with mammalian cells, routes of particle uptake into the cellular space, the fate of the particles inside the cell, and their elimination from the cell and the whole organism.

It is natural to suppose that the first cells GNPs encounter on their way into the mammalian organism are those of the immune system, in particular its phagocytic link (neutrophils, monocytes, macrophages, dendritic cells, and mast cells). Indeed, as early as in the first attempts to investigate colloidal gold biodistribution, which were performed in the 1960s–1980s on rabbits,²⁸ mice,²⁹ and rats,^{30,31} it was found that, after parenteral administration, colloidal gold particles are captured by liver cells, excreted through bile, and eliminated from the organism with feces. After injection, gold was identified mostly in Kupffer cells. Perhaps Scott et al.²⁸ were the first to note that the phagocytosis of GNPs is size-dependent (maximal accumulation and clearance were observed for 40-nm-diameter particles). Besides the work of Hardonk et al.,³⁰ the important role of Kupffer cells in the elimination of GNPs was established by Sadauskas et al.,³² who injected 2- and 40-nm GNPs intravenously in mice. Electron microscopy showed that, after injection, the GNPs accumulated in the macrophages of the liver (90%) and spleen (10%). The authors concluded that GNPs penetrate only phagocytes, primarily the Kupffer cells of the liver. In a subsequent study,³³

Received: November 4, 2012

Published: November 26, 2013

Sadauskas et al. reported that 40-nm GNPs get localized in lysosomes (endosomes) of Kupffer cells and can be retained there for up to 6 months.

With recent achievements in the fabrication of functionalized GNPs, which have controllable properties and are loaded with targeting molecules, the endocytosis of such GNPs has become crucial for successful biomedical applications. Understanding the mechanisms by which GNPs are taken up and the particles' fate after cellular internalization may help to avoid endocytic metabolism and to retain the biological activity of delivered cargoes. Despite the notable progress in this field, real quantitative control of endocytosis kinetics and of the traffic of GNPs to their intracellular targets is still quite limited. The existing gaps in understanding the mechanisms of endocytosis, together with the potential nanotoxicity of GNPs, hamper the transfer of nanoparticle-based technologies to clinical practice.

By now, there has been a large amount of original research on the mechanisms and critical parameters of GNP uptake into cells, and many reviews have dealt with the topic to this or that degree.^{23,34–53} The same topic is also addressed in several sections of the excellent book edited by Prokop.⁵⁴ However, as usually happens at the initial stages in the study of a complex problem, it is often difficult to compare and organize the available data because of the many important factors involved, which differ in different studies. In particular, most work on cellular GNP uptake has employed various cell lines *in vitro* and GNPs of various sizes, shapes, and structures [nanospheres (NSph's), nanorods (NRs), nanoshells (NSs), nanocages, nanostars, etc.]. The mechanisms and effectiveness of intracellular uptake have been investigated with a vast diversity of molecules used to functionalize the surface of GNPs. There is, consequently, a strong need to systematize literature data in a special review devoted entirely to the intracellular uptake of GNPs.

Keeping in mind the huge data volume and the high data-update rate, we restrict our attention to one particle type (gold or gold-based composites) and to mammalian cells, with the goal of providing a comprehensive analysis of the most recent data in the period January 2010–March 2013 (62% of the 361 works cited, Figure 1), although the overall coverage also includes pre-2010 publications.

In this review, we consider recent progress in understanding how size, shape, and surface properties of GNPs affect their uptake and intracellular fate. In particular, we discuss the selective penetration of GNPs into cancer and immune cells and the interaction of GNPs with immune cell receptors. We also analyze

recent theoretical models for endocytosis of spherical and nonspherical particles in relation to experimental data on the effects of particle geometry, ligand density, and cell membrane properties. In accordance with our major goal, we focus on experiments *in vitro*, with those *in vivo* being omitted from discussion. There are two reasons for our choice. One is that most data on the mechanisms of GNP uptake by animal cells have come from the use of models *in vitro*. The other reason is that studies of cellular uptake *in vivo* depend inevitably on particle biodistribution, which itself relies on the chosen model and on the nature of the functionalized GNPs.²⁵ Therefore, particle uptake into mammalian cells *in vivo* deserves separate consideration.

2. DEPENDENCE OF INTRACELLULAR UPTAKE ON GNP SIZE AND SHAPE

2.1. Effects of GNP Size

The most important geometrical parameters of particles, which should be responsible for their cellular uptake, are size and shape. Pioneering experimental work on GNPs was done by Chan's group. In 2006,⁵⁵ Chan and co-workers studied HeLa cell uptake of citrate gold NSph's with average diameters of 14, 30, 50, 74, and 100 nm and gold NRs with dimensions (length × diameter) of 40 × 14 and 74 × 14 nm. The surface of the as-prepared NRs was coated with a bilayer of cetyltrimethylammonium bromide (CTAB) molecules. The uptake effectiveness was determined quantitatively with inductively coupled plasma atomic emission spectroscopy (ICP–AES) by the amount of gold present in a homogenate of cells treated with different particles. With knowledge of the amount of gold accumulated in the cells and the geometrical dimensions of the particles, the average number of particles in a cell was calculated. Gold NSph's of ~50 nm were best able to enter the cell interior (Figure 2a). The accumulation of NRs in the cells was 3- and 6-fold less (for 40 × 14-nm and 74 × 14-nm NRs, respectively; Figure 2b). At first glance, these data seem unexpected, because the negatively charged citrate NSph's should have penetrated the negatively charged cells less effectively than the positively charged NRs. However, they can be explained by the effect of coating of cell-incubated citrate NSph's with serum proteins from Dulbecco's modified Eagle's medium (DMEM), which lowered the effect of charge. Further, citrate GNPs coated with serum proteins penetrated the cells much better than did those conjugated with transferrin—a blood plasma protein that mediates transport of Fe ions into cells via the transferrin receptors at the cell surface.⁵⁶ Chan and co-workers attributed this difference in uptake to the fact that the cell surface has many more receptors for serum proteins than it does for transferrin, and they concluded that the cellular uptake of GNPs is receptor-mediated endocytosis.

As is known, endocytosis^{49,57} is a process by which materials are engulfed by a cell through the invagination of a portion of the plasma membrane, with subsequent formation of vesicles with these materials inside the cell. Endocytosis can arbitrarily be divided into phagocytosis (actin-dependent, "professional" endocytosis), macropinocytosis (receptor-independent), and receptor-mediated (specific) endocytosis.⁵⁷ In turn, receptor-mediated endocytosis can be clathrin-, caveolin-, and raft-dependent. Clathrin and caveolin are proteins that mediate the invagination of a cell membrane, and rafts are specially organized domains of lipids in the plasma membrane. Receptor-mediated endocytosis is "turned on" for a quick and controlled uptake of the corresponding ligand by a cell. Vesicles rapidly lose their

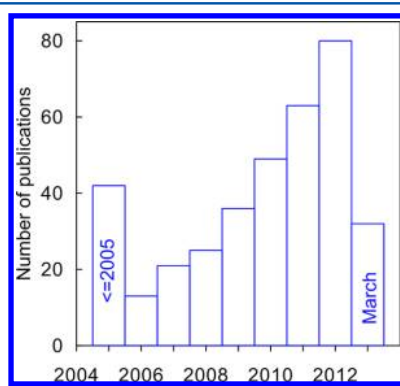


Figure 1. Distribution of the cited publications over years. The first column presents cumulative data published before 2006, and the last column shows the data published in March 2013.

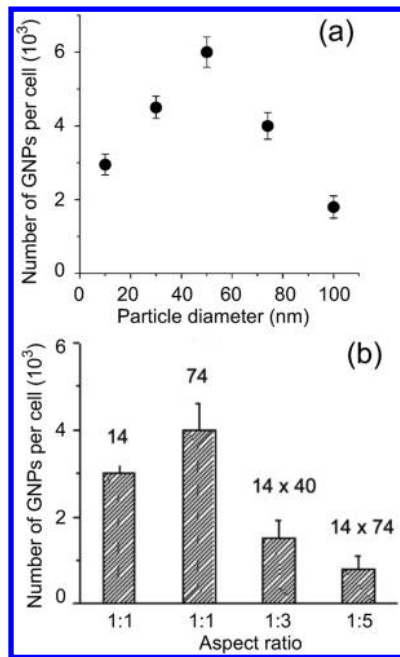


Figure 2. (a) Dependence of cellular uptake of spherical GNPs as a function of size. (b) Comparison of cellular uptake for rod-shaped nanoparticles (with aspect ratios of 1:3 and 1:5) and spherical GNPs. Recalculated data of ICP–AES after 6-h incubation of HeLa cells with GNPs. Adapted with permission from ref 55. Copyright 2006 American Chemical Society.

coats and fuse to form larger compartments, known as endosomes, which then fuse with the primary lysosomes, forming secondary lysosomes.^{58–60} Krpetić et al.,⁶¹ using transmission electron microscopy (TEM), identified three characteristic stages in the intracellular uptake of GNPs by macrophages: chemotaxis (including the formation of vacuoles at the cost of pseudopodia), phagocytosis (the formation of GNP-containing phagosomes and their merging with lysosomes), and digestion (the formation of phagolysosomes). According to Banerji and Hayes,⁶² a nonendocytic pathway for cellular GNP uptake through an intact lipid bilayer is impossible, although Xia et al.⁶³ and Taylor et al.⁶⁴ concluded that nonendosomal GNP uptake is possible in principle. A detailed discussion of endocytic pathways, trafficking, and endocytosis of nanoparticles can be found in a recent review by Canton and Battaglia.⁴⁹

Further to their research,⁵⁵ Chithrani and Chan⁶⁵ studied the mechanisms of intracellular uptake, accumulation, and elimination of transferrin-coated GNPs of different sizes and shapes. The cell lines STO, HeLa, and SNB19 served as models in this study. Uptake was evaluated by two methods: (i) laser confocal microscopy (LCM), using Texas red-labeled transferrin as a fluorescent probe, and (ii) TEM. To examine if the endocytosis of transferrin-coated GNPs is a receptor-mediated process,⁵⁵ the authors investigated cellular GNP uptake at low temperature and after cell treatment with sodium azide, an inhibitor of electron transport. In both cases, the level of uptake decreased by ~70%. Next, before GNPs were introduced, the cells had been treated with a hypertonic solution of sucrose or had been grown in a K^+ -deficient medium to disrupt the formation of clathrin-coated vesicles. This too resulted in a considerable decrease in the GNP uptake, leading the authors to speculate that GNP internalization may be clathrin-dependent. The best ability of spherical particles of ~50 nm to penetrate inside cells was explained by Chithrani and Chan⁶⁵ by the minimal time needed by the membrane to

wrap around spheres, in agreement with the previously reported thermodynamic calculations.⁵⁸

Another interesting point reported in ref 65 is the time of GNP elimination from the cells (exocytosis). The smaller the nanoparticles, the more rapidly they were removed from the cells. Specifically, 14-nm GNPs were eliminated two times faster than 74-nm particles, and this dependence was almost linear in the size range 10–100 nm. Transferrin-coated nanorods were taken up much less effectively than spherical particles with the same surface coating. However, the fraction of exocytosed nanorods was larger than that of spherical GNPs.

Continuing their work on size-dependent endocytosis, Chan's group studied the uptake of antibody-coated GNPs into tumor cells.⁶⁶ Specifically, they examined the interactions between herceptin and SK-BR-3 cells, which overexpress ErbB2 tyrosine kinase receptors. Herceptin is a recombinant humanized monoclonal G1 antibody that selectively interacts with the extracellular domain of the human epidermal growth factor receptor (EGFR) and blocks the proliferation of ErbB2-overexpressing human tumor cells. Most commonly, herceptin is used to treat breast cancer with overexpression of ErbB2 (early stages and metastatic cancer). GNP–herceptin complexes were first used for optoacoustic tomography imaging of deep tumors.⁶⁷ Chan and co-workers⁶⁶ conjugated herceptin to 2-, 10-, 25-, 40-, 50-, 70-, 80-, and 90-nm GNPs and assessed the degree of uptake by TEM and LCM. Similarly to the uptake of transferrin-coated GNPs,⁶⁵ the uptake of GNP–herceptin into tumor cells was also found to be size-dependent. Maximal uptake of GNPs, with localization in endosomes and lysosomes, was observed for 25–50-nm particles, whereas smaller or larger GNPs had much worse penetration of cells and appeared mostly on the plasma membrane. This was explained by the optimal quantity of antibodies adsorbed on the surface of 25–50-nm GNPs and interacting with the cellular ErbB2 receptors. Using LCM and colocalization of ErbB2 and transferrin receptors (Tfr's), Chan and co-workers⁶⁶ demonstrated that the GNP–Her conjugates and the ErbB2 receptors are internalized as a single complex and that this process is also size-dependent (Figure 3). What is more, herceptin conjugated with 25–50-nm GNPs caused the most damage to the cells. Thus, the authors provided additional strong evidence for a receptor-mediated mechanism of GNP endocytosis.

In 2011, Chan's group reported unusual correlations between the aggregation of GNPs and their intracellular uptake and cytotoxicity.⁶⁸ According to ICP–AES and TEM data, the amount of aggregated transferrin-coated GNPs taken up by HeLa cells was 25% smaller than that of nonaggregated particles. A similar picture was obtained for A549 cells. However, for MDA-MB-435 cells, the largest aggregates (98 nm) were accumulated the most—almost 2-fold more than were non-aggregated particles or small aggregates. This finding looks somewhat unexpected, because the surface of MDA-MB-435 cells contains the smallest number of receptors of transferrin CD71. Therefore, the authors proposed that, in addition to receptor-mediated endocytosis, MDA-MB-435 cells might use another mechanism of GNP internalization. Possibly, the asymmetrical geometry of the aggregates may add to the complexity of their interaction with the cell membrane. Inhomogeneous aggregates may interact with the cell membrane through various polyvalent interactions by following the receptor-independent pathway. One also should bear in mind the results of Kneipp et al.,⁶⁹ who showed that aggregates may

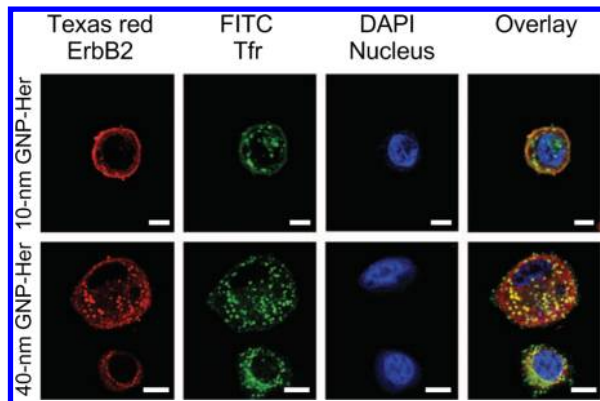


Figure 3. Size-dependent internalization of ErbB2 receptors. Laser confocal fluorescence microscopy of SK-BR-3 cells treated for 3 h with 10- and 40-nm GNPs conjugated to herceptin. Cells were then labeled with anti-ErbB2 (red) and antitransferrin receptor (Tfr) antibodies (green), and the nucleus was counterstained with DAPI (blue). Significant colocalization of ErbB2 and Tfr was observed in cells treated with 40-nm GNP-Her conjugates (yellow), whereas a fairly limited number of ErbB2 receptors were internalized in the case of 10-nm GNPs. Scale bars, 10 μm . Adapted with permission from ref 66. Copyright 2008 Nature Publishing Group.

form directly in endosomes after GNPs have entered the cytoplasm.

The effect of the concentration of introduced GNPs on uptake by MC3T3-E1 cells was explored by Mustafa et al.;⁷⁰ 12-nm GNPs at 160 $\mu\text{g}/\text{mL}$ formed aggregates on the cell surface and effectively penetrated the cells by endocytosis. Yet, at 10 $\mu\text{g}/\text{mL}$, the GNPs were found on the membranes mostly as isolated particles, suggesting diffusion to be the predominant uptake pathway in this case.

Mironava et al.⁷¹ compared intracellular uptake of 13- and 45-nm GNPs. From scanning electron microscopy (SEM) observations, it appeared that 45-nm GNPs were taken up into the intracellular space of CF-31 cells five times more effectively than were 13-nm GNPs, and they were localized in large lysosomes without entering the nuclei or mitochondria. To investigate the mechanism of GNP endocytosis, Mironava et al. pretreated the cells with phenylarsine oxide, an inhibitor of clathrin-dependent endocytosis. TEM analysis demonstrated that endocytosis was clathrin-dependent only for 45-nm GNPs and was inhibited considerably by phenylarsine oxide. For 13-nm GNPs, there was no significant difference in uptake between inhibitor-treated and nontreated cells. In this case, in the authors' opinion, a receptor-independent mechanism of endocytosis (macropinocytosis) was possibly involved. An effective way to detect a receptor-independent mechanism is to study endocytosis at lowered temperature, because this mechanism depends strongly on temperature (as distinct from the receptor-dependent mechanism). Specifically, the data of Mironava et al. showed that reducing the temperature to 4 °C brought about a 90% decrease in the endocytosis of 13-nm GNPs, whereas the endocytosis of 45-nm GNPs decreased only by 30%.

Sonavane et al.⁷² examined the size-dependent uptake of GNPs *in vitro* into rat skin and intestine treated with 15-, 100-, and 200-nm particles. The tissue content of the GNPs was determined by TEM, inductively coupled plasma mass spectrometry (ICP-MS), and energy-dispersive X-ray spectroscopy. The amount of GNPs taken up into the studied tissues was found to decrease in the order 15 > 100 > 200 nm.

Yen et al.⁷³ described the uptake of 3-, 6-, and 40-nm GNPs by murine macrophages (J774 A1). The tissue content of the GNPs was determined by TEM, UV-vis spectrophotometry, and ICP-MS. Compared with 3- and 6-nm GNPs, 40-nm particles were internalized better and were less cytotoxic. Yet, the smaller particles were responsible for enhanced production of proinflammatory cytokines [interleukins-1 and -6 (IL-1 and IL-6) and tumor necrosis factor α (TNF- α)]. The internalized GNPs in the macrophage cytoplasm were shown by TEM to be located inside coated vesicles, a finding indicative of receptor-mediated endocytosis. The authors associated this mechanism with adsorption of serum proteins from the cell culture medium onto the GNPs. Similar data were recorded by Coradeghini et al.⁷⁴ for 5- and 15-nm GNPs and mouse fibroblasts.

Wang et al.⁷⁵ used dark-field microscopy, TEM, and ICP-MS to investigate the endocytosis of GNPs (Figure 4). The

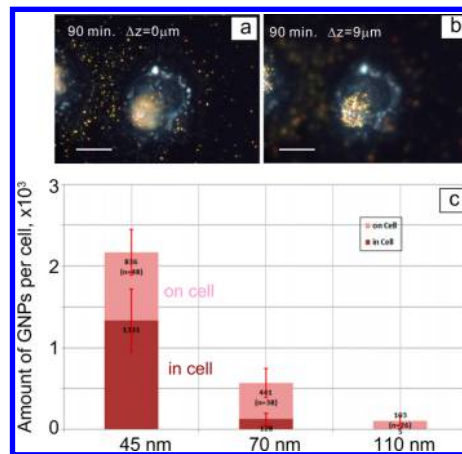


Figure 4. Dark-field images of a HeLa cell taken at the bottom (a) and top (b) of the cell at 90 min after interaction with 70-nm GNPs. The image (b) shows that many GNPs are localized on the cell membrane without being internalized. (c) Statistical data, as assessed by TEM and ICP-MS, for 45-, 70-, and 110-nm GNPs localized on (soft pink) and in (ruby red) HeLa cells illustrate the maximal total amounts of 45-nm GNPs interacting with the cells and the maximal percentage of 45-nm GNPs localized in the cells. Adapted with permission from ref 75. Copyright 2010 BioMed Central Ltd., part of Springer Science +Business Media.

experiments used 45-, 70-, and 110-nm particles and the cell lines CL1-0 and HeLa. The GNPs were functionalized with ssDNA—an aptamer to mucin, which is a cell-surface glycoprotein overexpressed in tumor cells. The best uptake in both types of cells was obtained with 45-nm GNPs. Conversely, the cell cytoplasm contained almost no 110-nm GNPs, which, however, appeared on the cell membranes. To explain what had caused the revealed effect, Wang et al. put forward a thermodynamic model for the ligand–receptor interaction occurring in receptor-mediated endocytosis.

Rieznichenko et al.⁷⁶ presented data on the uptake of 10-, 20-, 30-, and 45-nm GNPs by U937 tumor cells. GNP internalization was detected by TEM and LCM. The most active cellular accumulation was found for 30-nm GNPs, with maximal uptake occurring very fast (at 3–5 min). It is interesting to note that, for the same U937 cells, the uptake of 15-nm GNPs, from ICP-AES data, was ~1 order of magnitude lower than was that for HeLa cells.⁷⁷ This observation, along with the data of Albanese and Chan,⁶⁸ Coulter et al.,⁷⁸ Freese et al.,⁷⁹ and Cui et al.,⁸⁰ indicates

that the intracellular uptake of GNPs depends also on the cell type.

The same conclusion was drawn by Trono et al.⁸¹ from a study of uptake of 5-, 10-, 20-, 30-, 40-, and 50-nm GNPs by PK-1, PK-4S, and Panc-1 tumor cells. It was shown by atomic absorption spectrometry (AAS) that, unlike HeLa cells, the pancreas cancer cells were best able to internalize 20-nm particles. In addition, uptake efficacy was influenced by the time of incubation, the concentration of introduced GNPs, and the temperature conditions for the experiment. Quite recently, Zhou et al.⁸² showed that the thickness of the pericellular matrix of different cells is an important factor, which can enhance the retention and cellular uptake of nanoparticles.

Size-dependent endocytosis of single 4-, 12-, and 17-nm GNPs was examined by Shan et al.⁸³ with HeLa cells. The force of GNP interaction with the cell membrane was measured by atomic force microscopy (AFM). The interaction force of a single GNP with the cell membrane increased with increasing particle diameter. Pretreatment of the cells with methyl- β -cyclodextrin inhibited the endocytosis. Because methyl- β -cyclodextrin lowers the content of membrane cholesterol and, accordingly, decreases the formation of lipid rafts, the mechanism of GNP endocytosis was concluded to be raft-dependent. In their subsequent work,⁸⁴ the authors determined the endocytosis of small (4 nm) GNPs to be caveolin-dependent.

The endocytosis of variously sized GNPs that leads to lysosome impairment and to autophagosome accumulation was explored by Ma et al.⁸⁵ They used GNPs of 10, 25, and 50 nm and cells of the rat kidney (NRK) as a model object. The cellular content of the GNPs was determined by TEM (Figure 5), light

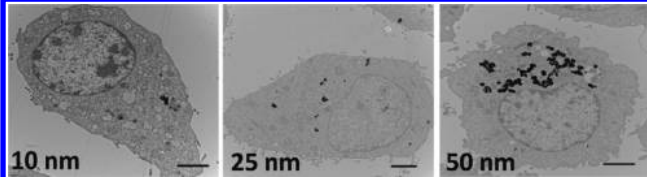


Figure 5. TEM images of rat kidney cells treated with 10-, 25-, and 50-nm GNPs. Adapted with permission from ref 85. Copyright 2011 American Chemical Society.

microscopy, and ICP-MS. Receptor-mediated endocytosis was found to increase with increasing particle diameter, reaching a maximum for 50-nm GNPs. Similar data were reported by Sobhan et al.⁸⁶ for 7-, 21-, and 31-nm GNPs and AR42J cells. Sabuncu et al.⁸⁷ demonstrated that 50-nm GNPs were taken up by tumor cells more effectively than were 25-nm GNPs and that uptake in Panc-1 cells was much more active than it was in Jurkat cells.

Different data were acquired by Huang et al.⁸⁸ in a TEM and ICP-MS study of uptake of 2-, 6-, and 15-nm tiopronin-functionalized GNPs by MCF-7 cells. The most active uptake was recorded for 2-nm GNPs (4×10^6 particles/cell); the uptake of 6- and 15-nm GNPs was ~ 1 order of magnitude less effective. Only 2- and 6-nm GNPs were present in the cell nuclei. However, in a subsequent study,⁸⁹ the same group compared the uptake of 50- and 100-nm tiopronin-functionalized GNPs by MCF-7 cells and concluded that the smaller, 50-nm nanoparticles demonstrated more advantages over the larger, 100-nm particles in the uptake and permeability in tumor cells and tissues. Yet, Arvizo et al.⁹⁰ demonstrated, by instrumental neutron activation analysis and TEM, that the uptake of 5- and 20-nm

unmodified GNPs in SKOV3-ip, OVCAR5, and A2780 cells was higher, compared with 50- and 100-nm GNPs. Trickler et al.⁹¹ examined the blood-brain barrier (BBB) in response to variously sized GNPs (3, 5, 7, 10, 30, and 60 nm) in vitro using primary rat brain microvessel endothelial cells (rBMEC). According to spectrophotometric measurements at 500 nm, the smaller GNPs (3–7 nm) showed higher rBMEC accumulation compared to the larger GNPs (10–60 nm). Even though slight changes in cell viability were observed with small GNPs, the rBMEC morphology appeared unaffected 24 h after exposure to GNPs with only mild changes in fluorescein permeability, indicating BBB integrity was unaltered.

A possible reason for the contradiction in the published data on size-dependent uptake can be related to the particle clusters formed prior to interaction with cells or during adsorption on the cell membrane. For example, Chithrani and Chan⁶⁵ observed single-particle uptake for 50-nm transferrin-coated GNPs, whereas 14-nm GNPs were taken up only as GNP clusters (at least six GNPs per cluster). By contrast, Lèvy et al.⁹² observed single-particle entry of 10-nm peptide-capped GNPs in HeLa cells (see endosomes containing single 10-nm nanoparticles in Figure 6). An obvious explanation for these apparently

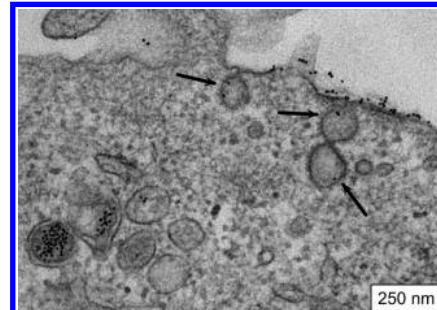


Figure 6. TEM image of single-particle uptake of 10-nm peptide-coated GNPs (6 nM) incubated with HeLa cells for 3 h in the presence of serum. The arrows indicate endosomes with a single and two GNPs. Adapted with permission from ref 92. Copyright 2004 American Chemical Society.

conflicting data may be the different surface functionalization of GNPs (transferrin versus peptide/PEG). This example, together with the data of Albanese and Chan,⁶⁸ clearly demonstrates the need for real-time single-particle techniques in order to better understand the impact of clustering on GNP uptake.

2.2. Effects of GNP Shape

We now shift to discuss particle shape effects. The effects of GNP shape on intracellular uptake were addressed by Bartczak et al.⁹³ They studied, by ICP-AES, the HUVEK cell uptake of four types of poly(ethylene glycol)-coated (PEGylated) GNPs, namely, NSph's (15 nm), NRs (47×17 nm), hollow NSs (91 nm, shell thickness of 9 nm), and NSs on silica cores (SiO_2 core of 43 nm, Au shell of 7 nm). The intracellular uptake of the GNPs decreased in the order NSph's (~ 2400 GNPs/cell) > NRs (~ 2200 GNPs/cell) > NSs on silica cores (~ 400 GNPs/cell) > hollow NSs (~ 200 GNPs/cell). It should be stressed that these results do not reflect any effect of the size and shape of particles in pure form, because the negative charge of the particles and the quantity of stabilizer molecules associated with them increased in the sequence from PEG-coated NSph's to hollow NSs. It is these two factors that are thought by the authors to be responsible for the obtained differences in uptake effectiveness.

Table 1. Size and Shape Effects of GNPs on Endocytosis

GNP type and size	cell line	coating	functionalization method	analysis methods	observed effects	type of endocytosis	ref
NSph's of 14, 30, 50, 74, and 100 nm NRs of 40 × 14 and 74 × 14 nm	HeLa	transferrin	physical adsorption	ICP–AES, TEM	endocytosis depends on size; maximal uptake occurs for 50-nm NSph's	receptor-mediated endocytosis	Chithrani 2006 ⁵⁵
NSph's of 14, 30, 50, 74, and 100 nm NRs of 40 × 14 and 74 × 14 nm	STO, HeLa, SNU19	transferrin	physical adsorption	TEM, LCM	endocytosis depends on size (linearly, inversely) and shape (NRs are eliminated faster than NSph's)	clathrin-dependent receptor-mediated endocytosis	Chithrani 2007 ⁶⁵
NSph's of 2, 10, 25, 40, 50, 70, 80, and 90 nm	SK-BR-3	herceptin	physical adsorption	TEM, LCM	endocytosis depends on size; maximal uptake occurs for 25–50-nm NSph's	receptor-mediated endocytosis	Jiang 2008 ⁶⁶
NSph's of 15, 30, 45, and 100 nm and their aggregates of 26, 49, and 98 nm	A549, MDA-MB-435, HeLa	transferrin	physical adsorption	ICP–AES, TEM	endocytosis depends on cell phenotype, as well as on GNP size	receptor-mediated and receptor-independent endocytosis	Albanese 2011 ⁶⁸
NSph's of 13 and 45 nm	CF-31	citrate	as prepared	SEM, TEM	endocytosis depends on size; maximal uptake occurs for 45-nm NSph's	clathrin-dependent endocytosis for 45-nm GNPs and receptor-independent endocytosis for 13-nm GNPs	Mironava 2010 ⁷¹
NSph's of 3, 6, and 40 nm	J774 A1	citrate	as prepared	TEM, UV-vis, ICP–MS	endocytosis depends on size; maximal uptake occurs for 40-nm NSph's	receptor-mediated endocytosis	Yen 2009 ⁷³
NSph's of 45, 70, and 110 nm	CL1-0, HeLa	aptamer (ssDNA)	chemical adsorption via an SH group	dark-field microscopy	endocytosis decreases in the order 45 > 70 > 100 nm	receptor-mediated endocytosis	Wang 2010 ⁷⁵
NSph's of 10, 20, 30, and 45 nm	U937	citrate	as prepared	TEM, LCM	endocytosis depends on size; maximal uptake occurs for 30-nm NSph's	receptor-mediated endocytosis	Rieznichenko 2010 ⁷⁶
NSph's of 5, 10, 20, 30, 40, and 50 nm	PK-1, PK-45, Panc-1	citrate	as prepared	AAS	endocytosis depends on size; maximal uptake occurs for 20-nm NSph's	receptor-mediated endocytosis	Trono 2011 ⁸¹
NSph's of 4, 12, and 17 nm	HeLa	L-cysteine	chemical adsorption via a PEG-SH linker	AFM	endocytosis increases with increasing particle diameter	raft-dependent endocytosis	Shan 2011 ⁸³
NSph's of 10, 25, and 50 nm	NRK	citrate	as prepared	TEM, light microscopy, ICP–MS	endocytosis increases with increasing particle diameter	receptor-mediated endocytosis	Ma 2011 ⁸⁵
NSph's of 7, 21, and 31 nm	AR42J		as prepared	dark-field microscopy, TEM, SEM	endocytosis increases with increasing particle diameter	clathrin-dependent endocytosis	Sobhani 2012 ⁸⁶
NSph's of 25 and 50 nm	Panc-1, Jurkat	carboxy-PEG	as prepared	ICP–AES	endocytosis increases with increasing particle diameter	receptor-mediated endocytosis	Sabuncu 2012 ⁸⁷
NSph's of 2, 6, and 15 nm	MCF-7	topronin	physical adsorption	ICP–MS, TEM	maximal uptake occurs for 2-nm GNPs	receptor-mediated endocytosis	Huang 2012 ⁸⁸
NSph's of 50 and 100 nm	MCF-7	topronin	physical adsorption	ICP–MS, TEM	maximal uptake occurs for 50-nm GNPs	receptor-mediated endocytosis	Huo 2013 ⁸⁹

Cho et al.⁹⁴ arrived at different conclusions in their UV-vis spectrophotometry study of the uptake of gold NSph's (15, 54, and 100 nm), nanocages (62 and 118 nm), and NRs (40 × 16 nm) into SK-BR-3, ATCC, and HTB-30 cells. After changing the experimental design to preclude any effects of GNP sedimentation, they showed that the effectiveness of intracellular uptake is affected by the rates of GNP diffusion and sedimentation much more than it is affected by the size and shape of nanoparticles, the density of stabilizer coating, or the GNP concentration.

Schaeublin et al.⁹⁵ pointed out differences in the character of uptake of NSph's and NRs into HaCaT cells. On the whole, NRs were taken up less effectively; furthermore, TEM analysis revealed that NSph's inside the cells were present as aggregates and NRs were present as isolated particles. The authors concluded that GNP shape not only affects intracellular uptake but also plays a crucial role in cellular response to particle introduction. Zhang et al.⁹⁶ demonstrated that the effectiveness of NR uptake by MDA-MB-231 cells, measured with UV-vis-NIR adsorption spectroscopy, is affected by the time of incubation and by the concentration of GNPs introduced into a cell suspension. In agreement with the data of Schaeublin et al.,⁹⁵ Tarantola et al.⁹⁷ showed that spherical GNPs (43 nm) with identical surface functionalization (CTAB) are generally more toxic and more efficiently ingested by MDCK II cells than are rod-shaped particles (38 × 17 nm). Their experiment confirmed more efficient intracellular uptake of spherical functionalized GNPs as compared with NRs, with other experimental conditions being equal. Accordingly, an increased intracellular release of CTAB from spherical GNPs resulted in their increased toxicity.

Hutter et al.⁹⁸ compared the uptake of gold NSph's, NRs, and nanosea-urchins (also named spiky nanoparticles or nanostars³) by phagocytic microglia cells and by nonphagocytic neurons. It was shown that gold NRs were mainly taken up by the neurons, whereas spiky nanoparticles were preferentially internalized by the microglia cells, thus indicating the selectivity of the cells with respect to particle shape. Liu et al.⁹⁹ used dark-field microscopy and ICP-AES to study the uptake of PEGylated gold NSs on silica nanorattles by MCF-7 cells. Uptake efficacy was found to decrease in the particle-size sequence 84 > 142 > 315. This conclusion agrees with the previously discussed data, as the actual particle shape was close to spherical.

Navarro et al.¹⁰⁰ investigated the uptake of PEGylated gold nanostars and bipyramids into melanoma B16-F10 cells. Dark-field microscopy showed that the biocompatible gold nanoparticles were easily internalized and most of them were localized within the cells. Avram et al.,¹⁰¹ using the same B16 melanoma cells but different particles (5-nm citrate-coated gold NSph's), presented similar data.

In a recent study in vitro, Plascencia-Villa et al.¹⁰² showed gold nanostars to be biocompatible with murine macrophages. For precise control of the size, shape, and structure of the nanostars, these were prepared through a seed-mediated route by using HEPES (2-[4-(2-hydroxyethyl)-1-piperazinyl]ethanesulfonic acid), a zwitterionic buffering compound. Such nanoparticles were efficiently adsorbed and internalized by the cells, as revealed by advanced field emission scanning electron microscopy (FE-SEM) and backscattered electron imaging of complete unstained uncoated cells.

Summing up the many experimental data reported in the cited articles (Table 1), we conclude that the endocytosis of GNPs is receptor-mediated and size-dependent.¹⁰³ Maximal effectiveness

of the intracellular uptake of GNPs is observed for 30–50-nm particles, depending on the cell type. Gold NRs—particularly those with large axial ratios¹⁰⁴—are taken up into cells much worse but can be eliminated faster from them. In the case of the receptor-independent mechanism, small particles are internalized the best.

It should be noted that all GNPs listed in Table 1, regardless of their surface functionalization, size, and shape, were negatively charged (zeta potentials ranging from −20 to −70 mV).

2.3. Experimental Methods and Theoretical Models

One of the most important problems in understanding the mechanisms of GNP endocytosis is to achieve a reliable statistical estimation of particles that enter cells or cell compartments.^{105,106} For instance, estimates of the amount of particles present in a cell are often based on the qualitative examination of TEM images and on the counting of the number of particles in various cellular structures. However, the statistical accuracy of such estimates is usually questionable if no special methods have been used for sampling.¹⁰⁷ The importance of quantitative judgment is well-illustrated by the strong dependence of endocytosis on the modification of the nanoparticle surface. From many published data points collected in this review, it follows that, for the same type of cell and similar geometrical parameters of GNPs, replacing the surface modifier may cause the number of particles per cell to change by 2 or even 3 orders of magnitude. Such a strong difference in the effectiveness of endocytosis calls for a thorough analysis of the techniques used to generate quantitative data and of their statistical reliability.

It is also important to choose a quantitative parameter for assessing the effectiveness of endocytosis: the number, mass, or surface of the particles. For example, it is obvious that TEM images are better suited for estimating the number of particles in a sample and that ICP-AES or ICP-MS is better suited for measuring the mass of particles per unit volume of that sample. For an ideal monodisperse ensemble of spherical particles of known size, the number of particles per unit volume can easily be converted into their mass or surface. For actual samples, however, such conversion requires knowledge of particle distribution by size, shape, composition, etc.—information that is usually unavailable.

As follows from the discussion of the experimental data presented in the two previous sections, the principal experimental methods to study intracellular uptake of GNPs in vivo and in vitro are TEM, LCM, dark-field microscopy, AFM, UV-vis spectrophotometry, ICP-AES, and ICP-MS. Other state-of-the-art methods have also been used for qualitative and quantitative analysis of cellular GNP uptake, including luminescence microscopy,¹⁰⁸ scanning transmission electron microscopy,¹⁰⁹ scanning transmission ion microscopy,¹¹⁰ differential interference contrast microscopy,¹¹¹ photothermal heterodyne imaging,¹¹² Rayleigh light scattering microscopy,¹¹³ fluorescence spectral imaging,¹¹⁴ laser desorption/ionization mass spectrometry,¹¹⁵ cell mass spectrometry,¹¹⁶ fluorescence correlation microscopy,¹¹⁷ anti-Stokes Raman scattering microscopy,¹¹⁸ confocal Raman microscopy,¹¹⁹ dynamic SERS imaging,¹²⁰ photothermal optical coherent tomography,¹²¹ high-resolution X-ray microscopy,¹²² X-ray computer tomography,¹²³ photoacoustic imaging,¹²⁴ and combinations of different methods.^{125,126} Elsaesser et al.¹⁰⁵ made a critical analysis of the basic methods used to determine nanoparticles in biological samples, and they compared particle types, biosystems, applications, and the strong and weak points of

such methods as light microscopy, TEM, radioactive labeling, mass spectrometry, magnetic NPs, and field-flow fractionation (Table 1¹⁰⁵).

Despite the large number of methods listed above, all of them fall into two major classes: destructive and nondestructive. Destructive methods are, in essence, analytical and permit only the total amount of gold in a sample to be determined, whereas nondestructive methods yield the distribution of GNPs over organs, cells, and cellular compartments. In addition, both classes of methods can take advantage of special labels for particle determination or estimate GNPs without the aid of any labels, by relying only on the properties of particles themselves (e.g., by using their high TEM contrast or enhanced plasmonic scattering and absorption of light).

Among the great diversity of destructive techniques, ICP–MS and ICP–AES yield the most reliable data.¹²⁷ Both have exceptional sensitivity within the detection range from ppt to ppm and are commonly employed in trace analysis of various substances. Therefore, ICP can be recommended as a method of choice to estimate both the biodistribution of GNPs over organs and the total gold content per cell. An evident, but not the only, weak point of ICP is the destructive character of the analysis, which rules out GNP localization in various cellular compartments or organ sites.¹²⁸ Another weak point stems from problems in sample preparation for analysis. Whereas gold nanoparticles can be relatively simply digested and measured in suspensions, a more sophisticated sample preparation procedure is needed to determine them within complex biological matrixes such as cells, blood, or tissues. It is common practice to use microwave digestion in closed pressure vials with high resistance to volatile compounds such as *aqua regia* or nitric acid. Because the sample preparation is complex, the results generated by ICP–AES/MS depend strongly on instrument calibration, and independent determinations of gold within one set of samples may show a large scatter of data. For this reason, the measured data should always be averaged over several samples, which makes the analysis even more labor-intensive.

The most reliable nondestructive method to estimate GNPs in cells or their compartments is TEM. As noted above, the localization of GNPs in TEM images presents no problems owing to the strong contrast with respect to the biological components of the sample. Compared to even the most advanced light microscopy methods,¹²⁹ TEM stands out because it provides an open view at high resolution on the cellular level by visualizing the inner structures in which GNPs are contained.¹⁰⁷ However, making statistically significant estimates of the average number of particles in a cell or its individual organelles is a nontrivial task. Usually, TEM images represent a selection of thin sections obtained after particle treatment of samples and their subsequent fixation and embedding in resins. For versatile quantification of the embedded nanoparticles, several basic principles need to be applied:¹⁰⁷ (i) unbiased selection of specimens by multistage random sampling; (ii) unbiased estimation of GNP number and compartment size; (iii) statistical testing of an appropriate null hypothesis. The work of Brandenberger et al.¹³⁰ is an instructive example of a thorough sampling to obtain reliable estimates of differences in the cellular uptake and trafficking of plain versus PEG-coated GNPs.

It should be stressed that TEM photos are actually a set of 2D images; therefore, attaining statistically sound results in 3D requires combining TEM with the principles of stereology. Stereology is a set of tools to estimate morphometric parameters of 3D objects, which is based on measurements made on two-

dimensional sections. For revealing the internal structure of cells or tissues at a sufficiently high level of lateral resolution, TEM images are usually obtained for thin or ultrathin (50–100 nm) sections. However, only structures with dimensions smaller than the section thickness will be seen without loss of dimensionality. For example, a mitochondrion or endosome will appear on the section plane as one or more section profiles of a certain area. Thus, combining TEM with stereology offers a set of tools that allows unbiased and efficient quantification of GNPs in 3D samples (cells, tissues, and organs) and versatile comparison between experimental groups or between compartments within one group.

The presence of a size dependence of endocytosis has been established for many types of nanoparticles and viruses⁴⁹ and has stimulated the development of various theoretical models, beginning with studies by Lipowsky and Döbereiner,¹³¹ Gao et al.,⁵⁸ and Bao and Bao.¹³² The attraction between the curved surface of a nanoparticle and the cell membrane deforms the membrane and causes the nanoparticle to be sucked up inside the membrane region being deformed. The attraction forces between nanoparticle and membrane on the one hand and the membrane rigidity on the other lead to the existence of a minimal radius for endocytosis.¹³³ Note that the attractive interaction and aggregation of small particles on the cell membrane will decrease the minimal size of particles, whereas nonspecific repulsive interactions will increase the minimal size for effective uptake.⁴⁹ The membrane-deformation model has been extended to receptor-mediated interactions involved in endocytosis.^{133–135} Decuzzi and Ferrari¹³⁶ generalized the original formulation by Gao et al.⁵⁸ to include the contribution of nonspecific interactions and a more realistic expression for the ligand–receptor binding energy.

In the initially developed theoretical models,^{58,132} the mechanisms of receptor-mediated endocytosis were treated from a kinetic point of view to elucidate the question of “how fast” a single nanoparticle can be transported into the cell. Zhang et al.¹⁰³ treated receptor-mediated endocytosis from a different standpoint by invoking thermodynamic arguments and considering a cell immersed in a solution with ligand-coated GNPs. The nanoparticle–cell system reaches a thermodynamic equilibrium at minimal free energy, which determines the number of bound receptors and the distribution of bound GNPs. Accordingly, this theory elucidates “how many” GNPs can be endocytosed in a sufficiently long period. Although the final results explained size-dependent endocytosis qualitatively, the minimal particle diameter was >40 nm, in contrast to the experimental observations.

Yuan et al.¹³⁴ provided a phase diagram (Figure 7) that correlates uptake efficiency with particle size and the density of the ligands expressed on the particle surface. The most efficient uptake was predicted for high ligand densities and for a particle radius of about 25–30 nm (the right-bottom part of phase II). The ligand-shortage phase corresponds to a critical ligand density, for which the cellular uptake vanishes, because the nanoparticle is too short of ligands (phase I in Figure 7). On the other hand, at critically large ligand density or particle size, the receptor density can reach an entropic limit at which adhesion becomes insufficient to overcome the membrane deformation cost. This entropic limit gives rise to a regime noted as “receptor shortage” (phase III in Figure 7).¹³⁴

The endocytosis of nonspherical particles, unlike that of spherical particles, has been the subject of few theoretical studies. Decuzzi and Ferrari¹³⁷ showed that only circular cylinders and

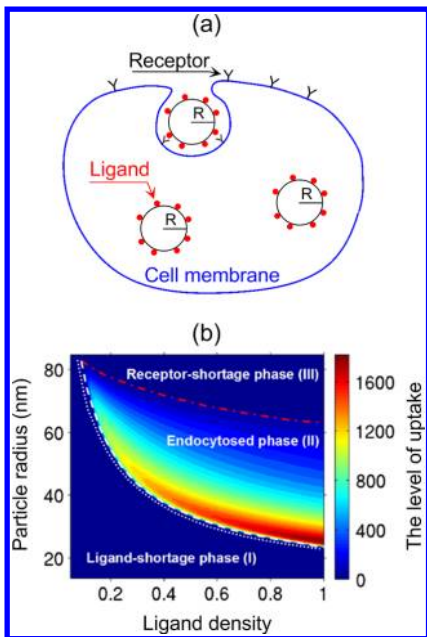


Figure 7. (a) Scheme of wrapped and endocytosed nanoparticles covered by ligands to cell-membrane receptors. (b) Dependence of cellular uptake on the particle radius R of spherical particles and the ligand density on their surface. The dashed and dash-dotted lines are the lower and upper transition boundaries, respectively, between effective endocytosis phase II and the other two phases, in which uptake is impossible. Adapted with permission from ref 134. Copyright 2010 American Physical Society.

those with moderate aspect ratios can be internalized, whereas particles with small and high aspect ratios cannot be taken up effectively. Recently,¹³⁸ Li developed a thermodynamic theoretical model to explain the size and shape effects of cigarlike nanoparticles (Figure 8) on endocytosis. In agreement with the previous theoretical considerations,⁴⁹ it was found that endocytosis needs to overcome a thermodynamic energy barrier

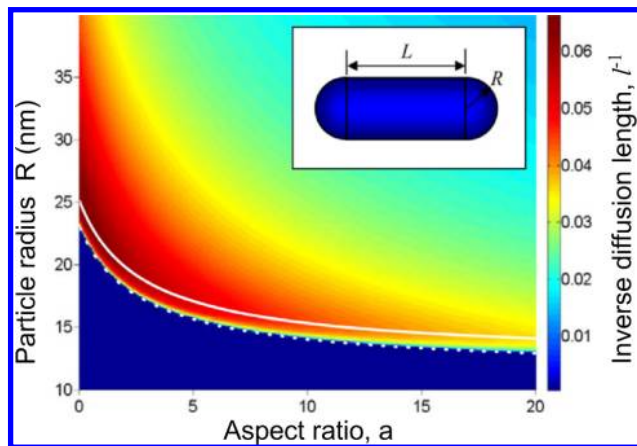


Figure 8. Endocytosis phase diagram in the space of the particle size R and aspect ratio a , as calculated by eq 2. The solid white line represents the theoretical optimal nanoparticle size for endocytosis according to eq 3, and the dotted white line is the threshold nanoparticle size for endocytosis according to eq 1. In the blue region, endocytosis is impossible. The color bar represents uptake efficiency in terms of the dimensionless inverse diffusion length, expressed in $A_0^{-1/2}$ units. Adapted with permission from ref 138. Copyright 2012 American Institute of Physics.

and that there exists a minimal nanoparticle radius for endocytosis. On the basis of the “diffusion length of receptors” concept,¹³⁸ Li obtained the following analytical expression for the minimal diameter of cigarlike particles: $R_{\min} = [A_0 \kappa (8 + a) / 2(2 + a)(\mu + \ln \xi_0)]^{1/2}$, where κ is the membrane bending modulus, $a = L/R$ is the aspect ratio of the length of the cylindrical part to the radius of the hemispherical parts, A_0 is the cross-sectional area of the receptor, μ is the released chemical energy caused by a ligand–receptor chemical binding, and ξ_0 is the initial density of receptors on the membrane surface. Note that the particle surface area $S = 2\pi R^2(2 + a)/A_0$ is measured in terms of A_0 , which is taken as unit area. Below the minimal size, the particle cannot be internalized through receptor-mediated endocytosis. For spherical particles, the aspect ratio $a = 0$, and the minimal size reduces to

$$R_{\min} = [2A_0 \kappa / (\mu + \ln \xi_0)]^{1/2} \quad (1)$$

which is close to the previously reported expressions of Gao et al.⁵⁸ and other authors.⁴⁹ As the wrapping of nanoparticles needs continuous binding of ligands to receptors diffused from the vicinity of the nanoparticles, there exists a diffusion length for full wrapping,

$$l_{\text{diff}} = [S(\xi_b^* - \xi_0) / \pi(\xi_f^* - \xi_0)]^{1/2} \quad (2)$$

where ξ_b^* and ξ_f^* are the densities of bound and free receptors, respectively, as defined by eq 6 in ref 138. Physically, the diffusion length is the distance from the nanoparticle to the farthest receptors that diffuse to it. Therefore, a small diffusion length corresponds to fast endocytosis. Accordingly, by minimizing the diffusion length with respect to the surface area, one can obtain the optimal size,¹³⁸

$$R_{\text{opt}} = \left\{ \frac{\kappa A_0 (8 + a)}{2(2 + a)[W(\xi_0 e^{\mu+1}) - 1]} \right\}^{1/2} \quad (3)$$

where the Lambert $W(x)$ function is defined as the inverse function $f(W) = W \exp(W)$. Using eqs 1–3, Li calculated a phase diagram (Figure 8) clarifying the relation between the geometry of nanoparticles and the rate of their endocytosis.

In general, all theoretical models confirm that there exists an optimal diameter (40–60 nm) for effective intracellular uptake and of a threshold size (depending on the model’s details), below which uptake is impossible. To conclude this section, we point to a recent theoretical study by Dobay et al.¹³⁹ in which a stochastic approach was applied to simulate nanoparticle uptake and intracellular distribution. These simulations were based on experimental TEM data obtained with human bronchial epithelial cells (Beas-2B) and with 4-nm GNPs.

3. EFFECT OF GNP FUNCTIONALIZATION ON INTRACELLULAR UPTAKE

3.1. Basic Methods for GNP Functionalization

Functionalization of GNPs with surface molecules is aimed at fabricating multifunctional nanoparticle bioconjugates possessing various modalities, such as active biosensing, enhanced imaging contrast, drug delivery, and tumor targeting. At present, bioconjugation chemistry, recently reviewed comprehensively by Sapsford et al.,¹⁴⁰ can be considered a separate specific branch of nanobiotechnology. The review by Sapsford et al. is based on 2 081 literature sources and covers a broad range of particle types (including GNPs) and a great variety of functionalization technologies. For more detailed information, we point readers

to this review; what follows is a description of only some general principles.

There are two basic approaches to functionalizing GNPs—the adsorptional and the chemosorptional. The adsorptional approach is based on the passive adsorption of a polymer on the surface of a particle through hydrophobic and electrostatic interactions or through sulfur bonding (Figure 9). Specifically,

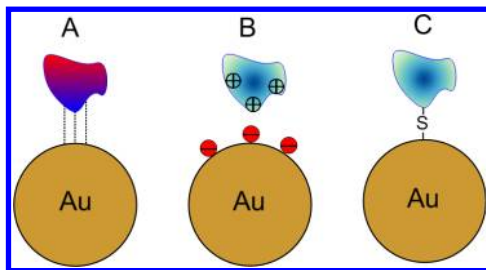


Figure 9. Schematic representation of adsorptional approaches to functionalizing GNPs with proteins. Proteins bind to the GNP surface by hydrophobic attractions (red, hydrophilic regions; blue, hydrophobic regions), which depend on the amino acids exposed to the particle surface (A), electrostatic interactions (B), and sulfur bonding (C).

proteins bind to gold colloids through sulfur bonding (cysteine and methionine), charge–charge attraction (lysine), and hydrophobic attraction (tryptophan).¹⁴¹ For example, electrostatic interactions were reported to occur between the H₂N groups of lysine and the citrate ions at the surface of GNPs produced by the method of Frens.¹⁴² Another example is the SH groups of cysteine molecules,¹⁴³ which are important for protein binding to the gold-particle surface. The strong point of the adsorptional approach is that the alterations in macromolecular structure are minimal and, consequently, the functional properties of the attached macromolecule are preserved. The weak points are possible desorption and competition with the binding sites on the target molecules. Typically, high-molecular-weight substances are adsorbed in amounts much larger than those needed for the formation of a monomolecular layer on the particle surface. In the case of dilute polymer solutions, the adsorption isotherms do not have inflections, the presence of which would attest to the formation of a discrete monolayer, as is observed for low-molecular-weight surfactants. In general, the adsorptional conjugation is irreversible, although long-term storage at high pH or in a buffer containing a surfactant may cause some proteins to dissociate.¹⁴¹

The chemical attachment of biomolecules to GNPs is based on the classical chemistry of thiols and thiolated linkers or macromolecules. It is known that gold and sulfur atoms can form a dative bond.¹⁴⁴ This property is widely employed in bioconjugation chemistry to form alkanethiol linkers for covalent attachment of various biomolecules to GNPs (the chemosorption method). The chemical formula of alkanethiols can be represented as HS(CH₂)_nR, where R stands for –COOH, –OH, or –SO₃H and the number of groups n usually varies from 11 to 22.¹⁴⁵ Interaction of alkanethiols with gold gives rise to Au(I) thiolates, nAu0×Au+S–(CH₂)_nR,¹⁴⁶ which are organized as a monolayer on the surface of a particle. In 1996, Mirkin et al. proposed a technique for attaching 3'-thiolated oligonucleotides to 13-nm gold particles.¹⁴⁷ As a result, stable conjugates were prepared that could aggregate and disaggregate at low and high temperature, respectively; this principle was used by the authors for colorimetric detection of DNA in solution. The same group also suggested the use of cyclic disulfides¹⁴⁸ and trihexylthiol

linkers¹⁴⁹ to prepare DNA conjugates with 30- and 100-nm GNPs, respectively. Walton et al.¹⁵⁰ and Ghosh et al.¹⁵¹ used thiolated proteins (immunoglobulins and avidin) to obtain conjugates with gold NSph's and NRs. In addition to alkanethiols, the linkers used include phosphine-, amine-, and carboxyl-containing ligands. The advantages of chemical attachment are evident for linear molecules (like DNA) and are determined by C-terminal immobilization, which ensures a strict spatial orientation of probes. The type of the bond between GNPs and functional molecules is, in particular, responsible for the release of the target substance inside a cell.¹⁵² Thus, the presence on the GNP surface of polymers and biological macromolecules that differ in chemical makeup and properties leads to differences in the cellular uptake of functionalized particles.

3.2. Formation of a GNP–Protein Corona in a Biological Environment

Immediately on contact of GNPs with blood, lymph, gastric juice, or any other biological liquid *in vivo*, as well as on contact with a culture medium *in vitro*, the interaction between GNPs and solvable proteins and other biomolecules results in the formation of a protein “corona”.^{153,154} Similarly to the concept of functionalized GNPs, the concept of a GNP–protein corona is important in tuning the surface physicochemical properties of GNPs, such as charge, hydrodynamic size, and colloidal stability. In fact, it is the GNP–protein corona that forms the first nano–bio interface and determines the first interactions of GNPs with or within living cells. This is because the GNP–protein corona is a dynamic biopolymer layer that can strongly affect cellular uptake owing to modification of the particle properties (the overall size, charge, etc.). Furthermore, owing to the GNP–protein interaction, the adsorbed proteins can change their conformations. It is a kind of change that exposes new functional groups and alters the protein functions, avidity effects, and so on (Figure 10).^{154,155} In general, the corona structure and properties depend on the prior history of particles, as the GNP surface may already be covered by various ligands coming from fabrication and stabilization procedures.¹⁵⁴

Although as much as 69 plasma proteins can bind to the GNP surface,^{156,157} only some of them, such as albumin, apolipoprotein, immunoglobulin, complement, and fibrinogen, are the most abundantly bound proteins forming the GNP–protein corona. After intravenous injection, the coating of GNPs by these proteins largely determines the particles' fate in the body—biodistribution over organs, tissues, and cells; the efficiency of cellular uptake and clearance; and so on.

Thus, the corona is a complex mixture of proteins adsorbed on the surface of nanoparticles. These proteins play an important role in determining what surface is actually presented to cells that take the nanostructure up and activate signaling pathways. The protein corona is composed of an inner layer of selected proteins with a lifetime of several hours in slow exchange with the environment (the hard corona) and an outer layer of weakly bound proteins that are characterized by a faster exchange rate with the free proteins (the soft corona). The biological impact of protein-coated NPs is mainly related to the hard corona and their specificity and suitable orientation for a particular receptor. Although low-affinity, high-abundance proteins may initially adsorb to the surface of NPs, proteins with lower abundance but higher affinity quickly replace them.¹⁵⁸

The corona formation process depends mainly on GNP size, charge, preliminary surface functionalization, particle curvature,

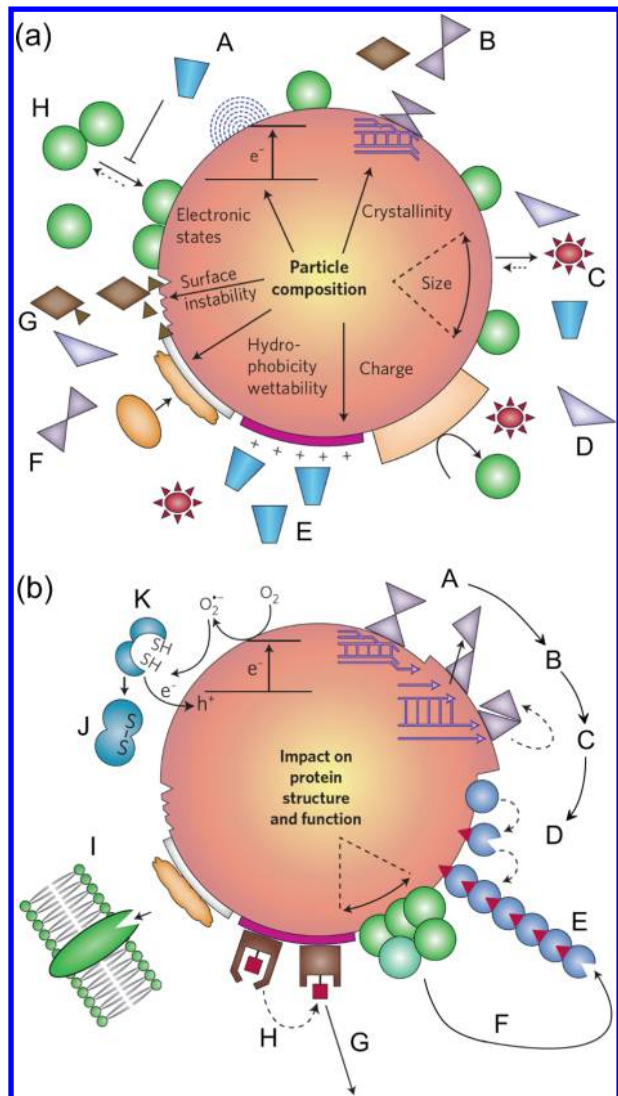


Figure 10. Effects of a GNP–protein corona. (a) The initial material characteristics of as-prepared GNPs contribute to the formation of the corona in a biological environment. The corona can change when particles move from one biological compartment to another. Symbol designations: A, competitive binding interactions depend on the protein concentration and the body fluid composition; B, binding interactions release surface free energy, leading to surface reconstruction; C, the available surface area, surface coverage, and angle of curvature determine the adsorption profiles; D, steric hindrance prevents binding; E, charge (e.g., cationic binding); F, hydrophilic or hydrophobic interactions; G, protein binding accelerates the dissolution of some materials; H, characteristic protein on/off rates depend on the material type and the protein characteristics. (b) Possible changes in corona structure and functions owing to interaction with the GNP surface. The colored symbols represent various types of proteins, including charged, lipophilic, and conformationally flexible proteins; catalytic enzymes with sensitive thiol groups; and proteins that crowd together or interact to form fibrils. Symbol designations: A, surface reconstruction; B, release of surface free energy; C, protein conformation, functional changes; D, protein fibrillation; E, amyloid fiber; F, protein crowding, layering, nucleation; G, immune recognition; H, exposure to cryptic epitopes; I, surface opsonization/liganding allows interaction with additional nano–bio interfaces; J, protein conformational changes cause loss of enzyme activity; K, electron–hole pairs lead to oxidative damage. Adapted with permission from ref 154. Copyright 2009 Nature Publishing Group.

and surface roughness. In turn, these factors determine the main physicochemical contributions to corona formation, namely, hydrodynamic, electrodynamic, electrostatic, solvent, steric, and polymer-bridging interactions.¹⁵⁴ The dynamic composition of the GNP–protein corona depends on association/dissociation constants, the concurrent binding processes, steric hindrance (which prevents binding), and the composition of the biological liquid surrounding GNPs.¹⁵⁹ Accordingly, Arvizo et al.¹⁶⁰ pointed out that the composition and properties of the GNP–protein corona should be considered in designing new GNP-based therapeutic targets.

3.3. Intracellular Uptake of PEGylated GNPs

In current nanotechnologies, extensive use has been made of GNPs functionalized with PEGs having different polymer-chain lengths and diverse functional group. This is due to a number of factors: PEGylated GNPs are less “recognized” by cells of the immune system because of the lower opsonization by serum proteins (stealth technologies) and are much more tolerant of salt aggregation than citrate- or CTAB-coated GNPs, which makes them able to circulate in the bloodstream for a longer time.^{161–163} In vivo, PEGylated nanoparticles preferentially accumulate in tumor tissue owing to the increased permeability of the tumor vessels and are retained in it owing to reduced lymph outflow.¹⁶⁴ Finally, PEG hydrophilizes the surface of nanoparticles and can serve as a ligand for the attachment of drugs or genes to deliver to target cells.^{165,166}

Shenoy et al.¹⁶⁷ used 10-nm GNPs coated with thiolated PEG1500 with attached coumarin, a fluorescent dye. This is an example of a “hetero-bifunctional” PEG, which has a thiogroup for binding to GNPs at one end and a mobile spacer for binding to a dye or to other ligands at the other. With the help of this structure, the authors investigated by LCM the uptake of GNPs in MDA-MB-231 cells. They showed that GNPs modified with coumarin–PEG-SH are taken up effectively within 1 h of incubation and localize mostly in the perinuclear space. Endocytosis proper begins as early as at 5 min; at 30 min, GNPs appear in endosomes. Despite the high rate of endocytosis, no GNPs could be found in the cell nuclei even after a day’s incubation. It was concluded that, with the aid of PEG-coated GNPs, it is possible to perform intracellular delivery of various ligands (dyes, antibodies, drugs, etc.).

Bergen et al.¹⁶⁸ explored the liver cell uptake in vivo of 50-, 80-, 100-, and 150-nm GNPs modified with PEG5000-SH and galactose–PEG5000-SH. The cellular concentration of gold was determined by neutron activation. The time of GNP circulation in blood and the amount of GNPs in the liver cells were found to be substantially affected by the particle size and by the presence of galactose in the surface ligand (Figures 11 and 12). The increased accumulation of GNPs coated with galactose–PEG5000-SH was attributed to receptor-mediated endocytosis of such GNPs by the Kupffer cells of the liver through galactose receptors or by hepatocytes through asialoglycoprotein receptors on their surface.

Cho et al.¹⁶⁹ made a TEM study of the toxicity and pharmacokinetics of 13-nm GNPs modified with PEG5000. In complete agreement with the data obtained by Sadauskas et al.^{32,33} for nonfunctionalized GNPs, the PEGylated particles accumulated mostly in Kupffer cells of the liver and in macrophages of the spleen. In addition, the results of TEM demonstrated that, inside the cells, GNPs were found in endosomes and lysosomes and were not associated with the nucleus, mitochondria, or the Golgi apparatus (Figure 13).

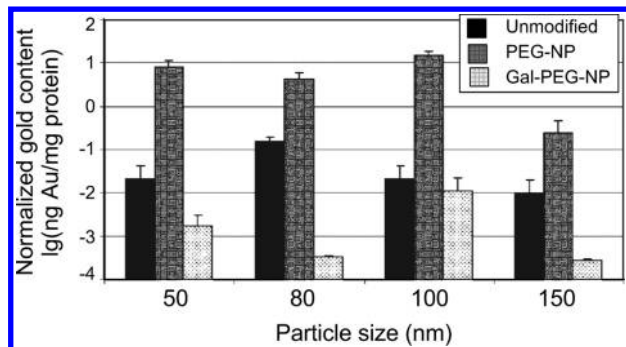


Figure 11. Normalized gold content in blood, in terms of $\text{lg}(\text{ng gold}/\text{mg protein}$ from four mice/group), at 2 h postinjection. Adapted with permission from ref 168. Copyright 2006 John Wiley & Sons, Inc.

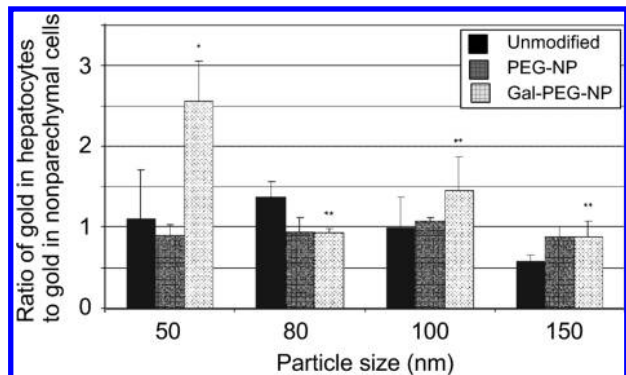


Figure 12. Liver-cell biodistribution of GNPs at 2 h postinjection. Values presented are the mean ratio of gold in hepatocytes to gold in nonparenchymal cells from four mice/group. *, significant statistical difference compared to the PEG-GNP control ($p < 0.05$). **, no significant statistical difference compared to the PEG-GNP control ($p > 0.05$). Adapted with permission from ref 168. Copyright 2006 John Wiley & Sons, Inc.

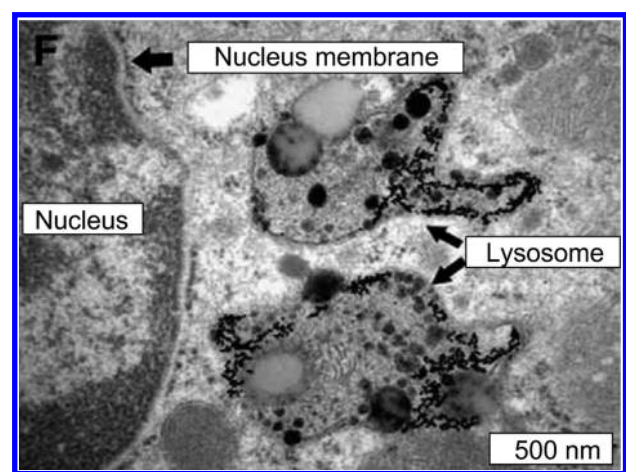


Figure 13. Thin-section TEM image of mouse spleen macrophages at 7 days after intravenous injection of PEG-modified GNPs. Magnification, 50 000 \times . Adapted with permission from ref 169. Copyright 2009 Elsevier B.V.

Similar data were reported by Cho et al. for 4- and 100-nm PEGylated GNPs.¹⁷⁰ Liu et al.¹⁷¹ also showed that 5-nm GNPs modified with PEG5000 were localized in the cytoplasm of CT26 cells and were not found in the nuclei. Zhang et al.¹⁷² reported that the most effective uptake *in vivo* into cells of the liver and

spleen was demonstrated by 20-nm GNPs modified with PEG5000 through thioctic acid.

Different data were gathered by Gu et al.,¹⁷³ who found by TEM, LCM, and ICP-MS that 3.7-nm GNPs successively coated with mercaptopropionic acid and PEG2000 can penetrate the nuclei of HeLa cells (Figure 14). Thus, as Gu et al.¹⁷³ concluded, PEGylated GNPs can be used for the delivery of drugs or genetic material directly to the nuclei of cells.

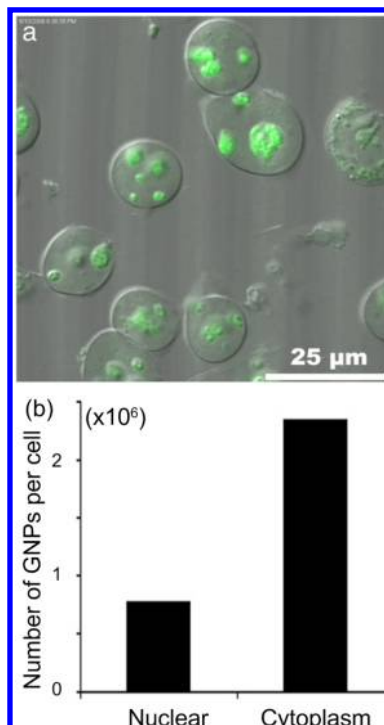


Figure 14. Confocal image of isolated nuclei of HeLa cells incubated with GNPs-PEG-FITC (a). The GNP concentration in the nuclei and cytoplasm of HeLa cells (data by ICP-MS) (b). Adapted with permission from ref 173. Copyright 2009 Elsevier B.V.

Brandenberger et al.¹³⁰ compared the uptake of 15-nm PEGylated (PEG5000) and plain GNPs by A549 cells. The GNPs in the cells were quantitatively analyzed by TEM. Both types of particles were found to be present in the cytoplasm as part of variously sized vesicles: <150 nm (primary endosomes), 150–1000 nm (endosomes), and >1000 nm (phagosomes and lysosomes). In the other cell compartments—the nucleus, mitochondria, endoplasmic reticulum, and Golgi apparatus—no GNPs were observed. After 4 h of incubation, the per-cell number of plain GNPs was 3500 and that of PEGylated GNPs was 1000. When the cells were treated with methyl- β -cyclodextrin, an inhibitor of caveolin- and clathrin-dependent endocytosis, the per-cell number of GNPs decreased particularly strongly for PEGylated GNPs—by 95% (for plain GNPs, the decrease was 50%). It was concluded that the uptake of non-PEGylated GNPs is effected both through macropinocytosis and through caveolin- and clathrin-dependent endocytosis and that the uptake of PEGylated GNPs occurs only via receptor-mediated endocytosis.

Lund et al.¹⁷⁴ presented data on the tumor cell (HCT-116, HT 29, LS154T, and SW640) uptake of two types of 2-nm GNPs: (i) those coated with PEG and (ii) those coated with 50% PEG/50% glucose. Particles of the latter type were found to be taken up into cells much more effectively. The authors inferred that the major

Table 2. Effect of the Concentration and Molecular Mass of PEG and the Diameter of NSs on the Phagocytosis of NSs

PEG conc (mmol/L)	uptake in macrophages ^a (%)	size of SiO ₂ /Au NSs (nm)	uptake in macrophages ^b (%)	molecular mass of PEG (Da)	uptake in macrophages ^c (%)
0	80	79/23	8.1	750	10.2
0.05	40	100/23	1.7	2 000	0.6
0.25	30	140/23	0.6	5 000	0.9
0.5	20	162/23	0.9	10 000	2.1
2.5	10	181/23	1.4	20 000	48.2
5.0	10	196/23	1.2		
10	10				
20	10				

^aNSs of 181/23 nm, PEG2000. ^bPEG2000, PEG concentration of 2.5 mmol/L. ^cNSs of 140/23 nm, PEG concentration of 2.5 mmol/L.

role in GNP internalization is played by the structural organization of the ligands on the nanoparticle surface, rather than by the charge of the functional groups. In addition, the authors suggested that apart from receptor-mediated endocytosis, an important role in the uptake of small GNPs is played by passive transport of GNPs through the pores of the plasma membrane.

An in-depth study of the uptake of PEGylated NSs by macrophages (RAW264.7) in vitro was described by Kah et al.¹⁷⁵ They synthesized gold NSs on SiO₂ cores, with diameters of 79, 100, 140, 162, 181, and 196 nm and a gold shell thickness of ~23 nm. For functionalization, they used different concentrations of methoxy-PEG-SH with different molecular masses, including 750, 2 000, 5 000, 10 000, and 20 000 Da. For visualization of gold NSs in the macrophages, dark-field microscopy and LCM were employed. The results showed that the intracellular uptake of NSs by macrophages was affected by the amount of PEG added. The highest uptake was exhibited by non-PEGylated NSs (80%). The percentage of phagocytosed NSs decreased to 40% with 0.05 mmol/L PEG, to 30% with 0.25 mmol/L PEG, to 20% with 0.5 mmol/L PEG, and to ~10% with 2.5–20 mmol/L PEG. It was also found that the phagocytosis of PEGylated NSs depends on the molecular mass of adsorbed PEG (2.5 mmol/L). The uptake of 140/30 NSs (core/shell, nm) in the macrophages, in percent of the amount of administered particles (2×10^{13} particles/mL), was 10.2% for PEG750, 0.6% for PEG2000, 0.9% for PEG5000, 2.1% for PEG10000, and 48.2% for PEG20000. Furthermore, phagocytosis depended on the nanoparticle size: the uptake of NS-PEG2000 was 8.1% for NSs of 79/23 nm, 1.7% for NSs of 100/23 nm, 0.6% for NSs of 140/23 nm, 0.9% for NSs of 162/23 nm, 1.4% for NSs of 181/23 nm, and 1.2% for NSs of 196/23 nm. Thus, the best ability to be taken up was displayed by NSs with a core diameter of 79 nm and NSs functionalized with PEG20000. For convenience, the data of ref 175 are summarized in Table 2.

Unlike gold NSph's and NSs, gold NRs are coated with the cationic surfactant CTAB, which is used in all seed-mediated synthetic protocols. CTAB-coated gold NRs actively and irreversibly penetrate into mammalian cells, and they are markedly cytotoxic. The cytotoxic effect is often reduced by replacing CTAB with inert polymers, specifically with PEG.¹⁶¹ Such replacement not only produces a sharp decrease in cytotoxicity but also appreciably lowers, according to several authors,^{98,176–179} the level of nonspecific uptake of gold NRs in various cells.

Arnida and co-workers^{180,181} compared the intracellular uptake of PEGylated and plain gold NSph's versus PEGylated gold NRs by PC-3 and RAW264.7 cells. They used NSph's with diameters of 30, 50, and 90 nm and NRs with length-by-diameter

dimensions of 35×10 and 45×10 nm. TEM and ICP-MS analysis showed that 50-nm non-PEGylated NSph's were taken up best. Modification of the surface with PEG led to a considerable decline in uptake, as also did the presence of serum proteins. PEGylated NRs (especially the shorter ones) were taken up by the cells much worse than NSph's.

Somewhat different data came from a study by Cho et al.,¹⁸² who compared the uptake by SK-BR-3 cells of 17-nm citrate-capped and PEGylated NSph's versus CTAB- and PEG5000-coated NRs (50 × 20 nm). They showed by UV-vis spectrophotometry that the levels of uptake of citrate-capped NSph's and NR-CTAB were approximately the same: 8×10^3 GNPs/cell. After PEGylation, the uptake level decreased approximately 4-fold (2×10^3 GNPs/cell) for NSph's and 2-fold (4×10^3 GNPs/cell) for NRs. Of interest is the fact that, when the cells were incubated with a mixture of NSph's and NRs, the latter were found in large amounts in the intracellular space regardless of the modification of the surface. Hence, as the authors concluded, it is the surface functionalization of nanoparticles, rather than their shape, that has a greater influence on the intracellular uptake of GNPs. In contrast to this conclusion, Puvanakrishnan et al.¹⁸³ showed that PEGylated NRs penetrated tumor cells 12-fold more actively than did PEGylated NSs and that the accumulation of these particles in the liver cells was approximately of the same level.

Although PEG functionalization ensures stealth properties of GNPs in a biological environment, this coating may be destroyed by some concurrent binding. For example, Larson et al.¹⁸⁴ showed that the physiological concentration of cysteine and cystine can displace methoxy-PEG-thiol molecules from the GNP surface. This displacement is accompanied by plasma protein coatings and by enlargement of the protein corona; as a result, the modified GNPs demonstrate enhanced cellular uptake. To avoid such loss of stealth properties and to greatly reduce the cellular uptake, the authors incorporated a small hydrophobic shield (alkyl linker) in between the GNP core and the hydrophilic PEG shell.¹⁸⁴

Thus, the existing data point to a combined effect of the shape and functionalization of the particles used in comparative experiments to study the effectiveness of intracellular uptake. Further work is needed to identify the effects of shape alone, without interference from the effects of surface molecules.

3.4. Uptake of GNPs Functionalized with Other Synthetic Polymers and Proteins

Apart from PEG, other polymer molecules are also frequently used to reduce the cytotoxicity of gold NRs, a practice that changes the level of uptake of such GNPs by mammalian cells. For example, Takahashi et al.¹⁸⁵ modified the surface of NRs (65 × 11 nm) with phosphatidylcholine and polyethyleneimine

(PEI). It is known that conjugating GNPs to PEI improves the effectiveness of transfection of plasmid DNA into cells.¹⁸⁶ According to the data of Takahashi et al., PEI-modified NRs were taken up by HeLa cells much better than were NR-phosphatidylcholine conjugates. Thus, for nonspherical particle shape, the effect of surface functionalization with PEI is evident.

Probably the most thorough analysis of the effect of functionalization on the intracellular uptake of NRs was reported by Chan's group¹⁸⁷ for a representative set of polymers. To modify the surface of NRs (40 × 18 nm), the authors used poly(4-styrenesulfonic acid) (PSS1), poly(diallyldimethylammonium chloride) (PDDAC), poly(allylamine hydrochloride) (PAH), and PSS-PDDAC-PSS (PSS2). NRs coated with CTAB (the initial ones), PDDAC, and PAH were charged positively, and those capped with PSS1 and PSS2 were charged negatively. Uptake was studied with HeLa cells by using TEM and ICP-AES. NRs (150 μM) were added to cells in DMEM containing fetal bovine serum and also to cells in DMEM serum-free medium. It was found that, in serum-free medium, PSS1- and PAH-coated NRs were taken up ~2-fold worse than CTAB-, PDDAC-, and PSS2-coated NRs (~50 000 GNPs/cell, as compared with ~100 000). The membrane of HeLa cells is charged negatively, and a possible explanation for the higher uptake of positively charged NRs could be the electrostatic interactions between the cell and the NR surface. In addition, the chemical nature of the coating polymer is probably important for the uptake of NRs. Specifically, NRs coated with quaternary amines (CTAB and PDDAC) were taken up by the cells much more effectively than were NRs coated with a primary amine (PAH). Experiments with cells in serum medium yielded somewhat different results. The highest uptake was demonstrated by NRs coated with PDDAC (~150 000 GNPs/cell). The average value yielded by CTAB-, PAH-, and PSS2-functionalized NRs was 25 000 GNPs/cell. PSS1-coated NRs displayed a fairly low uptake level: <10 000 GNPs/cell. This effect was explained by the differences in the adsorption of serum proteins onto the functionalized NRs and by the enhanced receptor-mediated endocytosis of GNPs covered with serum proteins.⁵⁵

Slightly different results for the same type of particle were reported by Alkilany et al.¹⁸⁸ They used TEM and ICP-MS to investigate the uptake of gold NRs ($\lambda_{\text{max}} = 840 \text{ nm}$, aspect ratio of 4.1) by HT-29 cells. Positively charged NRs were coated with CTAB and PAH, and negatively charged NRs were coated with poly(acrylic acid) (PAA). The best cellular uptake (in serum medium) was shown by PAH-coated NRs (final concentration of 0.2 nM; ~2 500 GNPs/cell); much worse uptake was shown by PAA-coated NRs (~300 GNPs/cell); and minimal uptake was shown by CTAB-coated NRs (~50 GNPs/cell). This is in disagreement with the data of Hauck et al.¹⁸⁷ for CTAB-coated NRs and for the average values for the taken-up particles. It should be noted that, after incubation of NRs in a medium containing serum proteins, the charge of all NRs leveled off, becoming approximately -20 mV. It is quite possible that the differences between the data of Hauck et al.¹⁸⁷ and those of Alkilany et al.¹⁸⁸ have to do with the different types of cells used, amounts of NRs added, geometrical parameters of the NRs, and incubation times (6 and 24 h, respectively). Also in conflict with the data of Hauck et al. is a closely related study by Parab et al.,¹⁸⁹ who used TEM to compare the uptake of CTAB- and PSS-coated NRs ($\lambda_{\text{max}} = 700 \text{ nm}$, aspect ratio of 2–3) by S-G and TW 2.6 cells. PSS-coated NRs were found to be taken up into the cell cytoplasm better than their CTAB-coated counterparts.

Fan et al.¹⁹⁰ reported that the uptake of PEG-coated NRs (65 × 12 nm) in MEF-1 and MRC-5 cells was much less effective than it was when the particles were functionalized with PSS and PDDAC. Goh et al.¹⁹¹ demonstrated that gold NRs encapsulated in Pluronic triblock copolymers effectively penetrated OSCC cells and were much less toxic than CTAB-coated NRs.

An in-depth study of the effect of NR geometry and surface functionalization on intracellular uptake was made by Qiu et al.,¹⁹² by using NRs with dimensions of 33 × 30 nm (1), 40 × 21 nm (2), 50 × 17 nm (3), and 55 × 14 nm (4). The NRs were coated with CTAB (the initial NRs, 1–4), PSS (1 and 4), and PDDAC (1 and 4). The uptake was examined with MCF-7 cells grown on Roswell Park Memorial Institute (RPMI) medium containing fetal bovine serum, and the methods used were TEM and ICP-MS. The results showed that, out of the initial NRs, the best uptake was observed for GNPs with smaller aspect ratios (almost spherical GNPs), whereas the NRs with the maximal aspect ratio exhibited the worst uptake. However, the effect of the geometrical parameters on uptake effectiveness was not as strong—9 × 10³ GNPs/cell for NR-1-CTAB and 5 × 10³ for NR-4-CTAB. A much stronger effect was produced by surface modification: 9 × 10³ GNPs/cell for NR-1-CTAB, 4 × 10³ GNPs/cell for NR-1-PSS, 1.2 × 10⁴ GNPs/cell for NR-1-PDDAC, 5 × 10³ GNPs/cell for NR-4-CTAB, 3 × 10³ GNPs/cell for NR-4-PSS, and 9 × 10⁴ GNPs/cell for NR-4-PDDAC (Figure 15).

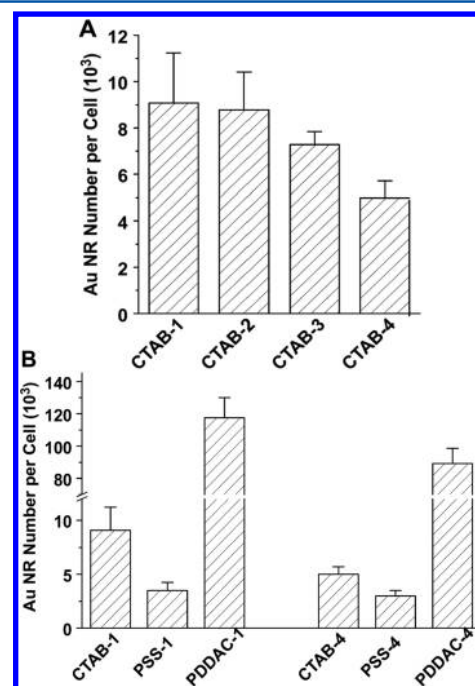


Figure 15. Effect of shape and functionalization on the intracellular uptake of NRs. The cellular amounts of CTAB-coated (A) and CTAB-, PSS-, and PDDAC-coated (B) NRs with four different aspect ratios after cell incubation with 70 pM NRs for 24 h. Adapted with permission from ref 192. Copyright 2010 Elsevier B.V.

As indicated by TEM, some of the CTAB-coated NRs inside the cells were localized in lysosomes and some were found in mitochondria (Figure 16a, b). It follows from the images (c, d) that the CTAB molecules in cells can cause swelling and stimulate the production of mitochondria, thus indicating a cellular inflammatory response.

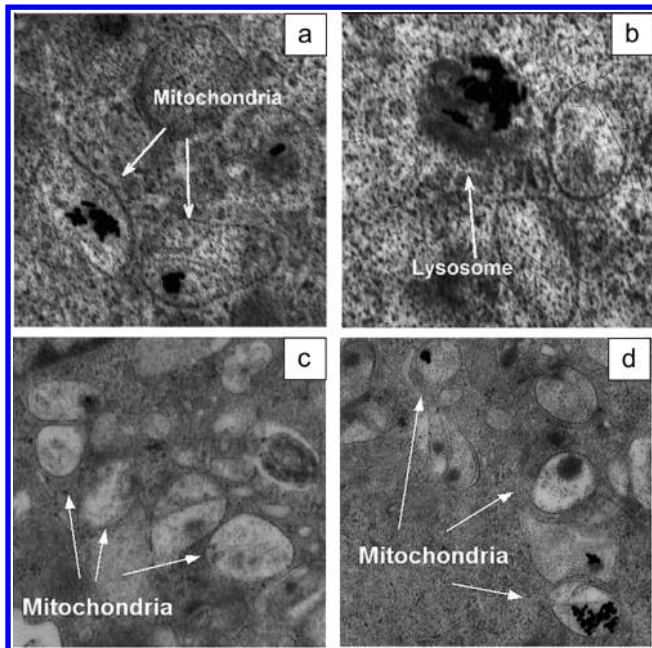


Figure 16. TEM images of cells incubated with CTAB-coated NRs. Some NRs are in mitochondria (a), whereas others are found in lysosomes (b). The CTAB molecules in cells can cause swelling and stimulate the production of mitochondria, which is an ordinary pathological indicator for cellular inflammatory responses (c, d). Adapted with permission from ref 192. Copyright 2010 Elsevier B.V.

On the basis of their findings, the authors reasoned that the major effect on the cellular uptake of NRs is produced by surface functionalization, rather than by geometrical parameters. They also proposed a scheme for the mechanism of intracellular uptake and cytotoxicity of NRs (Figure 17). In this mechanism, NRs are first covered rapidly by serum proteins, which mediate

endocytosis. Once taken up, the NR–protein complex is transported by vesicles to lysosomes, where the proteins are digested and CTAB is released. The NR aggregates are delivered to mitochondria, where they accumulate. The released CTAB molecules damage the mitochondria and induce cell apoptosis and death. If NRs are coated with an inert polymer, the lysosomal enzymes are unable to digest it; therefore, CTAB is not released and, consequently, the cytotoxic effect of NRs is relieved. Qiu et al.¹⁹² believe that PDDAC-complexed NRs with an aspect ratio of ~ 4 make the optimal nanocomposites for medical applications.

In a subsequent report from the same group,¹⁹³ the study of uptake of gold NRs into various types of cells was continued by using A549 carcinoma cells, 16HBE normal bronchial epithelial cells, and mesenchymal stem cells. The intracellular uptake of 55×13 -nm NRs functionalized with fetal bovine serum was examined by ICP–MS and TEM. It was found that uptake was more effective in the carcinoma and stem cells and was much worse in the normal cells. Exocytosis was more active in the stem cells. To investigate the mechanism of endocytosis, the authors used a variety of inhibitors. Sodium azide, 2-deoxy-D-glucose, and low temperature sharply decreased the endocytosis (to as low as 80%) and noticeably decreased ATP synthesis—that is, the endocytosis was energy-demanding. Chlorpromazine and a hypertonic solution of sucrose reduced NR uptake by 75 and 89%, respectively. It follows that the principal mechanism of endocytosis was clathrin-dependent. If nystatin, methyl- β -cyclodextrin, and dynamin served as inhibitors, the endocytosis decreased by 54, 48, and 42%, respectively, attesting that a raft-dependent endocytosis route is also possible. TEM data indicated that the intracellular localization of NRs was different in the three types of cells: only in the carcinoma cells were NRs present in mitochondria as well as in lysosomes. The authors associated the toxic effect of NRs on the cancer cells with mitochondrial damage by CTAB, which is released in the lysosomes of cancerous cells. Thus, cell viability is affected not only by endocytic routes but also (and primarily) by intracellular localization.

Very intriguing data on the influence of surface modification of NRs on their intracellular uptake were presented recently by Vigderman et al.¹⁹⁴ Using TEM, SEM, and ICP–AES, they demonstrated that replacing CTAB on the surface of NRs (42×10 nm) by its analogue, (16-mercaptohexadecyl)-trimethylammonium bromide, increased drastically (~ 200 -fold) the effectiveness of NR uptake by MCF-7 cells. In addition, these NRs were very stable and caused no toxicity.

Li et al.¹⁹⁵ examined the intracellular uptake of transferrin-functionalized and PEG-capped GNPs (25 nm) in tumor (Hs578T) and normal (3T3) cells. Dark-field microscopy and LCM showed that transferrin-coated GNPs were taken up by tumor cells via transferrin-receptor endocytosis 6-fold more effectively than were PEGylated GNPs. Blocking of transferrin receptors by cell pretreatment with native transferrin also brought about a 6-fold decrease in uptake effectiveness. In addition, the uptake of transferrin-capped GNPs by normal cells was 75% lower than that by tumor cells owing to the small number of transferrin receptors on the surface of normal cells.

The effect of coating GNPs with a thermoresponsive polyacrylamide polymer on the uptake of 18-nm GNPs by MCF-7 cells was explored by Salmaso et al.¹⁹⁶ They used ICP–AES and TEM to show that at 40°C polymer-capped GNPs were taken up 80-fold more effectively (12 000 particles/cell) than they were at 34°C (140 particles/cell). The intracellular uptake

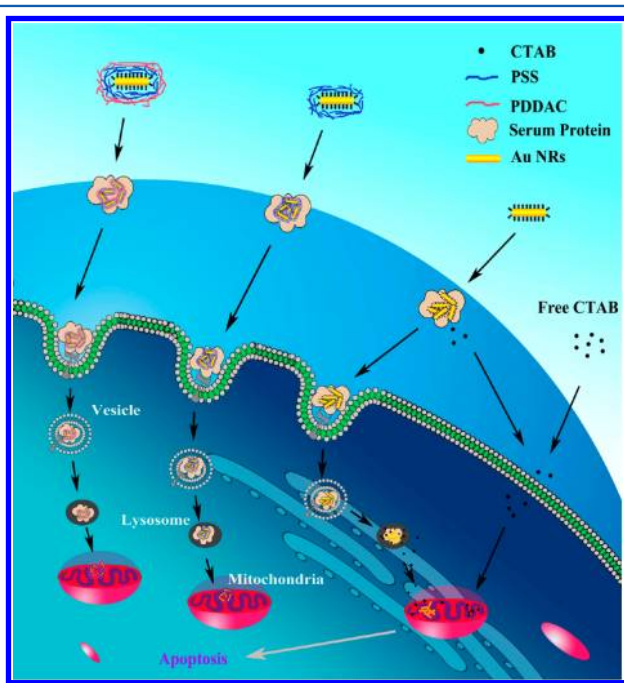


Figure 17. Scheme for the pathway of intracellular uptake and the mechanism of cytotoxicity of NRs. Adapted with permission from ref 192. Copyright 2010 Elsevier B.V.

of uncapped GNPs was 6 000 particles/cell and did not depend on temperature.

Dragoni et al.¹⁹⁷ reported that 5-nm polyvinylpyrrolidone-coated GNPs were found in endosomes of hepatocytes within 30 min of their addition and that, after 2 h, they appeared in endosomes of endothelial and Kupffer cells. Liu et al.¹⁹⁸ found that, as compared with GNP–PEG2000, 16-nm GNPs conjugated to zwitterionic surfactants were taken up much worse both by phagocytic (RAW 264.7) and nonphagocytic (HUVEC and HepG2) cells.

One of the most important effects of functionalization is the change of particle charge, because electrostatic interactions can control cellular uptake of particles much stronger than can, for example, hydrophobic or van der Waals interactions. The effect of surface-polymer charge on the intracellular uptake of spherical GNPs was investigated by several authors.^{199–205} It was demonstrated that GNPs coated with positively charged polymers were taken up best, as compared with negatively charged and neutral NSph's. These results are in harmony with the data obtained by Hauck et al.¹⁸⁷ for gold NRs. Cho et al.¹⁹⁹ explained the enhanced uptake of positively charged GNPs by the enhanced adsorption of positively charged GNPs onto the negatively charged cell surface, facilitating the higher uptake into cells. Yet, Liang et al.²⁰⁶ successfully demonstrated the use of an anionic group, *meso*-2,3-dimercaptosuccinic acid (DMSA), to enhance the uptake of gold NSs by RAW 265.7, A543, and BEL-7402 cells. The reason possibly lies in the nonspecific adsorption of serum proteins on the DMSA-modified gold NSs, which enhanced the cellular uptake. Arvizo et al.²⁰⁷ demonstrated that the surface charge of functionalized GNPs plays a prominent role in modulating the membrane potential of different malignant and normal cells and in subsequent intracellular uptake of GNPs. In particular, positively charged GNPs depolarized the membrane to the greatest extent, whereas NPs of other charges had negligible effect. Such membrane-potential disturbances resulted in an increased intracellular Ca^{2+} concentration, which in turn inhibited the proliferation of normal cells, whereas malignant cells remained unaffected. Furthermore, as shown by Lin et al.,²⁰⁸ the charge of coating polymers influences the mechanism of endocytosis, in particular the involvement of tubulin microtubules in this process.

Researchers who study the influence of various factors on the effectiveness of cellular GNP uptake should take into consideration the components of the cell growth medium they are using. Just like in the case of NRs, the composition of the cell growth medium may be profound for cellular uptake of gold NSph's. For instance, Maiorano et al.,²⁰⁹ using ICP–AES, reported that the uptake of 15-nm GNPs by HeLa cells grown on RPMI medium was ~3-fold more effective than the uptake by the same cells grown on DMEM medium. The authors' explanation for this finding is that, in RPMI medium, the diameter of the protein corona formed on GNPs is 2-fold greater than that observed in DMEM medium.

An interesting research direction is the use of hybrid particles, combining GNPs with components of liposomes, which are traditionally considered promising carriers for intracellular delivery. Pal et al.²¹⁰ and Boca et al.²¹¹ found that GNPs incorporated in liposomes or capped with chitosan were taken up by CHO cells better than native GNPs and also were less toxic. The data of Chithrani et al.²¹² indicate that 1.4-nm GNPs incorporated in liposomes were taken up in HeLa cells 1000-fold more effectively than were native GNPs. In addition, the biocompatibility of GNPs can be improved by the use of, e.g.,

gellan gum.²¹³ According to LCM data, 14-nm GNPs coated with this polysaccharide entered LN220 tumor cells much more effectively than they entered NIH-3T3 normal fibroblasts. It was also proposed that biocompatibility can be increased with lysozyme-conjugated GNPs, and such conjugates were found to be effective at entering the cells and nuclei of an NIH-3T3 culture by clathrin-dependent endocytosis.²¹⁴ Hao et al.²¹⁵ showed that phospholipid-coated GNPs were taken up by MCF-7 cells more effectively than were PEGylated GNPs. Wang and Petersen²¹⁶ also showed that lipid-coated GNPs were readily taken up by A549 cells. Similar data were published by Yang et al.²¹⁷ for high density lipoprotein–coated GNPs and lymphoma cells. Amarnath et al.²¹⁸ demonstrated that glutathione- or lipoic acid-coated GNPs entered HBL-100 tumor cells much more effectively than nonconjugated GNPs.

3.5. Uptake of GNPs Conjugated with Antibodies

The use of GNP–antibody conjugates was first suggested by Faulk and Taylor²¹⁹ for TEM identification of bacterial antigens. Currently, such conjugates are widely used in immunochemistry.^{1,3} In recent years, several publications have appeared describing the penetration of GNP–antibody conjugates into cancer cells, and in those studies, antibodies were employed mainly as target molecules.

Hu et al.²²⁰ compared the uptake by Panc-1 and MiaPaCa cells of gold NRs (40×14 nm) capped with PDDAC, transferrin, and antibodies developed to the cell surface antigens claudin 4 and mesothelin. Dark-field microscopy and TEM indicated that bioconjugates of NRs with transferrin and with the antibodies were taken up better than NR–PDDAC, a finding that corroborates the specific receptor-mediated nature of GNP endocytosis. Rejiya et al.²²¹ reported similar results. Using luminescence microscopy and ICP–AES, they examined the intracellular uptake by A431 cells of NRs (42×10 nm) modified with antibodies to the EGFR. The amount of nonconjugated (CTAB-capped) NRs that had entered the cellular space within 3 h proved to be 2-fold smaller than that of NR–antibody conjugates. Thus, modification of the NR surface with antibodies specific for cell-surface antigens improves the effectiveness of intracellular GNP uptake, which may prove to be useful both for targeted drug delivery and for photothermal therapy.²²²

Lapotko et al.²²³ demonstrated that 10- and 30-nm NSph's conjugated with antibodies to the CD33 receptor on the surface of K562 and AML cells accumulate in the cells more effectively than do nonconjugated GNPs. A possible explanation²²³ is that immunospecific conjugates form cell-surface clusters of ~20 particles, which is conducive to more active endocytosis. Furthermore, GNP clustering improves the effectiveness of photothermal therapy in the near-IR region, because the maximum of the clusters' plasmon resonance shifts to the longer wavelength region of the spectrum, as compared with the resonances of isolated GNPs.

Tumor cells are characterized by overexpression of EGFRs. Antibodies to these receptors also can serve for the selective entry of GNPs into tumor cells.⁶⁶ Specifically, Melancon et al.²²⁴ demonstrated that 30-nm hollow NSs complexed with anti-EGFR antibodies were effectively taken up by A431 cells in vitro and by cells of this tumor transplanted in mice, *in vivo*. In their further work,²²⁵ the authors successfully used the melanocyte-stimulating hormone, bound by the melacortin receptors of tumor cells, as a selective ligand. Marega et al.²²⁶ demonstrated that 5-nm GNPs coated with plasma-polymerized allylamine can be produced through plasma vapor deposition and can be

conjugated with a monoclonal antibody to EGFR. The resulting nanoconjugates displayed an antibody loading of ~1.7 nmol/mg and efficiently targeted EGFR-overexpressing cell lines, as ascertained by ELISA and Western blot assays. Similar results were reported by Raoof et al.²²⁷ for 10-nm GNPs coated with anti-EGFR antibodies. Such conjugates penetrated the endosomes of tumor cells, and this effect could be used in noninvasive radiofrequency-based cancer therapy.²²⁷ A new and rapidly growing field is the fabrication of multifunctional nanocarriers for anticancer drugs and the synthesis of plasmonic imaging probes to label specifically targeted cancer cells. For example, Song et al.²²⁸ fabricated GNPs conjugated with both anti-EGFR antibodies and doxorubicin.

Liu et al.²²⁹ aimed to demonstrate the potential of lymphotropic nanoparticle contrast agents designed to bind with high affinity to lymphoid cells overexpressing the CD45 antigen. To this end, 18-nm GNPs were prepared and conjugated with anti-CD45 antibodies through an optimized PEG coating to protect the particles from aggregation. By using a murine macrophage cell line as a model, the high binding affinity of the anti-CD45 nanoparticles for lymphoid cells was demonstrated in vitro. In contrast, unconjugated and nonspecific antibody-conjugated particles showed minimal nonspecific binding to the macrophage owing to the dense PEG coating. Similarly to spherical GNPs, gold NRs functionalized with anti-EGFR antibodies were taken up by CAL 27 cells much more effectively, as compared to NRs coated with chitosan oligosaccharides, PEG, PAA, PSS, or CTAB.²³⁰

In the huge arsenal of plasmonic nanoparticles being synthesized currently, gold nanocages are of special interest, because their size (~40–50 nm) is optimal for uptake into cells and also because their plasmon resonance is in the biological tissue optical window (~800 nm).³ Using two-photon luminescence and ICP–MS, Xia and co-workers²³¹ examined the intracellular uptake into U87MGwtEGFR cells of gold nanocages functionalized with PEG and with antibodies to the EGFR. Nanocage–antibody conjugates entered the cell interior by receptor-mediated endocytosis 4-fold better than did PEGylated GNPs. The endocytosis also depended on the time and temperature of incubation, the size of nanocages (35 > 50 > 90 nm), and the amount of antibody molecules immobilized on each GNP. The same group concluded²³² that, although both size and shape of nanoparticles do affect intracellular uptake—15-nm NSph's were taken up more effectively than 45-nm NSph's, 33-nm nanocages were taken up more effectively than 55-nm nanocages, and NSph's were taken up more effectively than nanocages—the major contribution to internalization is made by functionalization of the GNP surface. With SK-BR-3 cells as an example, the authors showed by ICP–MS that the effectiveness of intracellular uptake of both types of functionalized GNPs increased in the order PAA ≫ antibodies > PEG. Another interesting fact they observed²³³ was that, as shown by two-photon microscopy, U87-MG cells did not have equal amounts of nanocages at division.

4. USE OF PENETRATING PEPTIDES FOR THE DELIVERY OF GNPs INTO CELLS

Penetrating peptides are short peptides that facilitate the cellular uptake of various molecular cargoes, from small chemical molecules and nanosized particles to large DNA fragments. The cargoes are associated with the peptides either through covalent bonds or through noncovalent interactions.

As a rule, penetrating peptides have relatively high contents of positively charged amino acids, such as lysine or arginine, or they contain sequences of polar (charged) amino acids interspersed with nonpolar (hydrophobic) ones. These two types of structures are named polycationic and amphipathic, respectively.^{234,235} Peptides capable of entering cells have been isolated from proteins of various organisms, from viruses (HIV-1, SV40, adenovirus, herpes virus, influenza virus) to vertebrates.^{236–238} The penetrating peptides most commonly used in a complex with GNPs are listed in Table 3.

Table 3. Most Commonly Used Penetrating Peptides

amino acid composition	source or function
CGGGPKKKRKVGG	SV40 large T, NLS (nuclear localization signal peptide)
AAVALLPAVLLALLAP	SV40 large T, RME (receptor-mediated endocytosis peptide)
PKKKRKVAAVALLPAVLLALLAP	SV40 large T, NLS, and RME
CGGFSTSLRARKA	adenoviral, NLS
CKKKKKKSEDEYPYVPN	adenoviral, RME
CKKKKKKKSEDEYPYVPNFSTSLRARKA	adenoviral fiber protein, NLS, and RME
CGGRKKRQRRRAP	HIV 1 TAT (transactivator of transcription) protein, NLS
GRQIKIWFQNRRMKWKK	pANTN from <i>Antennapedia</i> protein from <i>Drosophila</i> , NLS
CKKKKKKGGRGDMFG	integrin binding domain and oligosyme
CALNN (CALNNR, CALND, CALNS)	GNP-stabilizing peptides

Most often, penetrating peptides are used to deliver GNPs loaded with target molecules via the cytoplasm to the cell nucleus. Pioneering work in this area was performed by Feldheim and colleagues.²³⁹ Specifically, they described the delivery into the nuclei of HepG2 cells of 20-nm GNPs coated with bovine serum albumin (BSA), which was conjugated to four penetrating peptides: CGGGPKKKRKVGG, CGGFSTSLRARKA, CKKKKKKSEDEYPYVPN, and CKKKKKKSEDEYPYVPNFSTSLRARKA. Peptide 3 facilitates receptor-mediated endocytosis, peptides 1 and 2 interact with the nucleopore complex, and peptide 4 has both mechanisms of entry. The entry of GNPs into the cells and nuclei was monitored by TEM and differential interference contrast microscopy. GNP–BSA complexes conjugated to peptides 1 and 3 entered the cells and were found in endosomes, those conjugated to peptide 2 did not enter the cells, and only those conjugated to peptide 4 entered the nuclei. However, GNPs carrying both peptides 2 and 3 were best able to enter the nuclei. Similar data were reported by Mandal et al.²⁴⁰ for 5-nm GNPs and TE85 cells. Thus, in order to achieve efficient nuclear penetration, it is necessary to use GNP conjugates with peptides (a single peptide or a complex of them) able to penetrate both through membrane receptors and through nuclear pores. In a subsequent study,²⁴¹ Feldheim's group showed that the entry of GNPs complexed with penetrating peptides depends on the type of cell, the nature of the peptide (adenovirus, SV40, or HIV-1 origin), the time of incubation, and the temperature conditions for the experiment.

Later,²⁴² the same group described the dependence of the intracellular entry of GNPs on the particle size and on the number of peptide molecules at the surface of GNP–BSA. According to ICP–AES data, the GNP uptake into HeLa cells was highest with 20-nm GNPs, lower with 15-nm GNPs, and still

lower with 10-nm GNPs. Moreover, the effectiveness of nuclear penetration depended almost directly on the number of peptide molecules present on the surface of GNPs (Table 4). Similar

Table 4. Number of GNPs per Cell, Depending on the Amount of Peptide Used (Reprinted with Permission from Ref 242; Copyright 2007 American Chemical Society)

no. peptide molecules per GNP	no. GNPs per cell	no. GNPs per cytosolic fraction	no. GNPs per nuclear fraction	% GNPs in nucleus
0 (native BSA)	3.48×10^4	1.33×10^4	8.18×10^3	37.5
30	3.52×10^4	5.22×10^3	9.23×10^3	62.5
70	1.21×10^5	1.54×10^4	7.04×10^3	82.4
80	4.97×10^5	3.21×10^4	1.73×10^5	84.4
110	1.16×10^6	4.74×10^4	9.61×10^5	95.3
130	1.80×10^6	8.97×10^4	1.47×10^6	94.2
150	5.44×10^6	1.20×10^5	3.11×10^6	96.3

results were also attained for GNP–PEG conjugated to penetrating peptides.²⁴³ Liu and Franzen²⁴⁴ showed that it is possible to use GNP-conjugated penetrating peptides for the delivery of oligonucleotides to the nuclei of HeLa cells. Ghosh et al.²⁴⁵ reported on the capacity of 3-nm GNPs complexed with a penetrating short cationic peptide, HKRK, for intracellular delivery of large protein (β -galactosidase) molecules, which under usual conditions are membrane impermeable.

de la Fuente and Berry²⁴⁶ compared the intracellular entry of GNPs with that of GNPs conjugated to TAT peptide. TEM showed that both types of 3-nm GNPs entered the cytoplasm of hTERT-BJ1 cells but that only GNPs functionalized with the penetrating peptide appeared in the cell nucleus. A similar result came from Oh et al.,²⁴⁷ in addition, the authors, using LCM, demonstrated that 2.4-nm GNP–PEG–TAT complexes were localized in the nucleus; 5.5- and 8.2-nm complexes were localized in the perinuclear space; and 16-nm complexes were localized in the cytoplasm of COS-1 cells.

Krpetić et al.²⁴⁸ found that modifying GNPs with the cell-penetrating peptide TAT enhances HeLa cell uptake and leads to an unusual distribution pattern, by which particles are found initially in the cytosol, the nucleus, and the mitochondria and later within densely filled vesicles, from which they can be released again. Once inside the cell, these particles appear to overcome intracellular membrane barriers quite freely, including the possibility of direct membrane transfer. Ultimately, in the absence of extracellular nanoparticles, the gold is completely cleared from the cells. Combined conjugation of 13-nm GNPs with penetrating and lysosomal sorting peptides was suggested by Dekiwadia et al.²⁴⁹ to minimize cytotoxic effects and ensure selective delivery of nanoparticles into cell lysosomes.

Several researchers have employed the CALNN pentapeptide and its derivatives as a penetrating peptide to conjugate with GNPs. This pentapeptide transforms citrate-stabilized GNPs to GNPs that are extremely stable in aqueous solution and have some chemical properties that are analogous to those of proteins.⁹² Nativo et al.²⁵⁰ provided TEM and ICP–AES data on the uptake of 16-nm CALNN-stabilized GNPs by HeLa cells. Citrate- and CALNN-stabilized GNPs effectively entered the cell cytoplasm and localized in endosomes, whereas GNP–PEG complexes were absent from the cells. However, when penetrating peptides (TAT, pANTN) were attached to GNP–PEG, such complexes were detected not only in the cytoplasm but also in the nuclei of the cells.

Sun et al.²⁵¹ explored the HeLa cell uptake of 30-nm GNPs coated with an arginine derivative of the CALNN peptide—CALNNRRRRRRRR (CALNNR₈). As indicated by dark-field microscopy and ICP–AES, GNPs complexed with CALNNR₈ entered the cell cytoplasm much more effectively than did those complexed with CALNN. However, the best nuclear penetration was shown by GNPs conjugated to a 1:9 CALNNR₈/CALNN mixture. Finally, it was reported recently²⁵² that, as compared with citrate-capped GNPs, GNP–CALNN conjugates were much more effective at penetration *in vivo* of the endosomes of rat liver Kupffer cells.

Penetrating peptides serve to modify not only NSph's but also NRs, NSs, and nanostars. Oyelere et al.²⁵³ modified NRs with a virus (SV40) NLS peptide. The results by dark-field microscopy and Raman spectroscopy demonstrated that such NRs entered both the cytoplasm and the nucleus of the cells much better than did CTAB-capped NRs. Furthermore, they entered the nuclei of tumor cells (HSC) much more effectively than they entered normal cells (HaCat). This fact was explained by disruption of the normal cellular processes and by damage to the nuclear membranes in the tumor cells. Accordingly, the authors discussed the possibility of using NRs modified with penetrating peptides for the diagnosis of tumors and for the delivery of target substances to the nuclei of cancer cells. Also, as early as in their subsequent work,²⁵⁴ they demonstrated that NR–peptide conjugates can enter the cell nuclei, damaging DNA, arresting cytokinesis and cell division, and, ultimately, inducing cell apoptosis.

Yuan et al.²⁵⁵ showed that TAT-peptide-functionalized gold nanostars enter cells much better than bare or PEGylated nanostars and that the major uptake mechanism involves actin-driven lipid raft-mediated macropinocytosis, in which particles accumulate primarily in macropinosomes but may also leak out into the cytoplasm. Liu et al.²⁵⁶ investigated the uptake by normal and tumorous liver cells of gold NSs conjugated to the A54 (AGKGTPSLETTP) peptide, which specifically adheres to liver tumor cells. TEM and ICP–AES data suggested that the A54-functionalized NSs were efficiently taken up into tumor cells (BEL-7404 and BEL-7402) and were not taken up into normal ones (HL-7702).

The rate of GNP uptake can also be determined by the terminal amino acid residues in the ligand shell.²⁵⁷ For example, by replacing only 5–10% of the terminal amino acids of the peptide ligands from glutamic acid to tryptophan or serine, one can dramatically increase or decrease the GNP uptake.²⁵⁷

Wang et al.²⁵⁸ showed that 20-nm KDEL-peptide-covered GNPs penetrated Sol8 cells very rapidly (within 5–15 min) and were localized only in the endoplasmic reticulum. These data indicate that the GNP–KDEL nanoconstructs are internalized via a clathrin-mediated pathway and are trafficked to the endoplasmic reticulum via a retrograde transport pathway, bypassing the lysosomal degradation pathway. Thus, this novel approach to developing nanoconstruct-based drug delivery has the potential to evade intracellular degradation, enhancing drug efficacy.

The use of cyclic peptide-coated GNPs containing tryptophan and arginine residues for intracellular delivery of antitumor drugs was proposed by Shirazi et al.²⁵⁹ Their complexes exhibited approximately 12 and 15 times higher cellular uptake than that of antitumor drugs alone in CCRF-CEM cells and SK-OV-3 cells, respectively. Recently, Yao et al.²⁶⁰ demonstrated a significant enhancement of tumor cell (HeLa-GFP) uptake of GNPs conjugated with pH (low) insertion peptide.

Thus, the use of penetrating peptides conjugated to variously sized and shaped GNPs can enhance the entry of GNPs into the cell cytoplasm and nucleus. This may become a basis for the development of diagnostic and therapeutic nanoplatforms to actively deliver target substances inside cells.²⁶¹ However, it should be considered that serum proteins can affect the transport function of penetrating peptides, decreasing the effectiveness of uptake.²⁶²

5. INTRACELLULAR UPTAKE OF OLIGONUCLEOTIDE-COATED GNPS

Currently, oligonucleotide-conjugated nanoparticles enjoy active use in molecular diagnostics, gene therapy, and vaccination methods. Therefore, the study of the mechanisms responsible for the effective delivery of genes to cells is of major importance. The study of intracellular uptake of GNPs functionalized with nucleic acids is foremost associated with the work of Mirkin's group addressed to intracellular gene regulation.²⁶³ Specifically, Giljohann et al.²⁶⁴ reported on the uptake of GNPs modified with antisense oligonucleotides (28 bases) into C-166, HeLa, and A594 cells. With ICP-MS, they examined the uptake of 13-nm GNPs functionalized with different numbers of oligonucleotide chains (from 0 to 80 per particle). It turned out that uptake of the conjugates was best in HeLa cells: 3×10^7 GNPs/cell (for comparison, uptake in C-166 cells was 1×10^7 GNPs/cell and that in A594 cells was 1×10^6 GNPs/cell). The uptake depended strongly on the density of the oligonucleotide coating on GNPs, increasing from 1×10^3 GNPs/cell for the least laden GNPs to 1.3×10^6 GNPs/cell at a load of 60–80 molecules/particle (for A594 cells). In addition, uptake efficacy increased with an increasing amount of GNP-adsorbed serum proteins in the cell growth medium and with increasing concentration of added GNPs. In another report from the same group,²⁶⁵ it was shown that, when GNPs are coated with a combination of oligonucleotides and penetrating peptides, the effectiveness of intracellular uptake increases.

Subsequently,²⁶⁶ Mirkin's group demonstrated that GNP uptake into HeLa cells is affected not only by the factors mentioned above, which influence the internalization of GNPs conjugated with different nucleic acids, but also by the nature of the adsorbate. As measured by ICP-MS, the highest uptake was shown by GNPs conjugated to double-stranded RNA; somewhat lower uptake was shown by GNPs conjugated to single-stranded DNA; and the lowest uptake was shown by BSA-conjugated GNPs (Figure 18).

Jewell et al.²⁶⁷ found that the level of GNP-oligonucleotide uptake is also affected by the methods used to attach oligonucleotides to the particle surface. They used thiol-modified oligonucleotides to conjugate with GNPs, but they also modified the GNP surface with the linkers mercapto-1-undecanesulfonate (MUS) and mercapto-1-undecanesulfonate-1-octanethiol (MUS-OT). These ligands increased substantially the effectiveness of GNP-oligonucleotide uptake by B16-F0 tumor cells (5-fold for GNP-MUS-oligonucleotide and 10-fold for GNP-MUS-OT-oligonucleotide).

Bonoiu et al.²⁶⁸ presented data for the uptake of siRNA-modified NRs by DAN cells. Dark-field microscopy and LCM indicated that such complexes were taken up by the cells much better than were native siRNAs. A similar result was obtained by Crew et al.²⁶⁹ for the transfection of 13-nm GNPs conjugated to microRNA into MM.1S cells. Guo et al.²⁷⁰ reported more effective intracellular uptake of siRNA conjugated to GNPs and polyelectrolytes, as compared to that of siRNA conjugated to

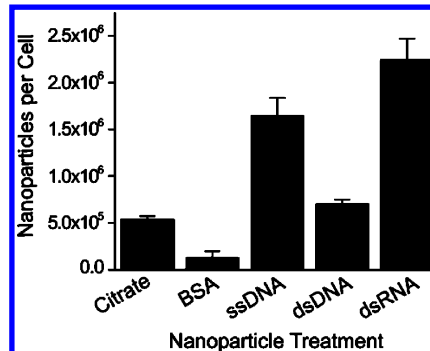


Figure 18. Quantification of HeLa cell uptake of nanoparticles after 24 h of treatment with 10-nm GNPs functionalized with various surface ligands. The mean and STD values were determined from three separate experiments. Adapted with permission from ref 266. Copyright 2010 American Chemical Society.

lipofectamine, a commercial transfection agent. A similar finding was reported by Ghosh et al.²⁷¹ for the uptake of 13-nm cysteamine-functionalized GNPs conjugated to microRNA into neuroblastoma (NGP, SH-SY5Y) and ovarian cancer (HEYA8, OVCAR8) cells.

Braun et al.²⁷² developed a gold NS functionalized with a TAT-lipid (TAT-peptide–lipid cell internalizing agent) layer for transfection and selective release of siRNA. The TAT-lipid coating mediated the cellular uptake of the nanomaterial, whereas the release of the siRNA was dependent on NIR laser pulses.

Apart from that, DNA or RNA transfection into cells is enhanced with GNPs complexed with PEI,^{186,273,274} cationic lipids,^{275,276} bacterial toxins,⁴¹ poly-L-lysine,²⁷⁷ and hyaluronic acid,²⁷⁸ or it can be enhanced with functionalized GNPs in combination with conventional transfection reagents.²⁷⁹

Elbakry et al.²⁸⁰ studied the size-dependent uptake of 20-, 30-, 50-, and 80-nm GNPs into a variety of mammalian cell lines. The GNPs were coated with nucleic acids and PEI using a layer-by-layer approach. In contrast to other studies, the optimal particle diameter for cellular uptake and the number of therapeutic cargo molecules per cell were determined. It was found that 20-nm GNPs, with diameters of ~32 nm after the coating process and ~88 nm (including the protein corona) after incubation in cell culture medium, yield the largest number of nanoparticles and therapeutic DNA molecules per cell.

6. SELECTIVE INTERNALIZATION OF ENGINEERED GNPS INTO CANCER CELLS

The GNP-internalization mechanisms discussed above are based mostly on the nonspecific interaction of nanoparticles with the cell surface and on the subsequent endocytosis of GNPs. Of major importance in current biomedicine, however, is the selective recognition of cells at the cost of interaction of functionalized GNPs with specific receptors of cells, in particular tumorous cells. Such selective interaction will allow, e.g., one to perform targeted delivery of drugs or to treat GNP-containing cells with various types of irradiation.^{281,282}

Specific receptors, in particular, include folate receptors, which are high-affinity cell receptors for folic acid and some of its derivatives. In humans, four types of receptors from this family have been described. Folate receptors ensure the delivery to cells of 5-tetrahydrofolate, a cofactor necessary for cellular proliferation. For this reason, folate receptors are targeted by anticancer therapy, since blocking of folate transport to cancer cells prevents

their further proliferation. Consequently, the use of folic acid as part of nanocomposites seems very promising for the selective interaction with tumor cells.²⁸³

Dixit et al.²⁸⁴ explored the uptake of 10-nm PEGylated GNPs functionalized with folic acid into KB tumor cells with overexpression of folate receptors. Using TEM, they showed that folic acid-conjugated GNP–PEG1500 complexes were taken up effectively by KB cells through receptor-mediated endocytosis. The uptake effectiveness decreased substantially when cell lines with low expression of folate receptors were used, when the receptors were inhibited with native folic acid, and when GNP–PEG conjugates were folate uncoated. Similar results emerged from a study by Li et al.,²⁸⁵ who used HeLa cells and 18-nm non-PEGylated GNPs capped with folate, and also from that by Tong et al.²⁸⁶ with folic acid–NR (46 × 12 nm) conjugates.

Bhattacharya et al.²⁸⁷ investigated the uptake of GNP–folate conjugates by cells of seven tumor lines. The level of uptake depended on the number of folate molecules on GNPs; in turn, this number depended on the molecular mass of the PEG conjugated to GNPs. For the conjugates used, the uptake level decreased in the sequence folate–GNP–PEG20000 > folate–GNP–PEG10000 > folate–GNP–PEG2000, in agreement with the data of Kah et al.¹⁷⁵ for NSs.

The use of folate-coated GNPs for intracellular delivery of the antitumor drug 6-mercaptopurine was proposed by Park et al.²⁸⁸ Their method enabled tumor cell (HeLa and KB) death to be increased by 20%, as compared with other drug delivery techniques.

Paciotti et al.²⁸⁹ proposed the use of TNF in complex with 26-nm GNPs for selective uptake in tumor cells *in vivo*. Shao et al.²⁹⁰ demonstrated that maximal uptake of TNF–GNP conjugates was in cancer cells (SCK), compared to no or low uptake in mouse red blood cells and white blood cells. For selective delivery to cancerous cells, Li et al.¹⁰⁸ used 20-nm GNPs conjugated to anti-EGFR aptamers, and Wang et al.⁷⁵ used GNPs conjugated to aptamers specific for mucin, which was overexpressed on the surface of cancer cells.

An interesting approach to delivering drugs to the tumor cell nucleus was put forward by Dam and co-workers.^{291,292} Gold nanostars were conjugated with an aptamer to nucleolin, a protein overexpressed in cancer cells and found both on the cell surface and in the cell interior. Owing to the aptamer–protein interaction, GNPs are delivered to the cell nucleus, after which the DNA aptamer is released from the nanostars and begins to act as a drug, causing cell death. As well as making it possible to load a large drug amount, the nanostar shape helps to concentrate light intensity near the sharp particle ends, thus enhancing light–heat conversion and facilitating drug release in these regions.

Kumar and co-workers^{293,294} suggested the use of multifunctionalized GNPs (conjugated with a combination of specific antibodies, penetrating peptides, and PEG) for intracellular delivery of GNPs and for bioimaging. Lukianova-Hleb et al.²⁹⁵ enhanced therapeutic effectiveness simultaneously with (i) gold NSs attached to anti-EGFR and (ii) liposomal doxorubicin.

Yet another important target for GNP interactions with the tumor cell surface is vascular endothelial growth factor receptors, which play a central role in angiogenesis. Mukherjee et al.²⁹⁶ presented TEM data for the preferential internalization by CLL-B cells of GNPs complexed with antibodies to vascular endothelial growth factor receptors, as compared with that of nonconjugated 5-nm GNPs. Such internalization resulted in an enhancement of tumor cell apoptosis. Kalishwaralal et al.²⁹⁷

showed that, after 50-nm GNPs had been internalized by BREC cells, they could be detected by TEM in multivesicular bodies. If the cells were incubated with GNPs conjugated to vascular endothelial growth factor, the particles were found mostly in the membrane, with only a small number of them being present in the cytoplasm. GNPs were also found to inhibit angiogenesis.

Wang et al.²⁹⁸ proposed the use of gold nanocages conjugated to the low-molecular-weight ligand SV119, which specifically interacts with sigma-2 receptors on the surface of tumor cells, as a platform for a theranostic agent. The resultant conjugate effectively entered MDA-MB-231 and PC-3 cancer cells overexpressing sigma-2 receptors. Yet another ligand that selectively interacts with tumor cells is 5-aminovaleric acid. Using LCM, Krpetić et al.²⁹⁹ demonstrated that 7-nm GNPs coated with this acid selectively penetrated into K562 cancer cells and almost did not penetrate into normal epithelial cells.

Kasten et al.³⁰⁰ fabricated 5-nm GNPs coated with a prostate-specific membrane antigen inhibitor (CTTS4). These conjugates exhibited selective, significantly higher uptake into LNCaP prostate tumor cells, as compared to the nontargeted control GNPs.

Huang et al.³⁰¹ studied the biodistribution and localization of gold NRs labeled with three types of probing molecules: (i) an scFv fragment of antibodies to the EGFR; (ii) an amino terminal fragment (ATF) peptide that recognizes the urokinase plasminogen activator receptor; and (iii) a cyclic RGD peptide that recognizes the $\alpha_5\beta_3$ integrin receptor. By dark-field microscopy and ICP–MS, the authors showed that the effectiveness of A549 cell uptake decreased in the order NR–RGD (~9000 NRs/cell) > NR–ATF (~6500 NRs/cell) > NR–scFv (~2500 NRs/cell) > NR–PEG (~100 NRs/cell). By contrast, the biodistribution data from xenograft animal models did not reveal any significant effect of active targeting on the total tumor uptake of long-circulating gold NRs, although their localization was quite different for different targeting ligands.

In a study by Song et al.,³⁰² HeLa and MCF-7 cancer cells took up more glucose-capped GNPs than naked GNPs and the uptake curve showed size- and cell-dependent uptake. The glucose-capped GNPs were mainly located in the cytoplasm, and endocytosis was concluded to be the mechanism behind the internalization of both naked and glucose-capped GNPs.

Interesting data came from Li et al.³⁰³ Five-nm GNPs conjugated with a dual ligand—folic acid and glucose—penetrated KB cells 3.9- and 12.7-fold more effectively than did GNP–folate and GNP–glucose, respectively. Thus, a definite synergistic effect of the two ligands was found. Bhattacharyya et al.³⁰⁴ also used two ligands, conjugated to 50-nm GNPs: antibodies to folate receptors and anti-EGFR antibodies (cetuximab). Evaluation of conjugate uptake into OVCAR-5 and Skov3-ip tumor cells by using TEM and neutron activation indicated that GNPs complexed with the dual ligand were internalized best, as compared with those complexed with antibodies to one receptor. The same group^{305,306} studied the mechanisms of tumor cell endocytosis of GNPs conjugated with anti-EGFR antibodies. These studies revealed an important role of the intracellular GTFases dynamin (caveolin-dependent endocytosis) and Cdc42 (pinocytosis/phagocytosis).

The use of multifunctionalized GNPs was also addressed by Hosta-Rigau et al.³⁰⁷ They suggested the conjugation of 20-nm GNPs simultaneously with an analogue of the peptide Bombesin (interacting with gastrin-releasing receptors, which are overexpressed on the cancer cell surface) and the therapeutic antitumor peptide RAF. Such complexes were found to possess high

efficacy and selectivity of uptake and also marked therapeutic activity.

Kumar et al.³⁰⁸ conjugated 2-nm GNPs also with two peptides: the peptide CRGDK, selectively binding to neuropilin-1 receptors, and the therapeutic peptide PMI (p12). As found by ICP-MS and MTT assay, the GNPs coated with the two peptides were effectively taken up by MDA-MB-321 cells, exerting a pronounced cytotoxic effect.

Heo et al.³⁰⁹ reported on effective and selective tumor uptake of GNPs conjugated to the antitumor drug paclitaxel and to biotin. Biotin interacts with the biotin receptors, which are overexpressed on the tumor cell surface. As a result, uptake of functionalized GNPs by tumor cells (HeLa, A549, and MG63) was more effective than that by normal cells (NIH3T3) and, correspondingly, cytotoxicity increased because of the larger amount of paclitaxel that had entered the cells.

Several authors have described the tumor uptake, via specific receptor-mediated endocytosis, of GNPs functionalized with antitumor drugs (daunorubicin,³¹⁰ herceptin,^{117,311} tamoxifen,³¹² doxorubicin,^{313,314} prospidine,³¹⁵ chloroquine,³¹⁶ topotecan,³¹⁷ and docetaxel³¹⁸). The ultimate goal of such studies is to increase the effectiveness of drugs already used in oncology through conjugation to GNPs. Additionally, Comenge et al.³¹⁹ demonstrated that GNPs not only act as carriers but also protect the drug from deactivation by plasma proteins until conjugates are internalized in cells and cisplatin is released. For better drug penetration of the cell nuclei, it was suggested to use small-sized (2–3 nm)³²⁰ or dextran-capped GNPs.³²¹

7. INTERACTION OF GNPS WITH IMMUNE CELLS

7.1. Immunostimulation Effects of GNPs

As noted above, the immune system cells constitute the first barrier to nanoparticle penetration of animal tissues and cells. Therefore, the study of GNP interactions with phagocytes, the mechanisms of intracellular uptake, and the responses of immune cells to GNPs is undoubtedly of major interest. Perhaps the first detailed consideration of these issues can be found in the paper by Shukla et al.,³²² who, using three microscopic methods (TEM, LCM, and AFM), examined the uptake of 3-nm GNPs into RAW264.7 macrophage cells. The conclusion from this study was that small GNPs enter macrophages through pinocytosis and get localized mostly in lysosomes and in the perinuclear space. On the whole, the data of Shukla et al. indicate that the GNPs are biocompatible, noncytotoxic, and nonimmunogenic and that they suppress the production of reactive oxygen species and do not cause elaboration of the proinflammatory cytokines TNF- α and IL1- β (which contradicts the data of Yen et al.⁷³). We emphasize that the data of Shukla et al.³²² were obtained for very small (3-nm) particles. However, Lim et al.,³²³ using much larger (60-nm) hollow NSph's capped with dextran, and Zhang et al.,³²⁴ using 60-nm GNPs, achieved results similar to the findings of Shukla et al.³²² for the same cell culture. Choi et al.³²⁵ even proposed a new method for the photothermal therapy of tumors that employs a "Trojan horse" in the form of monocytes and macrophages laden with phagocytosed gold NSs. For these purposes, Dreaden et al.³²⁶ suggested the use of GNPs conjugated with macrolide antibiotics, which can accumulate in tumor-specific macrophages and induce their cytotoxicity, causing tumor cells to die. Thus, particle size and structure in these studies were not critical to macrophage uptake.

Quite interesting data were acquired by Bastús et al.^{327,328} From their results, it follows that, indeed, 10-nm nonconjugated

GNPs, on entry into murine bone marrow macrophages, do not affect the production of proinflammatory cytokines. However, if the GNP surface is modified with the peptide AGIP (amyloid growth inhibitory peptide, LPFFD) or SAP [sweet arrow peptide, (VRLPPP)₃], GNPs, on entry into the macrophages, involve the induction of NO synthase and proinflammatory cytokines such as TNF- α , IL-1 β , and IL-6. In addition, they inhibit macrophage proliferation. The recognition of GNP-peptide conjugates was effected through toll-like receptors 4 (TLR-4) on the surface of the macrophages. Yet, Staroverov et al.³²⁹ demonstrated that both 15-nm nonconjugated GNPs and their conjugates with high- and low-molecular-weight antigens, on entry into murine peritoneal macrophages, enhance their respiratory activity. Lee et al.³³⁰ reported that the penetration of gold NRs and SiO₂-coated gold NRs into macrophages induces the release of inflammatory mediators (cytokines, prostaglandins, etc.) and the activation of immune response genes. The activation of macrophages by GNPs, found by these authors,^{327–330} can serve as a basis for the development of new vaccine adjuvants. It is important to point out that the previously found adjuvant effect of GNPs^{10,331} was recently confirmed for gold NRs.³³² This property was used to develop an experimental DNA vaccine against HIV infection that was based on NRs complexed with plasmid DNA coding for viral envelope protein (Env).³³² As in the usual cellular uptake, immunoactivity depended strongly on the particle size: 5-nm particles conjugated with disaccharides performed far better than smaller, 2-nm ones.³³³

Yet another means of activating macrophages with GNPs was proposed by Wei et al.³³⁴ For this purpose, they used 15- and 30-nm GNPs conjugated to CpG oligonucleotides. As is known, these oligonucleotides are demethylated sites of microbial DNA that can activate macrophage immune response by interacting with the TLR-9 receptors and subsequently triggering a cascade of immune response signals. The immunostimulating activity of synthetic oligonucleotides containing CpG motifs (cytosine-phosphate-guanosine) may be analogous to that of oligonucleotides from bacterial DNA.³³⁵ According to Wei et al.,³³⁴ GNP-CpG conjugates were effective in enhancing nanoparticle internalization in RAW264.7 macrophages, and they greatly increased the secretion of TNF- α and IL-6 (15-nm conjugates did so to a greater degree than 30-nm ones did). The immunostimulatory effect of GNP-CpG was much greater than that of native CpG at the same concentrations.

A recent study³³⁶ examined the influence of the size of PEGylated GNPs on the activation of the TLR-9 receptors of RAW264.7 murine macrophages by CpG oligonucleotides. GNPs with diameters of 4, 11, 19, 35, and 45 nm inhibited CpG-induced elaboration of TNF- α and IL-6 and the activity of the TLR-9 receptors. This effect was markedly size-dependent, with a peak for 4-nm GNPs, which penetrated the cells most intensively.

Massich et al.³³⁷ examined the immune response of macrophages after the phagocytosis of GNPs functionalized with polyvalent oligonucleotides. The effectiveness of uptake and the level of interferon production were found to depend on the density of DNA molecules on the GNP surface. Kim et al.³³⁸ showed that the uptake effectiveness of oligonucleotide-functionalized GNPs differs for cells isolated from peripheral blood (mononuclear cells) and those introduced into a 293T culture. In addition, only in the first type of cell did the uptake of GNP conjugates activate the expression of immune response genes.

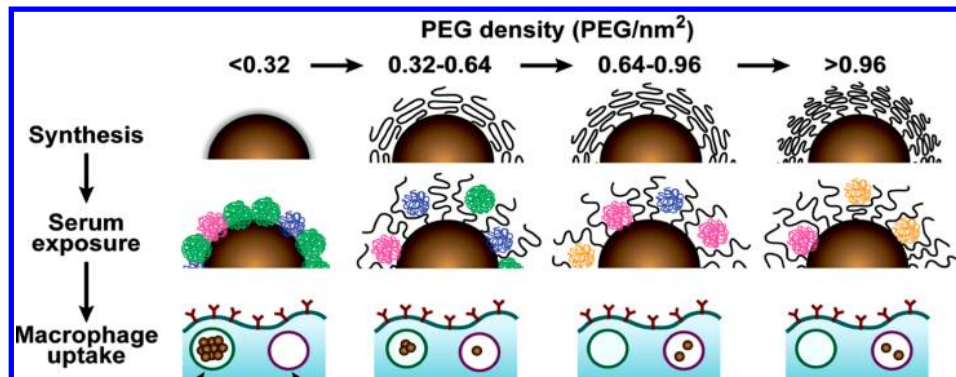


Figure 19. Scheme for the influence of the PEG coating density on the adsorption of serum proteins to GNPs and their subsequent uptake by macrophages. Reprinted with permission from ref 339. Copyright 2012 American Chemical Society.

A recent article by Walkey et al.³³⁹ described a thorough study of the effect of coating GNPs with serum proteins and PEG on macrophage uptake (Figure 19). The authors studied the adsorption of 70 blood serum proteins to PEG-coated GNPs with different densities of PEG coating.

Increasing the PEG coating density reduced serum protein adsorption and changed the composition of the adsorbed protein layer (Figure 19). Particle size also affected serum protein adsorption through a change in the steric interactions between the PEG molecules. Both the density of PEG molecules on the GNP surface and the size of GNPs determined the mechanism and effectiveness of macrophage uptake, possibly because of regulation of the composition of adsorbed blood serum proteins and their availability to cells. If the density of PEG coating was lower than ~0.16 PEG molecules/nm², the macrophage uptake of GNPs depended on the presence of adsorbed proteins (serum-dependent uptake). If the density was higher than ~0.64 PEG molecules/nm², there was serum-independent uptake. Serum-dependent uptake was more effective than serum-independent uptake, apparently because of the difference in the energy of the GNP–cell interaction. Interestingly, serum-independent uptake was more effective for large GNPs (90 nm), and serum-dependent uptake was more effective for 50-nm GNPs.

Liu et al.³⁴⁰ showed that PEGylated GNPs were internalized more quickly by lipopolysaccharide-activated RAW264.7 cells than by unstimulated cells, reaching saturation within 24 h. The PEGylated GNPs enhanced LPS-induced production of NO and IL-6 and inducible nitric oxide synthase expression in RAW264.7 cells, partly by activating p38 mitogen-activated protein kinases and nuclear factor- κ B pathways.

García et al.³⁴¹ studied the cellular uptake of GNPs with or without exposure of cells to Latrunculin-A, a phagocytosis inhibitor. The results indicate a size dependence of the internalization mechanisms for macrophage (THP-1) cells. The internalization of larger GNPs (15 and 35 nm) was blocked in the presence of Latrunculin-A, although they could attach to the cell membrane. Smaller GNPs (5 nm), though, were not blocked by actin-dependent processes.

Of considerable interest are studies on the uptake of GNPs by other cells of the immune system, in particular dendritic cells. In the past decade, dendritic cells have attracted increased interest owing to the ease of their isolation from peripheral blood monocytes and to their ability to effectively present antigens to T cells. By now, a great deal of work has been done on the modulation of immune response in patients with chronic infections and oncological diseases by using antigen-primed

dendritic cells.³⁴² Among other carriers, GNPs proved to be useful for antigen delivery to dendritic cells. For example, Cheung et al.³⁴³ described the use of 15-nm GNPs for presenting to dendritic cells a peptide antigen associated with Epstein–Barr virus. According to TEM data, peptide-functionalized GNPs penetrated into the dendritic cell cytoplasm but were not found in the nuclei. The uptake of GNPs by dendritic cells resulted in an increased content of γ -interferon, the presentation by major histocompatibility complex I (MHC-I) of the antigen to CD4+ T cells, and, correspondingly, activation of an epitope-specific immune response by cytotoxic T cells.

Cruz et al.³⁴⁴ addressed dendritic cell uptake of and immune response activation by 13-nm GNPs conjugated to prostate cancer peptide antigens. By TEM, LCM, and flow cytometry, GNPs functionalized with the peptides and with the Fc fragments of IgG were shown to interact with the Fc γ receptors of dendritic cells and to be distributed diffusely over the cytoplasm. Internalization of antigen-conjugated GNPs in dendritic cells brought about an increase in the immune response, as compared with the effect obtained from the use of the native antigen (enhanced lymphocyte proliferation). Such an approach, in the authors' opinion, opens up the way to create an effective system for the development of antitumor and other vaccines.

Villiers et al.³⁴⁵ reported on the effect of 10-nm non-antigen-functionalized GNPs on the immune functions of dendritic cells. From their findings, the GNPs that had entered cell endosomes were not cytotoxic and did not affect the production of the proinflammatory cytokine IL-6. However, they did promote the secretion of interleukin IL-12p70, which is directly involved in the activation of T cells and, thus, in the regulation of an antigen-specific immune response. Villiers et al. also noted the development of long dendrites and an increase in the cell-surface amount of MHC-II molecules, which present antigens to T lymphocytes. Thus, even nonfunctionalized GNPs are immunostimulatory to both dendritic cells and macrophages.⁷³

Ye et al.³⁴⁶ used TEM and flow fluorocytometry to quantify the uptake of gold NRs by dendritic cells and the particle effect on their functions. Compared to spherical GNPs, gold NRs entered dendritic cells more effectively and induced higher expression of CD86 immunostimulatory molecules, which are characteristic of dendritic cells.

Lin et al.³⁴⁷ reported that GNPs in complex with peptides derived from tumor-associated antigens are taken up effectively by dendritic cells. Moreover, dendritic cells take up GNPs with minimal toxicity and can process the vaccine peptides on the particles to stimulate cytotoxic T lymphocytes. A high peptide density on the GNP surface can stimulate cytotoxic T

lymphocytes better than can free peptides. Thus, GNPs have great potential as carriers for various vaccine types.

To estimate the functional impact of GNPs on B-lymphocytes, Sharma et al.³⁴⁸ treated a murine B-lymphocyte cell line (CH12.LX) with 10-nm citrate-stabilized GNPs. This treatment activated an NF- κ B-regulated luciferase reporter, and this activation correlated with the altered B lymphocyte function (i.e., with increased antibody expression). According to TEM images, GNPs could penetrate the cellular membrane and, therefore, could interact with the intracellular components of the NF- κ B signaling pathway.

Bartneck and co-workers^{349,350} reported on the interaction of GNPs with human neutrophil granulocytes, monocytes, and macrophages. On the basis of their study, involving variously shaped and sized particles, the mechanism of nanoparticle trapping can be classified as macropinocytosis rather than phagocytosis. Particle shape was found to affect strongly the particle trapping by the immune system cells; specifically, CTAB-coated gold NRs (50×15 nm) could be trapped faster than CTAB-coated gold NSph's (15 and 50 nm). Replacing CTAB by poly(ethylene oxide) greatly reduced uptake effectiveness for both types of GNPs. Nanoparticle uptake by the immune cells was accompanied by activation of the genes of proinflammatory cytokines and by a corresponding change in the cell phenotype. A characteristic fact is that the “professionally” phagocytic cells took up GNPs 2 orders of magnitude more effectively than did, e.g., HeLa cells. In addition, the authors revealed an alternative elimination mechanism whereby GNPs can be cleared from peripheral blood via an extracellular network (“trap”) produced by neutrophil granulocytes.

The same group presented data³⁵¹ on the uptake of GNPs into various cells of the reticuloendothelial system: monocytes, macrophages, immature and mature dendritic cells, and endothelial cells. The greatest uptake ability was demonstrated by macrophages, endothelial cells, and immature dendritic cells. Positively charged GNPs penetrated into cells of the reticuloendothelial system more effectively. Moreover, GNPs intensified the induction of several cytokines, including γ -interferon, IL-8 (both in dendritic cells and in macrophages), IL-1 β , and IL-6 (only in dendritic cells). Interestingly, in mature dendritic cells, GNPs accumulate in the MHC-II compartment; consequently, they may affect antigen processing.

7.2. Immune Cell Receptors Involved in the Interaction with GNPs

Phagocytic cells of the immune system have a multitude of various receptors on their surface, through which they bind and take up foreign material. Six types of phagocytosis receptors are differentiated: (i) mannose receptors (or C-type lectin receptors); (ii) integrins (the complement receptors); (iii) Fc receptors (Ig receptors); (iv) LRR receptors (or CD14, LPS receptors); (v) scavenger receptors (receptors of sialic acid derivatives); and tyrosine kinase receptors.³⁵² Unlike these, toll-like receptors are not directly involved in the uptake of foreign material; however, they do take part in the regulation of phagosome formation and in inflammatory reactions.³⁵³

As shown above, interactions with various types of receptors and, consequently, various types of GNP endocytosis depend in many ways on nanoparticle size and shape but especially on surface functionalization (including opsonization by proteins from the culture medium or blood plasma³⁵⁴) and on the presence of mannose-containing polysaccharides on the GNP surface.³⁵⁵ Some researchers believe that the key role in

macrophage uptake of GNPs is played by scavenger receptors (SRs),^{356,357} which are involved mainly in the endocytosis of apoptotic cells and which, unlike other macrophage receptors, release no proinflammatory cytokines.

More specifically, Patel et al.³⁵⁸ demonstrated that the mammalian cell uptake of GNPs functionalized with polyvalent oligonucleotides is mediated primarily by SRs. Cell preincubation with fucoidan and polyinosinic acid, which are agonists for these receptors, decreased the level of uptake by 60% (Figure 20). However, baflomycin A1 and methyl- β -cyclodextrin did not

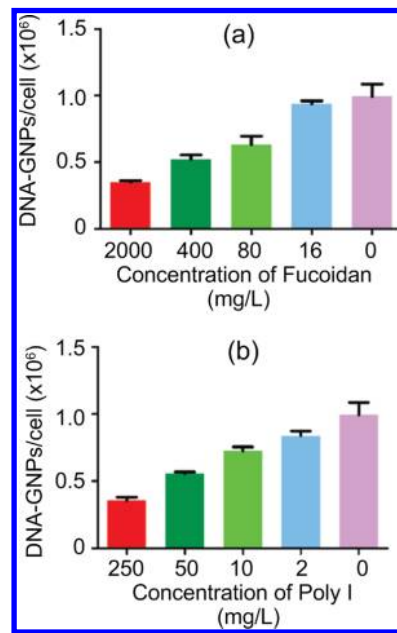


Figure 20. Cellular endocytosis of GNPs is mediated by scavenger receptors. Cell preincubation with fucoidan (a) and polyinosinic acid (b), which are agonists for these receptors, decreased the level of uptake by 60%. Adapted with permission from ref 358. Copyright 2010 American Chemical Society.

inhibit GNP uptake, because these pharmacological agents inhibit other modes of cellular entry. Coating of GNP conjugates with serum proteins also reduced uptake effectiveness.

An in-depth study on the involvement of scavenger receptors in macrophage uptake of GNPs was published by França et al.³⁵⁹ Their data show that macrophages take up opsonized GNPs through SR-mediated pathways (both 30- and 150-nm GNPs), as well as through clathrin- and caveolin-dependent pinocytosis (only 30-nm GNPs). Thus, the smaller (30-nm) particles use a broader range of internalization routes, in contrast to the larger (150-nm) GNPs. Noteworthy is the fact that, as demonstrated by inhibition analysis, phagocytosis began with an interaction of GNPs with scavenger receptors and was not attended by induction of proinflammatory cytokines.

8. CONCLUDING REMARKS

Without doubt, the use of various nanoparticles, including GNPs, to deliver genetic, medicinal, or other materials into cells is a leading trend in current nanobiotechnology and its biomedical applications. The data available on the cellular uptake of GNPs are still insufficient to gain a complete understanding of the physical chemistry and biology of endocytosis and its dependence on particle parameters and cell type. Nevertheless, the information presented in this review leads to several conclusions,

which have been confirmed in independent experiments by different research groups and also in existing theoretical models.

(1) The cellular uptake of spherical GNPs is a receptor-mediated process, the effectiveness of which depends on the size of particles and on the density of ligand coating. Most experimental data accrued for colloidal gold particles confirm the existence of an optimal diameter range (30–50 nm), whereas the specific optimal size for uptake may depend on cell type. It seems likely that the inner structure of spherical gold particles (and, in particular, their average density) has no large role; therefore, gold NSs are amenable to the same regularities concerning size dependence as the usual GNPs. Specifically, 60-nm NSs are taken up by cells better than are larger, 110-nm particles, and among NSs with outer diameters of 130–250 nm, the smallest particles are the best to take up. It is remarkable that, in all experimental cases, optimally sized NSPh's enter cells more effectively than large NSs. The effectiveness of GNP endocytosis also depends on the time and temperature of incubation and on the concentration of GNPs used.³⁶⁰ According to current theoretical models, the universal character of endocytosis can be expressed in terms of phase diagrams, which relate uptake efficiency to the particle size and aspect ratio and to the ligand surface density (Figures 7 and 8).

(2) With an increase in the particle aspect ratio, the effectiveness of GNP uptake into cells decreases; the exocytosis time may also decrease. The theoretical data for thick NRs with diameters of 50–60 nm are in harmony with experimental data; for thinner NRs, however, theory predicts a more complex dependence on particle shape. Because the size, shape, and surface functionalization of nonspherical particles can change cellular uptake, additional experimental and theoretical studies are required to elucidate the dependence of endocytosis on particle shape only, with all other factors being equal. The importance of such work is determined also by the specific peculiarity of uptake of CTAB-coated NRs into tumor cell mitochondria followed by cell apoptosis, which has not been observed for gold NSPh's.

(3) Functionalization of gold NSPh's with PEG molecules reduces the effectiveness of endocytosis, possibly because of the switching of GNP uptake from receptor-mediated pathways to other mechanisms. A similar effect was recorded for NSs and NRs as well, with uptake effectiveness diminishing with increasing surface density of PEG. The dependence of GNP uptake on the molecular mass of PEG is nonmonotonic and calls for further studies. Evidence shows that PEGylated NRs enter tumor cells an order of magnitude more actively than do PEGylated NSs, but both particle types accumulate in liver cells in approximately the same amounts. This property is important for the use of GNPs in photothermal therapy.

(4) Although the effect of surface functionalization of GNPs on their intracellular uptake has been studied for a wide variety of molecules, it seems that, in one way or another, all data reflect the influence of the principal factor—the surface charge of particles. On the whole, it should be considered proven that the best uptake is observed for particles coated with positively charged polymers, as compared to those coated with negatively charged and neutral polymers. Apart from the positive charge value itself, the chemical nature of the coating polymer also may be important, as shown for uptake of NRs capped with quaternary amines (CTAB and PDDAC, effective uptake) and primary amines (PAH, less effective uptake).

(5) In further work with functionalized GNPs, it is important to account for the role of the protein components of the medium

used for cell culturing or of blood serum. It was shown that surface hydrophobicity is a critical factor for controlling serum protein binding, which in turn decreases the cellular uptake of GNPs.³⁶¹ Protein adsorption may strongly interfere with the influence of the polymers used to coat functionalized particles. Specifically, culture-medium serum proteins may affect the transport function of penetrating peptides, reducing the uptake effectiveness. Overall, though, the existing data attest to elevated uptake of particles coated with penetrating peptides into the cell cytoplasm and nucleus. For nanoparticle functionalization with oligonucleotides, an opposite effect was observed: the uptake increased with increasing serum protein concentration in the medium. On the whole, however, the basic parameter for conjugates of this type is the density of the surface oligonucleotide coating, a change in which may cause uptake effectiveness to change by 3 orders of magnitude.

(6) Functionalization of GNPs with molecular vectors to tumor cell receptors leads to a marked enhancement of uptake into target cells and is, undoubtedly, a promising direction for the delivery of antitumor drugs inside cells. However, this question deserves additional studies, as recent reexamination of biodistribution data from xenograft animal models did not reveal any significant effect of active targeting on the total tumor uptake of long-circulating gold NRs, although their localization was quite different for different targeting ligands.³⁰¹ It should also be admitted that, in this area, GNPs compete strongly with biodegradable and other biocompatible carriers.

(7) Interestingly, GNP uptake into cells of the immune system activates the production of proinflammatory cytokines, a finding that indicates directly that GNPs are immunostimulatory. The activation of immune cells by GNPs, shown by several authors, may serve as a basis to develop new vaccine adjuvants. As in the case of the usual cells, interactions with various types of receptors on the surface of immune cells and, correspondingly, various types of GNP endocytosis depend largely on the surface functionalization of GNPs. Many researchers believe that the key role in macrophage uptake of GNPs is played by scavenger receptors. However, the interaction of functionalized GNPs with cells of the immune system is still far from being understood in more or less detail and requires further study.

(8) As justly noted by Canton and Battaglia,⁴⁹ it is hardly probable that there will emerge an all-purpose nanocarrier for all types of cargoes. Rather, the type of carrier should be optimized for both the payload to be carried and the biological target. In particular, for biosensorics and bioimaging, the optical properties of GNPs and the valence properties of surface ligands are most important. For therapy and drug delivery, the stability of conjugates in the bloodstream and their weak interaction with nontarget and immune cells should be combined with effective uptake and accumulation in targets. Perhaps these goals could be achieved with nanoscale systems, whose properties can be switched and activated dynamically on demand. For example, one can expect rapid progress in the development of multifunctional nanocomposites, combining controllable physical properties (magnetic, optical, photodynamic, radioactive, etc.) with advantages in the molecular surface targeting to meet the emerging theranostic demands.

(9) Sensitive and reliable determination of GNPs in cells or tissues is key when GNP uptake and biodistribution over different organs, cells, or cellular compartments are assessed. Although various techniques with labeled and label-free GNPs have been developed, tested, and applied to GNP quantification, only a few of them can be recommended as best compromises

between statistically sound and unbiased estimations on the one hand and preparative and measuring complexity on the other. Specifically, ICP–MS and ICP–AES are most suitable for sensitive determination of the total gold content in a cell or a tissue sample, provided that the sampling procedures are properly optimized. For example, simply mixing GNPs with cell suspensions may lead to significant errors owing to aggregation of GNPs before their intracellular uptake. At present, only TEM in combination with stereology sampling principles enables statistically reliable estimation of GNPs with high resolution at the cell compartment level.

(10) Although the ICP–MS technique is sensitive and reliable, there are serious problems associated with extrapolating from ICP–MS data to estimate GNP number per cell. On the one hand, such extrapolation depends on the particle size and shape distribution model assumptions. On the other hand, assessing the number of cells in which the estimated number of GNP resides is a difficult task. Clearly, both factors can lead to an unwanted bias in the ultimate results for individual cellular uptake. It should be emphasized that some of the estimates of GNP number per cell presented in this review (see, e.g., Table 4, Figure 18, and Figure 20) are several orders higher than those shown in Figures 2 and 4, which are more consistent with the results obtained by unbiased TEM/stereology approaches. One may assume that the potential systematic bias of any particular method is the same across all experimental groups. Therefore, it would be reasonable to use the GNP-per-cell data in a comparative manner within a particular study, as the experimental conditions can be quite different. For example, the data of Figure 2 were obtained after 6 h of incubation of cells with GNPs,⁵⁵ whereas the data shown in Figure 4⁷⁵ correspond to 1.5 h of incubation. Similarly, Mirkin and co-workers^{266,358} measured GNP uptake after 24 h of incubation, whereas Ryan et al.²⁴² (Table 4) used 6 h of incubation in combination with penetrating peptides. In any case, this important question deserves further study.

AUTHOR INFORMATION

Corresponding Author

*Phone: +78453970403. Fax: +78452970383. E-mails: dykman@ibppm.sgu.ru (L.A.D.), khlebtsov@ibppm.sgu.ru (N.G.K.).

Notes

The authors declare no competing financial interest.

Biographies



Dr. Lev A. Dykman is a lead researcher at the Immunochemistry Laboratory of the Russian Academy of Sciences' Institute of

Biochemistry and Physiology of Plants and Microorganisms. He has published over 280 scientific works, including two monographs on colloidal gold nanoparticles. His current research interests are in immunochemistry, fabrication of gold nanoparticles, and their applications to biological and medical studies. In particular, his research is focused on the interaction of nanoparticles and conjugates with immunocompetent cells and on the delivery of engineered particles to target organs, tissues, and cells.



Professor Nikolai G. Khlebtsov is head of the Nanobiotechnology Laboratory at the Russian Academy of Sciences' Institute of Biochemistry and Physiology of Plants and Microorganisms. He also heads the *kafedra* (a division in the department) of Biophysics at Saratov State University. He has published over 350 scientific works, including two monographs and five book chapters. His current research interests are in biophotonics and nanobiotechnology of plasmon-resonant particles, biomedical applications of metal nanoparticles, static and dynamic light scattering by small particles and clusters, and programming and computer simulation of light scattering and absorption by various metal and dielectric nanostructures. Professor Khlebtsov also serves as associate editor for the *Journal of Quantitative Spectroscopy and Radiative Transfer*.

ACKNOWLEDGMENTS

We acknowledge support from the Russian Foundation for Basic Research (Grants 13-02-12413, 12-04-00629-a, 12-02-00379-a, 11-02-00128-a, and 13-02-12413), the Russian Academy of Sciences Presidium Programs “Basic Sciences for Medicine” and “Basic Technologies for Nanostructures and Nanomaterials”, and the Government of the Russian Federation (Grant No. 11.G.34.31.0030 to support research projects supervised by lead scientists at Russia’s institutions of higher learning). We also thank Mr. D. N. Tychinin (IBPPM RAS) for his help in preparation of the manuscript.

REFERENCES

- Dreaden, E. C.; Alkilany, A. M.; Huang, X.; Murphy, C. J.; El-Sayed, M. A. *Chem. Soc. Rev.* **2012**, *41*, 2740.
- Sau, T. P.; Goia, D. In *Fine Particles in Medicine and Pharmacy*; Matijević, E., Ed.; Springer: New York, 2012; pp 101–145.
- Dykman, L. A.; Khlebtsov, N. G. *Chem. Soc. Rev.* **2012**, *41*, 2256.
- Mayer, K. M.; Hafner, J. H. *Chem. Rev.* **2011**, *111*, 3828.
- Kennedy, L. C.; Bickford, L. R.; Lewinski, N. A.; Coughlin, A. J.; Hu, Y.; Day, E. S.; West, J. L.; Drezek, R. A. *Small* **2011**, *7*, 169.
- Duncan, B.; Kim, C.; Rotello, V. M. *J. Controlled Release* **2010**, *148*, 122.
- Vigderman, L.; Zubarev, E. R. *Adv. Drug Delivery Rev.* **2013**, *65*, 663.
- Kumar, A.; Zhang, X.; Liang, X.-J. *Biotechnol. Adv.* **2013**, *31*, 593.
- Pissuwan, D.; Niidome, T.; Cortie, M. B. *J. Controlled Release* **2011**, *149*, 65.

- (10) Dykman, L. A.; Staroverov, S. A.; Bogatyrev, V. A.; Shchyogolev, S. Y. *Nanotechnol. Russia* **2010**, *5*, 748.
- (11) Bhattacharya, R.; Mukherjee, P. *Adv. Drug Delivery Rev.* **2008**, *60*, 1289.
- (12) Stern, S. T.; Hall, J. B.; Yu, L. L.; Wood, L. J.; Paciotti, G. F.; Tamarkin, L.; Long, S. E.; McNeil, S. E. *J. Controlled Release* **2010**, *146*, 164.
- (13) Brown, C. L.; Whitehouse, M. W.; Tiekkari, E. R. T.; Bushell, G. R. *Inflammopharmacology* **2008**, *16*, 133.
- (14) Chen, X. *Theranostics* **2011**, *1*, 1.
- (15) Warner, S. *Scientist* **2004**, *18*, 38.
- (16) Kelkar, S. S.; Reineke, T. M. *Bioconjug. Chem.* **2011**, *22*, 1879.
- (17) Funkhouser, J. *Curr. Drug Discov.* **2002**, *2*, 17.
- (18) Picard, F. J.; Bergeron, M. G. *Drug Discov. Today* **2002**, *7*, 1092.
- (19) Loo, C.; Lin, A.; Hirsch, L.; Lee, M.-H.; Barton, J.; Halas, N.; West, J.; Drezek, R. *Technol. Cancer Res. Treat.* **2004**, *3*, 33.
- (20) Lapotko, D.; Lukianova, E.; Oraevsky, A. *Lasers Surg. Med.* **2006**, *38*, 631.
- (21) Hleb, Y.; Hafner, J. H.; Myers, J. N.; Hanna, E. Y.; Rostro, B. C.; Zhdanok, S. A.; Lapotko, D. O. *Nanomedicine (Lond.)* **2008**, *3*, 647.
- (22) Lukianova-Hleb, E.; Hanna, E. Y.; Hafner, J. H.; Lapotko, D. O. *Nanotechnology* **2010**, *21*, 085102.
- (23) Alkilany, A.; Murphy, C. *J. Nanopart. Res.* **2010**, *12*, 2313.
- (24) Thakor, A. S.; Jokerst, J.; Zavaleta, C.; Massoud, T. F.; Gambhir, S. *Nano Lett.* **2011**, *11*, 4029.
- (25) Khlebtsov, N. G.; Dykman, L. A. *Chem. Soc. Rev.* **2011**, *40*, 1647.
- (26) Sabella, S.; Galeone, A.; Vecchio, G.; Cingolani, R.; Pompa, P. P. *J. Nanosci. Lett.* **2011**, *1*, 145.
- (27) Yokel, R.; Grulke, E.; MacPhail, R. *WIREs Nanomed. Nanobiotechnol.* **2013**, *5*, 346.
- (28) Scott, G. B.; Williams, H. S.; Marriott, P. M. *Br. J. Exp. Pathol.* **1967**, *48*, 411.
- (29) Singer, J. M.; Adlersberg, L.; Sadek, M. *J. Reticuloendothel. Soc.* **1972**, *12*, 658.
- (30) Hardonk, M. J.; Harms, G.; Koudstaal, J. *Histochemistry* **1985**, *83*, 473.
- (31) Renaud, G.; Hamilton, R. L.; Havel, R. *Hepatology* **1989**, *9*, 380.
- (32) Sadauskas, E.; Wallin, H.; Stoltenberg, M.; Vogel, U.; Doering, P.; Larsen, A.; Danscher, G. *Part. Fibre Toxicol.* **2007**, *4*, 10.
- (33) Sadauskas, E.; Danscher, G.; Stoltenberg, M.; Vogel, U.; Larsen, A.; Wallin, H. *Nanomedicine* **2009**, *5*, 162.
- (34) Xu, Z. P.; Zeng, Q. H.; Lu, G. Q.; Yu, A. B. *Chem. Eng. Sci.* **2006**, *61*, 1027.
- (35) Unfried, K.; Albrecht, C.; Klotz, L.-O.; von Mikecz, A.; Grether-Beck, S.; Schins, R. P. F. *Nanotoxicology* **2007**, *1*, 52.
- (36) Sperling, R. A.; Gil, P. R.; Zhang, F.; Zanella, M.; Parak, W. J. *Chem. Soc. Rev.* **2008**, *37*, 1896.
- (37) Roca, M.; Haes, A. *J. Nanomedicine (Lond.)* **2008**, *3*, 555.
- (38) Boisselier, E.; Astruc, D. *Chem. Soc. Rev.* **2009**, *38*, 1759.
- (39) Giljohann, D. A.; Seferos, D. S.; Daniel, W. L.; Massich, M. D.; Patel, P. C.; Mirkin, C. A. *Angew. Chem., Int. Ed.* **2010**, *49*, 3280.
- (40) Chithrani, B. D. *Mol. Membr. Biol.* **2010**, *27*, 299.
- (41) Lévy, R.; Shaheen, U.; Cesbron, Y.; Sée, V. *Nano Rev.* **2010**, *1*, 10.
- (42) Verma, A.; Stellacci, F. *Small* **2010**, *6*, 12.
- (43) Johnston, H. J.; Hutchison, G.; Christensen, F. M.; Peters, S.; Hankin, S.; Stone, V. *Crit. Rev. Toxicol.* **2010**, *40*, 328.
- (44) Chithrani, B. D. *Insciences J.* **2011**, *1*, 115.
- (45) Jiang, X.-M.; Wang, L.-M.; Chen, C.-Y. *J. Chin. Chem. Soc.* **2011**, *58*, 273.
- (46) Cobley, C. M.; Chen, J.; Cho, E. C.; Wang, L. V.; Xia, Y. *Chem. Soc. Rev.* **2011**, *40*, 44.
- (47) Chou, L. Y. T.; Ming, K.; Chan, W. C. W. *Chem. Soc. Rev.* **2011**, *40*, 233.
- (48) Zhao, F.; Zhao, Y.; Liu, Y.; Chang, X.; Chen, C.; Zhao, Y. *Small* **2011**, *7*, 1322.
- (49) Canton, I.; Battaglia, G. *Chem. Soc. Rev.* **2012**, *41*, 2718.
- (50) Podkolodnaya, O. A.; Ignatjeva, E. V.; Podkolodnyy, N. L.; Kolchanov, N. A. *Biol. Bull. Rev.* **2012**, *2*, 279.
- (51) Albanese, A.; Tang, P. S.; Chan, W. C. W. *Annu. Rev. Biomed. Eng.* **2012**, *14*, 1.
- (52) Zhu, M.; Nie, G.; Meng, H.; Xia, T.; Nel, A.; Zhao, Y. *Acc. Chem. Res.* **2013**, *46*, 622.
- (53) Cheng, L.-C.; Jiang, X.; Wang, J.; Chen, C.; Liu, R.-S. *Nanoscale* **2013**, *5*, 3547.
- (54) *Intracellular Delivery: Fundamentals and Applications*; Prokop, A.; Springer: New York, 2011.
- (55) Chithrani, B. D.; Ghazani, A. A.; Chan, W. C. W. *Nano Lett.* **2006**, *6*, 662.
- (56) Yang, P.-H.; Sun, X.; Chiu, J.-F.; Sun, H.; He, Q.-Y. *Bioconjug. Chem.* **2005**, *16*, 494.
- (57) Mukherjee, S.; Ghosh, R. N.; Maxfield, F. R. *Physiol. Rev.* **1997**, *77*, 759.
- (58) Gao, H.; Shi, W.; Freund, L. B. *Proc. Natl. Acad. Sci. U.S.A.* **2005**, *102*, 9469.
- (59) Boraschi, D.; Costantino, L.; Italiani, P. *Nanomedicine (Lond.)* **2012**, *7*, 121.
- (60) Chithrani, B. D.; Stewart, J.; Allen, C.; Jaffray, D. A. *Nanomedicine* **2009**, *5*, 118.
- (61) Krpetić, Z.; Porta, F.; Caneva, E.; Dal Santo, V.; Scarì, G. *Langmuir* **2010**, *26*, 14799.
- (62) Banerji, S. K.; Hayes, M. A. *Langmuir* **2007**, *23*, 3305.
- (63) Xia, T.; Rome, L.; Nel, A. *Nat. Mater.* **2008**, *7*, 519.
- (64) Taylor, U.; Klein, S.; Petersen, S.; Kues, W.; Barcikowski, S.; Rath, D. *Cytom. Part A* **2010**, *77*, 439.
- (65) Chithrani, B. D.; Chan, W. C. W. *Nano Lett.* **2007**, *7*, 1542.
- (66) Jiang, W.; Kim, B. Y. S.; Rutka, J. T.; Chan, W. C. W. *Nat. Nanotechnol.* **2008**, *3*, 145.
- (67) Copland, J. A.; Egahedari, M.; Popov, V. L.; Kotov, N.; Mamedova, N.; Motamedi, M.; Oraevsky, A. A. *Mol. Imaging Biol.* **2004**, *6*, 341.
- (68) Albanese, A.; Chan, W. C. W. *ACS Nano* **2011**, *5*, 5478.
- (69) Kneipp, J.; Kneipp, H.; McLaughlin, M.; Brown, D.; Kneipp, K. *Nano Lett.* **2006**, *6*, 2225.
- (70) Mustafa, T.; Watanabe, F.; Monroe, W.; Mahmood, M.; Xu, Y.; Saeed, L. M.; Karmakar, A.; Casciano, D.; Ali, S.; Biris, A. S. J. *Nanomedic. Nanotechnol.* **2011**, *2*, 118.
- (71) Mironava, T.; Hadjiahyrou, M.; Simon, M.; Jurukovski, V.; Rafailovich, M. H. *Nanotoxicology* **2010**, *4*, 120.
- (72) Sonavane, G.; Tomoda, K.; Sano, A.; Ohshima, H.; Terada, H.; Makino, K. *Colloids Surf, B* **2008**, *65*, 1.
- (73) Yen, H.-J.; Hsu, S.-h.; Tsai, C.-L. *Small* **2009**, *5*, 1553.
- (74) Coradeghini, R.; Gioria, S.; García, C. P.; Nativo, P.; Franchini, F.; Gilliland, D.; Ponti, J.; Rossi, F. *Toxicol. Lett.* **2013**, *217*, 205.
- (75) Wang, S.-H.; Lee, C.-W.; Chiou, A.; Wei, P.-K. *J. Nanobiotechnology* **2010**, *8*, 33.
- (76) Rieznichenko, L. S.; Shpyleva, S. I.; Gruzina, T. G.; Dybkova, S. N.; Ulberg, Z. R.; Chekhun, V. F. *Rep. Natl. Acad. Sci. Ukraine* **2010**, *2*, 170 (in Ukrainian).
- (77) Sabella, S.; Brunetti, V.; Vecchio, G.; Galeone, A.; Maiorano, G.; Cingolani, R.; Pompa, P. P. *J. Nanopart. Res.* **2011**, *13*, 6821.
- (78) Coulter, J. A.; Jain, S.; Butterworth, K. T.; Taggart, L. E.; Dickson, G. R.; McMahon, S. J.; Hyland, W. B.; Muir, M. F.; Trainor, C.; Hounsell, A. R.; O'Sullivan, J. M.; Schettino, G.; Currell, F. J.; Hirst, D. G.; Prise, K. M. *Int. J. Nanomed.* **2012**, *7*, 2673.
- (79) Freese, C.; Ubaldi, C.; Gibson, M. I.; Unger, R. E.; Weksler, B. B.; Romero, I. A.; Couraud, P.-O.; Kirkpatrick, C. *J. Part. Fibre Toxicol.* **2012**, *9*, 23.
- (80) Cui, L.; Zahedi, P.; Saraceno, J.; Bristow, R.; Jaffray, D.; Allen, C. *Nanomedicine* **2013**, *9*, 264.
- (81) Trono, J. D.; Mizuno, K.; Yusa, N.; Matsukawa, T.; Yokoyama, K.; Uesaka, M. *J. Radiat. Res.* **2011**, *52*, 103.
- (82) Zhou, R.; Zhou, H.; Xiong, B.; He, Y.; Yeung, E. S. *J. Am. Chem. Soc.* **2012**, *134*, 13404.
- (83) Shan, Y.; Ma, S.; Nie, L.; Shang, X.; Hao, X.; Tang, Z.; Wang, H. *Chem. Commun.* **2011**, *47*, 8091.
- (84) Hao, X.; Wu, J.; Shan, Y.; Cai, M.; Shang, X.; Jiang, J.; Wang, H. *J. Phys.: Condens. Matter.* **2012**, *24*, 164207.

- (85) Ma, X.; Wu, Y.; Jin, S.; Tian, Y.; Zhang, X.; Zhao, Y.; Yu, L.; Liang, X.-J. *ACS Nano* **2011**, *5*, 8629.
- (86) Sobhan, M. A.; Sreenivasan, V. K. A.; Withford, M. J.; Goldys, E. M. *Colloids Surf., B* **2012**, *92*, 190.
- (87) Sabuncu, A. C.; Grubbs, J.; Qian, S.; Abdel-Fattah, T. M.; Stacey, M. W.; Beskok, A. *Colloids Surf., B* **2012**, *95*, 96.
- (88) Huang, K.; Ma, H.; Liu, J.; Huo, S.; Kumar, A.; Wei, T.; Zhang, X.; Jin, S.; Gan, Y.; Wang, P. C.; He, S.; Zhang, X.; Liang, X.-J. *ACS Nano* **2012**, *6*, 4483.
- (89) Huo, S.; Ma, H.; Huang, K.; Liu, J.; Wei, T.; Jin, S.; Zhang, J.; He, S.; Liang, X.-J. *Cancer Res.* **2013**, *73*, 319.
- (90) Arvizu, R. R.; Saha, S.; Wang, E.; Robertson, J. D.; Bhattacharya, R.; Mukherjee, P. *Proc. Natl. Acad. Sci. U.S.A.* **2013**, *110*, 6700.
- (91) Trickler, W. J.; Lantz, S. M.; Murdock, R. C.; Schrand, A. M.; Robinson, B. L.; Newport, G. D.; Schlager, J. J.; Oldenburg, S. J.; Paule, M. G.; Slikker, W., Jr.; Hussain, S. M.; Ali, S. F. *Nanotoxicology* **2011**, *5*, 479.
- (92) Lèvy, R.; Thanh, N. T. K.; Doty, R. C.; Hussain, I.; Nichols, R. J.; Schiffirin, D. J.; Brust, M.; Fernig, D. G. *J. Am. Chem. Soc.* **2004**, *126*, 10076.
- (93) Bartczak, D.; Muskens, O. L.; Nitti, S.; Sanchez-Elsner, T.; Millar, T. M.; Kanaras, A. G. *Small* **2012**, *8*, 122.
- (94) Cho, E. C.; Zhang, Q.; Xia, Y. *Nat. Nanotechnol.* **2011**, *6*, 385.
- (95) Schaeublin, N. M.; Braydich-Stolle, L. K.; Maurer, E. I.; Park, K.; MacCuspie, R. I.; Afroz, A. R. M. N.; Vaia, R. A.; Saleh, N. B.; Hussain, S. M. *Langmuir* **2012**, *28*, 3248.
- (96) Zhang, W.; Ji, Y.; Meng, J.; Wu, X.; Xu, H. *PLoS ONE* **2012**, *7*, e31957.
- (97) Tarantola, M.; Pietuch, A.; Schneider, D.; Rother, J.; Sunnick, E.; Rosman, C.; Pierrat, S.; Sönnichsen, C.; Wegener, J.; Janshoff, A. *Nanotoxicology* **2011**, *5*, 254.
- (98) Hutter, E.; Boridy, S.; Labrecque, S.; Lalancette-Hébert, M.; Kriz, J.; Winnik, F. M.; Maysinger, D. *ACS Nano* **2010**, *4*, 2595.
- (99) Liu, H.; Liu, T.; Li, L.; Hao, N.; Tan, L.; Meng, X.; Ren, J.; Chen, D.; Tang, F. *Nanoscale* **2012**, *4*, 3523.
- (100) Navarro, J. R. G.; Manchon, D.; Lerouge, F.; Blanchard, N. P.; Marotte, S.; Leverrier, Y.; Marvel, J.; Chaput, F.; Micouin, G.; Gabudean, A.-M.; Mosset, A.; Cottancin, E.; Baldeck, P. L.; Kamada, K.; Parola, S. *Nanotechnology* **2012**, *23*, 465602.
- (101) Avram, M.; Bălan, C. M.; Petrescu, I.; Schiopu, V.; Mărculescu, C.; Avram, A. *Plasmonics* **2012**, *7*, 717.
- (102) Plascencia-Villa, G.; Bahena, D.; Rodríguez, A. R.; Ponce, A.; José-Yacamán, M. *Metalloomics* **2013**, *5*, 242.
- (103) Zhang, S.; Li, J.; Lykotrafitis, G.; Bao, G.; Suresh, S. *Adv. Mater.* **2009**, *21*, 419.
- (104) Kuo, C.-W.; Lai, J.-J.; Wei, K. H.; Chen, P. *Adv. Funct. Mater.* **2007**, *17*, 3707.
- (105) Elsaesser, A.; Taylor, A.; de Yanes, G. S.; McKerr, G.; Kim, E.-M.; O'Hare, E.; Howard, C. V. *Nanomedicine (Lond.)* **2010**, *5*, 1447.
- (106) Elsaesser, A.; Barnes, C. A.; McKerr, G.; Salvati, A.; Lynch, I.; Dawson, K. A.; Howard, C. V. *Nanomedicine (Lond.)* **2011**, *6*, 1189.
- (107) Mayhew, T. M.; Mühlfeld, C.; Vanhecke, D.; Ochs, M. *Ann. Anat.* **2009**, *191*, 153.
- (108) Li, N.; Larson, T.; Nguyen, H. H.; Sokolov, K. V.; Ellington, A. D. *Chem. Commun.* **2010**, *46*, 392.
- (109) Peckys, D. B.; de Jonge, N. *Nano Lett.* **2011**, *11*, 1733.
- (110) Chen, X.; Chen, C.-B.; Udalagama, C. N. B.; Ren, M.; Fong, K. E.; Yung, L. Y. L.; Giorgia, P.; Bettoli, A. A.; Watt, F. *Biophys. J.* **2013**, *104*, 1419.
- (111) Gu, Y.; Sun, W.; Wang, G.; Fang, N. *J. Am. Chem. Soc.* **2011**, *133*, 5720.
- (112) Berciaud, S.; Cognet, L.; Tamarat, P.; Lounis, B. *Nano Lett.* **2005**, *5*, 515.
- (113) Louit, G.; Asahi, T.; Tanaka, G.; Uwada, T.; Masuhara, H. *J. Phys. Chem. C* **2009**, *113*, 11766.
- (114) Hartsuiker, L.; Petersen, W.; Rayavarapu, R. G.; Lenferink, A.; Poot, A. A.; Terstappen, L. W. M. M.; van Leeuwen, T. G.; Manohar, S.; Otto, C. *Appl. Spectrosc.* **2012**, *66*, 66.
- (115) Zhu, Z.-J.; Ghosh, P. S.; Miranda, O. R.; Vachet, R. W.; Rotello, V. M. *J. Am. Chem. Soc.* **2008**, *130*, 14139.
- (116) Lin, H.-C.; Lin, H.-H.; Kao, C.-Y.; Yu, A. L.; Peng, W.-P.; Chen, C.-H. *Angew. Chem., Int. Ed.* **2010**, *49*, 3460.
- (117) Chen, J.; Irudayraj, J. *ACS Nano* **2009**, *3*, 4071.
- (118) Rago, G.; Bauer, B.; Svedberg, F.; Gunnarsson, L.; Ericson, M. B.; Bonn, M.; Enejder, A. *J. Phys. Chem. B* **2011**, *115*, 5008.
- (119) Shah, N. B.; Dong, J.; Bischof, J. C. *Mol. Pharm.* **2011**, *8*, 176.
- (120) Ando, J.; Fujita, K.; Smith, N. I.; Kawata, S. *Nano Lett.* **2011**, *11*, 5344.
- (121) Jung, Y.; Reif, R.; Zeng, Y.; Wang, R. K. *Nano Lett.* **2011**, *11*, 2938.
- (122) Chen, H.-H.; Chien, C.-C.; Petibois, C.; Wang, C.-L.; Chu, Y. S.; Lai, S.-F.; Hua, T.-E.; Chen, Y.-Y.; Cai, X.; Kempson, I. M.; Hwu, Y.; Margaritondo, G. *J. Nanobiotechnol.* **2011**, *9*, 14.
- (123) Menk, R. H.; Schültke, E.; Hall, C.; Arfelli, F.; Astolfo, A.; Rigon, L.; Round, A.; Ataelmannan, K.; MacDonald, S. R.; Juurlink, B. H. J. *Nanomedicine* **2011**, *7*, 647.
- (124) Nam, S. Y.; Ricles, L. M.; Suggs, L. J.; Emelianov, S. Y. *Opt. Lett.* **2012**, *37*, 4708.
- (125) Park, J.-H.; Park, J.; Dembereldorj, U.; Cho, K.; Lee, K.; Yang, S. I.; Lee, S. Y.; Joo, S.-W. *Anal. Bioanal. Chem.* **2011**, *401*, 1631.
- (126) Rosman, C.; Pierrat, S.; Henkel, A.; Tarantola, M.; Schneider, D.; Sunnick, E.; Janshoff, A.; Sönnichsen, C. *Small* **2012**, *8*, 3683.
- (127) Tan, S. H.; Horlick, G. *Appl. Spectrosc.* **1986**, *40*, 445.
- (128) Tanner, S. D.; Baranov, V. I. *J. Am. Soc. Mass Spectrom.* **1999**, *10*, 1083.
- (129) Stender, A. S.; Marchuk, K.; Liu, C.; Sander, S.; Meyer, M. W.; Smith, E. A.; Neupane, B.; Wang, G.; Li, J.; Cheng, J.-X.; Huang, B.; Fang, N. *Chem. Rev.* **2013**, *113*, 2469.
- (130) Brandenberger, C.; Mühlfeld, C.; Ali, Z.; Lenz, A.-G.; Schmid, O.; Parak, W. J.; Gehr, P.; Rothen-Rutishauser, B. *Small* **2010**, *6*, 1669.
- (131) Lipowsky, R.; Döbereiner, H. G. *Europhys. Lett.* **1998**, *43*, 219.
- (132) Bao, G.; Bao, X. R. *Proc. Natl. Acad. Sci. U.S.A.* **2005**, *102*, 9997.
- (133) Chaudhuri, A.; Battaglia, G.; Golestanian, R. *Phys. Biol.* **2011**, *8*, 046002.
- (134) Yuan, H.; Li, J.; Bao, G.; Zhang, S. *Phys. Rev. Lett.* **2010**, *105*, 138101.
- (135) Yi, X.; Shi, X.; Gao, H. *Phys. Rev. Lett.* **2011**, *107*, 098101.
- (136) Decuzzi, P.; Ferrari, M. *Biomaterials* **2007**, *28*, 2916.
- (137) Decuzzi, P.; Ferrari, M. *Biophys. J.* **2008**, *94*, 3790.
- (138) Li, X. *J. Appl. Phys.* **2012**, *111*, 024702.
- (139) Dobay, M. P. D.; Piera Alberola, A.; Mendoza, E. R.; Rädler, J. O. *J. Nanopart. Res.* **2012**, *14*, 821.
- (140) Sapsford, K. E.; Algar, W. R.; Berti, L.; Gemmill, K. B.; Casey, B. J.; Oh, E.; Stewart, M. H.; Medintz, I. L. *Chem. Rev.* **2013**, *113*, 1904.
- (141) Festag, G.; Klenz, U.; Henkel, T.; Csáki, A.; Fritzsch, W. Biofunctionalization of Metallic Nanoparticles and Microarrays for Biomolecular Detection. In *Biofunctionalization of Nanomaterials*; Kumar, C. S. S. R., Ed.; Wiley: Weinheim, Germany, 2005; pp 150–182.
- (142) Hermanson, G. T. *Bioconjugate Techniques*; Academic Press: San Diego, 1996.
- (143) Shenton, W.; Davis, S. A.; Mann, S. *Adv. Mater.* **1999**, *11*, 449.
- (144) Dubois, L. H.; Nuzzo, R. G. *Annu. Rev. Phys. Chem.* **1992**, *43*, 437.
- (145) Lowe, C. R. *Curr. Opin. Struct. Biol.* **2000**, *10*, 428.
- (146) Ulman, A. *Chem. Rev.* **1996**, *96*, 1533.
- (147) Mirkin, C. A.; Letsinger, R. L.; Mucic, R. C.; Storhoff, J. J. *Nature* **1996**, *382*, 607.
- (148) Letsinger, R. L.; Elghanian, R.; Viswanadham, G.; Mirkin, C. A. *Bioconjug. Chem.* **2000**, *11*, 289.
- (149) Li, Z.; Jin, R. S.; Mirkin, C. A.; Letsinger, R. L. *Nucleic Acids Res.* **2002**, *30*, 1558.
- (150) Walton, I. D.; Norton, S. M.; Balasingham, A.; He, L.; Oviso, D. F.; Gupta, D.; Raju, P. A.; Natan, M. J.; Freeman, R. G. *Anal. Chem.* **2002**, *74*, 2240.
- (151) Ghosh, S. S.; Kao, P. M.; McCue, A. W.; Chappelle, H. L. *Bioconjug. Chem.* **1990**, *1*, 71.

- (152) Cheng, Y.; Samia, A. C.; Li, J.; Kenney, M. E.; Resnick, A.; Burda, C. *Langmuir* **2010**, *26*, 2248.
- (153) Lynch, I.; Dawson, K. A. *Nano Today* **2008**, *3*, 40.
- (154) Nel, A. E.; Mädler, L.; Velez, D.; Xia, T.; Hoek, E. M. V.; Somasundaran, P.; Klaessig, F.; Castranova, V.; Thompson, M. *Nat. Mater.* **2009**, *8*, 543.
- (155) Tsai, Y.-S.; Chen, Y.-H.; Cheng, P.-C.; Tsai, H.-T.; Shiau, A.-L.; Tzai, T.-S.; Wu, C.-L. *Small* **2013**, *9*, 2119.
- (156) Dobrovolskaia, M. A.; Patri, A. K.; Zheng, J.; Clogston, J. D.; Ayub, N.; Aggarwal, P.; Neun, B. W.; Hall, J. B.; McNeil, S. E. *Nanomedicine* **2009**, *5*, 106.
- (157) Lacerda, S. H. D. P.; Park, J. J.; Meuse, C.; Pristinski, D.; Becker, M. L.; Karim, A.; Douglas, J. F. *ACS Nano* **2010**, *4*, 365.
- (158) Mahmoudi, M.; Lynch, I.; Ejtehadi, M. R.; Monopoli, M. P.; Bombelli, F. B.; Laurent, S. *Chem. Rev.* **2011**, *111*, 5610.
- (159) Goy-López, S.; Juárez, J.; Alatorre-Meda, M.; Casals, E.; Puntes, V. F.; Taboada, P.; Mosquera, V. *Langmuir* **2012**, *28*, 9113.
- (160) Arvizo, R. R.; Giri, K.; Moyano, D.; Miranda, O. R.; Madden, B.; McCormick, D. J.; Bhattacharya, R.; Rotello, V. M.; Kocher, J.-P.; Mukherjee, P. *PLoS ONE* **2012**, *7*, e33650.
- (161) Niidome, T.; Yamagata, M.; Okamoto, Y.; Akiyama, Y.; Takahashi, H.; Kawano, T.; Katayama, Y.; Niidome, Y. *J. Controlled Release* **2006**, *114*, 343.
- (162) Jokerst, J. V.; Lobovkina, T.; Zare, R. N.; Gambhir, S. S. *Nanomedicine (Lond.)* **2011**, *6*, 715.
- (163) Karakoti, A. S.; Das, S.; Thevuthasan, S.; Seal, S. *Angew. Chem., Int. Ed.* **2011**, *50*, 1980.
- (164) Jain, R. K.; Booth, M. F. *J. Clin. Invest.* **2003**, *112*, 1134.
- (165) Otsuka, H.; Nagasaki, Y.; Kataoka, K. *Adv. Drug Delivery Rev.* **2003**, *55*, 403.
- (166) Sperling, R. A.; Parak, W. J. *Philos. Trans. R. Soc. A* **2010**, *368*, 1333.
- (167) Shenoy, D.; Fu, W.; Li, J.; Crasto, C.; Jones, G.; Dimarzio, C.; Sridhar, S.; Amiji, M. *Int. J. Nanomedicine* **2006**, *1*, 51.
- (168) Bergen, J. M.; von Recum, H. A.; Goodman, T. T.; Massey, A. P.; Pun, S. H. *Macromol. Biosci.* **2006**, *6*, 506.
- (169) Cho, W.-S.; Cho, M.; Jeong, J.; Choi, M.; Cho, H.-Y.; Han, B. S.; Kim, S. H.; Kim, H. O.; Lim, Y. T.; Chung, B. H.; Jeong, J. *Toxicol. Appl. Pharmacol.* **2009**, *236*, 16.
- (170) Cho, W.-S.; Cho, M.; Jeong, J.; Choi, M.; Han, B. S.; Shin, H.-S.; Hong, J.; Chung, B. H.; Jeong, J.; Cho, M.-H. *Toxicol. Appl. Pharmacol.* **2010**, *245*, 116.
- (171) Liu, C. J.; Wang, C. H.; Chien, C. C.; Yang, T. Y.; Chen, S. T.; Leng, W. H.; Lee, C. F.; Lee, K. H.; Hwu, Y.; Lee, Y. C.; Cheng, C. L.; Yang, C. S.; Chen, Y. J.; Je, J. H.; Margaritondo, G. *Nanotechnology* **2008**, *19*, 295104.
- (172) Zhang, G.; Yang, Z.; Lu, W.; Zhang, R.; Huang, Q.; Tian, M.; Li, L.; Liang, D.; Li, C. *Biomaterials* **2009**, *30*, 1928.
- (173) Gu, Y.-J.; Cheng, J.; Lin, C.-C.; Lam, Y. W.; Cheng, S. H.; Wong, W.-T. *Toxicol. Appl. Pharmacol.* **2009**, *237*, 196.
- (174) Lund, T.; Callaghan, M. F.; Williams, P.; Turmaine, M.; Bachmann, C.; Rademacher, T.; Roitt, I. M.; Bayford, R. *Biomaterials* **2011**, *32*, 9776.
- (175) Kah, J. C.; Wong, K. Y.; Neoh, K. G.; Song, J. H.; Fu, J. W.; Mhaisalkar, S.; Olivo, M.; Sheppard, C. *J. Drug Target* **2009**, *17*, 181.
- (176) Huff, T. B.; Hansen, M. N.; Zhao, Y.; Cheng, J.-X.; Wei, A. *Langmuir* **2007**, *23*, 1596.
- (177) Rayavarapu, R. G.; Petersen, W.; Hartsuiker, L.; Chin, P.; Janssen, H.; van Leeuwen, F. W. B.; Otto, C.; Manohar, S.; van Leeuwen, T. G. *Nanotechnology* **2010**, *21*, 145101.
- (178) Grabinski, C.; Schaeublin, N.; Wijaya, A.; D'Couto, H.; Baxamusa, S. H.; Hamad-Schifferli, K.; Hussain, S. M. *ACS Nano* **2011**, *5*, 2870.
- (179) Alkilany, A. M.; Shatanawi, A.; Kurtz, T.; Caldwell, R. B.; Caldwell, R. W. *Small* **2012**, *8*, 1270.
- (180) Arnida; Malugin, A.; Ghandehari, H. *J. Appl. Toxicol.* **2010**, *30*, 212.
- (181) Arnida; Janát-Amsbury, M. M.; Ray, A.; Peterson, C. M.; Ghandehari, H. *Eur. J. Pharm. Biopharm.* **2011**, *77*, 417.
- (182) Cho, E. C.; Liu, Y.; Xia, Y. *Angew. Chem., Int. Ed.* **2010**, *49*, 1976.
- (183) Puvanakrishnan, P.; Park, J.; Chatterjee, D.; Krishnan, S.; Tunnell, J. W. *Int. J. Nanomed.* **2012**, *7*, 1251.
- (184) Larson, T. A.; Joshi, P. P.; Sokolov, K. *ACS Nano* **2012**, *6*, 9182.
- (185) Takahashi, H.; Niidome, T.; Kawano, T.; Yamada, S.; Niidome, Y. *J. Nanopart. Res.* **2008**, *10*, 221.
- (186) Thomas, M.; Klipanov, A. M. *Proc. Natl. Acad. Sci. U.S.A.* **2003**, *100*, 9138.
- (187) Hauck, T. S.; Ghazani, A. A.; Chan, W. C. W. *Small* **2008**, *4*, 153.
- (188) Alkilany, A. M.; Nagaria, P. K.; Hexel, C. R.; Shaw, T. J.; Murphy, C. J.; Wyatt, M. D. *Small* **2009**, *5*, 701.
- (189) Parab, H. J.; Chen, H. M.; Lai, T.-C.; Huang, J. H.; Chen, P. H.; Liu, R.-S.; Hsiao, M.; Chen, C.-H.; Tsai, D.-P.; Hwu, Y.-K. *J. Phys. Chem. C* **2009**, *113*, 7574.
- (190) Fan, Z.; Yang, X.; Li, Y.; Li, S.; Niu, S.; Wu, X.; Wei, J.; Nie, G. *Biointerphases* **2012**, *7*, 10.
- (191) Goh, D.; Gong, T.; Dinish, U. S.; Maiti, K. K.; Fu, C. Y.; Yong, K.-T.; Olivo, M. *Plasmonics* **2012**, *7*, 595.
- (192) Qiu, Y.; Liu, Y.; Wang, L.; Xu, L.; Bai, R.; Ji, Y.; Wu, X.; Zhao, Y.; Li, Y.; Chen, C. *Biomaterials* **2010**, *31*, 7606.
- (193) Wang, L.; Liu, Y.; Li, W.; Jiang, X.; Ji, Y.; Wu, X.; Xu, L.; Qiu, Y.; Zhao, K.; Wei, T.; Li, Y.; Zhao, Y.; Chen, C. *Nano Lett.* **2011**, *11*, 772.
- (194) Vigderman, L.; Manna, P.; Zubarev, E. R. *Angew. Chem., Int. Ed.* **2012**, *51*, 636.
- (195) Li, J.-L.; Wang, L.; Liu, X.-Y.; Zhang, Z.-P.; Guo, H.-C.; Liu, W.-M.; Tang, S.-H. *Cancer Lett.* **2009**, *274*, 319.
- (196) Salmaso, S.; Caliceti, P.; Amendola, V.; Meneghetti, M.; Magnusson, J. P.; Pasparakis, G.; Alexander, C. *J. Mater. Chem.* **2009**, *19*, 1608.
- (197) Dragoni, S.; Franco, G.; Regoli, M.; Bracciali, M.; Morandi, V.; Sgaragli, G.; Bertelli, E.; Valotti, M. *Toxicol. Sci.* **2012**, *128*, 186.
- (198) Liu, X.; Jin, Q.; Ji, Y.; Ji, J. *J. Mater. Chem.* **2012**, *22*, 1916.
- (199) Cho, E. C.; Xie, J.; Wurm, P. A.; Xia, Y. *Nano Lett.* **2009**, *9*, 1080.
- (200) Liang, M.; Lin, I.-C.; Whittaker, M. R.; Minchin, R. F.; Monteiro, M. J.; Toth, I. *ACS Nano* **2010**, *4*, 403.
- (201) Lin, I.-C.; Liang, M.; Liu, T.-Y.; Ziora, Z. M.; Monteiro, M. J.; Toth, I. *Biomacromolecules* **2011**, *12*, 1339.
- (202) Freese, C.; Gibson, M. I.; Klok, H.-A.; Unger, R. E.; Kirkpatrick, C. *J. Biomacromolecules* **2012**, *13*, 1533.
- (203) Ojea-Jiménez, I.; García-Fernández, L.; Lorenzo, J.; Puntes, V. F. *ACS Nano* **2012**, *6*, 7692.
- (204) Choi, S. Y.; Jang, S. H.; Park, J.; Jeong, S.; Park, J. H.; Ock, K. S.; Lee, K.; Yang, S. I.; Joo, S.-W.; Ryu, P. D.; Lee, S. Y. *J. Nanopart. Res.* **2012**, *14*, 1234.
- (205) Hühn, D.; Kantner, K.; Geidel, C.; Brandholt, S.; De Cock, I.; Soenen, J. H.; Rivera Gil, P.; Montenegro, J.-M.; Braeckmans, K.; Müllen, K.; Nienhaus, G. U.; Klapper, M.; Parak, W. J. *ACS Nano* **2013**, *7*, 3253.
- (206) Liang, Z.; Liu, Y.; Li, X.; Wu, Q.; Yu, J.; Luo, S.; Lai, L.; Liu, S. J. *Biomed. Mater. Res. A* **2011**, *98A*, 479.
- (207) Arvizo, R. R.; Miranda, O. R.; Thompson, M. A.; Pabelick, C. M.; Bhattacharya, R.; Robertson, J. D.; Rotello, V. M.; Prakash, Y. S.; Mukherjee, P. *Nano Lett.* **2010**, *10*, 2543.
- (208) Lin, I.-C.; Liang, M.; Liu, T.-Y.; Monteiro, M. J.; Toth, I. *Nanomedicine* **2012**, *8*, 8.
- (209) Maiorano, G.; Sabella, S.; Sorce, B.; Brunetti, V.; Malvindi, M. A.; Cingolani, R.; Pompa, P. P. *ACS Nano* **2010**, *4*, 7481.
- (210) Pal, A.; Shah, S.; Kulkarni, V.; Murthy, R. S. R.; Devi, S. *Mater. Chem. Phys.* **2009**, *113*, 276.
- (211) Boca, S. C.; Potara, M.; Toderas, F.; Stephan, O.; Baldeck, P. L.; Astilean, S. *Mater. Sci. Eng., C* **2011**, *31*, 184.
- (212) Chithrani, D. B.; Dunne, M.; Stewart, J.; Allen, C.; Jaffray, D. A. *Nanomedicine* **2010**, *6*, 161.
- (213) Dhar, S.; Mali, V.; Bodhankar, S.; Shiras, A.; Prasad, B. L. V.; Pokharkar, V. *J. Appl. Toxicol.* **2011**, *31*, 411.
- (214) Lee, Y.; Geckeler, K. E. *J. Biomed. Mater. Res. A* **2012**, *100A*, 848.
- (215) Hao, Y.; Yang, X.; Song, S.; Huang, M.; He, C.; Cui, M.; Chen, J. *Nanotechnology* **2012**, *23*, 045103.

- (216) Wang, M.; Petersen, N. O. *Biochim. Biophys. Acta* **2013**, *1831*, 1089.
- (217) Yang, S.; Damiano, M. G.; Zhang, H.; Tripathy, S.; Luthi, A. J.; Rink, J. S.; Ugolkov, A. V.; Singh, A. T. K.; Dave, S. S.; Gordon, L. I.; Thaxton, C. S. *Proc. Natl. Acad. Sci. U.S.A.* **2013**, *110*, 2511.
- (218) Amarnath, K.; Mathew, N. L.; Nellore, J.; Siddarth, C. R. V.; Kumar, J. *Cancer Nano* **2011**, *2*, 121.
- (219) Faulk, W. P.; Taylor, G. M. *Immunochemistry* **1971**, *8*, 1081.
- (220) Hu, R.; Yong, K.-T.; Roy, I.; Ding, H.; He, S.; Prasad, P. N. J. *Phys. Chem. C* **2009**, *113*, 2676.
- (221) Rejiya, C. S.; Kumar, J.; Raji, V.; Vibin, M.; Abraham, A. *Pharmacol. Res.* **2012**, *65*, 261.
- (222) Pissuwan, D.; Valenzuela, S. M.; Killingsworth, M. C.; Xu, X.; Cortie, M. B. *J. Nanoparticle Res.* **2007**, *9*, 1109.
- (223) Lapotko, D. O.; Lukianova-Hleb, E. Y.; Oraevsky, A. A. *Nanomedicine (Lond.)* **2007**, *2*, 241.
- (224) Melancon, M. P.; Lu, W.; Yang, Z.; Zhang, R.; Cheng, Z.; Elliot, A. M.; Stafford, J.; Olson, T.; Zhang, J. Z.; Li, C. *Mol. Cancer Ther.* **2008**, *7*, 1730.
- (225) Lu, W.; Xiong, C.; Zhang, G.; Huang, Q.; Zhang, R.; Zhang, J. Z.; Li, C. *Clin. Cancer Res.* **2009**, *15*, 876.
- (226) Marega, R.; Karmani, L.; Flamant, L.; Nageswaran, P. G.; Valembois, V.; Masereel, B.; Feron, O.; Borght, T. V.; Lucas, S.; Michiels, C.; Gallez, B.; Bonifazi, D. *J. Mater. Chem.* **2012**, *22*, 21305.
- (227) Raoof, M.; Corr, S. J.; Kaluarachchi, W. D.; Massey, K. L.; Briggs, K.; Zhu, C.; Cheney, M. A.; Wilson, L. J.; Curley, S. A. *Nanomedicine* **2012**, *8*, 1096.
- (228) Song, J.; Zhou, J.; Duan, H. *J. Am. Chem. Soc.* **2012**, *134*, 13458.
- (229) Liu, T.; Cousins, A.; Chien, C.-C.; Kempson, I.; Thompson, S.; Hwu, Y.; Thierry, B. *Cancer Lett.* **2013**, *328*, 271.
- (230) Charan, S.; Sanjiv, K.; Singh, N.; Chien, F.-C.; Chen, Y.-F.; Nergui, N. N.; Huang, S.-H.; Kuo, C. W.; Lee, T.-C.; Chen, P. *Bioconjug. Chem.* **2012**, *23*, 2173.
- (231) Au, L.; Zhang, Q.; Cobley, C. M.; Gidding, M.; Schwartz, A. G.; Chen, J.; Xia, Y. *ACS Nano* **2010**, *4*, 35.
- (232) Cho, E. C.; Au, L.; Zhang, Q.; Xia, Y. *Small* **2010**, *6*, 517.
- (233) Cho, E. C.; Zhang, Y.; Cai, X.; Moran, C. M.; Wang, L. V.; Xia, Y. *Angew. Chem., Int. Ed.* **2013**, *125*, 1190.
- (234) Wagstaff, K. M.; Jans, D. A. *Curr. Med. Chem.* **2006**, *13*, 1371.
- (235) Okuyama, M.; Laman, H.; Kingsbury, S. R.; Visintin, C.; Leo, E.; Eward, K. L.; Stoeber, K.; Boshoff, C.; Williams, G. H.; Selwood, D. L. *Nat. Methods* **2007**, *4*, 153.
- (236) Frankel, A. D.; Pabo, C. O. *Cell* **1988**, *55*, 1189.
- (237) Feldherr, C. M.; Lanford, R. E.; Akin, D. *Proc. Natl. Acad. Sci. U.S.A.* **1992**, *89*, 11002.
- (238) Vivès, E.; Schmidt, J.; Pèlegrin, A. *Biochim. Biophys. Acta* **2008**, *1786*, 126.
- (239) Tkachenko, A. G.; Xie, H.; Coleman, D.; Glomm, W.; Ryan, J.; Anderson, M. F.; Franzen, S.; Feldheim, D. L. *J. Am. Chem. Soc.* **2003**, *125*, 4700.
- (240) Mandal, D.; Maran, A.; Yaszemski, M. J.; Bolander, M. E.; Sarkar, G. J. *Mater. Sci.: Mater. Med.* **2009**, *20*, 347.
- (241) Tkachenko, A. G.; Xie, H.; Liu, Y.; Coleman, D.; Ryan, J.; Glomm, W. R.; Shipton, M. K.; Franzen, S.; Feldheim, D. L. *Bioconjug. Chem.* **2004**, *15*, 482.
- (242) Ryan, J.; Overton, K. W.; Speight, M. E.; Oldenburg, C. N.; Loo, L.; Robarge, W.; Franzen, S.; Feldheim, D. L. *Anal. Chem.* **2007**, *79*, 9150.
- (243) Liu, Y.; Shipton, M. K.; Ryan, J.; Kaufman, E. D.; Franzen, S.; Feldheim, D. L. *Anal. Chem.* **2007**, *79*, 2221.
- (244) Liu, Y.; Franzen, S. *Bioconjug. Chem.* **2008**, *19*, 1009.
- (245) Ghosh, P.; Yang, X.; Arvizu, R.; Zhu, Z.-J.; Agasti, S. S.; Mo, Z.; Rotello, V. M. *J. Am. Chem. Soc.* **2010**, *132*, 2642.
- (246) de la Fuente, J. M.; Berry, C. C. *Bioconjug. Chem.* **2005**, *16*, 1176.
- (247) Oh, E.; Delehanty, J. B.; Sapsford, K. E.; Susumu, K.; Goswami, R.; Blanco-Canosa, J. B.; Dawson, P. E.; Granek, J.; Shoff, M.; Zhang, Q.; Goering, P. L.; Huston, A.; Medintz, I. L. *ACS Nano* **2011**, *5*, 6434.
- (248) Krpetić, Ž.; Saleemi, S.; Prior, I. A.; Sée, V.; Qureshi, R.; Brust, M. *ACS Nano* **2011**, *5*, 5195.
- (249) Dekiwadia, C. D.; Lawrie, A. C.; Fecondo, J. V. *J. Pept. Sci.* **2012**, *18*, 527.
- (250) Nativo, P.; Prior, I. A.; Brust, M. *ACS Nano* **2008**, *2*, 1639.
- (251) Sun, L.; Liu, D.; Wang, Z. *Langmuir* **2008**, *24*, 10293.
- (252) Morais, T.; Soares, M. E.; Duarte, J. A.; Soares, L.; Maia, S.; Gomes, P.; Pereira, E.; Fraga, S.; Carmo, H.; Bastos, M. deL. *Eur. J. Pharm. Biopharm.* **2012**, *80*, 185.
- (253) Oyelere, A. K.; Chen, P. C.; Huang, X.; El-Sayed, I. H.; El-Sayed, M. A. *Bioconjug. Chem.* **2007**, *18*, 1490.
- (254) Kang, B.; Mackey, M. A.; El-Sayed, M. A. *J. Am. Chem. Soc.* **2010**, *132*, 1517.
- (255) Yuan, H.; Fales, A. M.; Vo-Dinh, T. *J. Am. Chem. Soc.* **2012**, *134*, 11358.
- (256) Liu, S.-Y.; Liang, Z.-S.; Gao, F.; Luo, S.-F.; Lu, G.-Q. *J. Mater. Sci.: Mater. Med.* **2010**, *21*, 665.
- (257) Yang, H.; Fung, S.-Y.; Liu, M. *Angew. Chem., Int. Ed.* **2011**, *50*, 9643.
- (258) Wang, G.; Norton, A. S.; Pokharel, D.; Song, Y.; Hill, R. A. *Nanomedicine* **2013**, *9*, 366.
- (259) Shirazi, A. N.; Mandal, D.; Tiwari, R. K.; Guo, L.; Lu, W.; Parang, K. *Mol. Pharmacol.* **2013**, *10*, 500.
- (260) Yao, L.; Danniels, J.; Moshnikova, A.; Kuznetsov, S.; Ahmed, A.; Engelmann, D. M.; Reshetnyak, Y. K.; Andreev, O. A. *Proc. Natl. Acad. Sci. U.S.A.* **2013**, *110*, 465.
- (261) Park, H.; Tsutsumi, H.; Mihara, H. *Biomaterials* **2013**, *34*, 4872.
- (262) Wang, G.; Papasani, M. R.; Cheguru, P.; Hrdlicka, P. J.; Hill, R. A. *Nanomedicine* **2012**, *8*, 822.
- (263) Rosi, N. L.; Giljohann, D. A.; Thaxton, C. S.; Lytton-Jean, A. K. R.; Han, M. S.; Mirkin, C. A. *Science* **2006**, *312*, 1027.
- (264) Giljohann, D. A.; Seferos, D. S.; Patel, P. C.; Millstone, J. E.; Rosi, N. L.; Mirkin, C. A. *Nano Lett.* **2007**, *7*, 3818.
- (265) Patel, P. C.; Giljohann, D. A.; Seferos, D. S.; Mirkin, C. A. *Proc. Natl. Acad. Sci. U.S.A.* **2008**, *105*, 17222.
- (266) Massich, M. D.; Giljohann, D. A.; Schmucker, A. L.; Patel, P. C.; Mirkin, C. A. *ACS Nano* **2010**, *4*, 5641.
- (267) Jewell, C. M.; Jung, J.-M.; Atukorale, P. U.; Carney, R. P.; Stellacci, F.; Irvine, D. J. *Angew. Chem., Int. Ed.* **2011**, *50*, 12312.
- (268) Bonoiu, A. C.; Mahajan, S. D.; Ding, H.; Roy, I.; Yong, K.-T.; Kumar, R.; Hu, R.; Bergey, E. J.; Schwartz, S. A.; Prasad, P. N. *Proc. Natl. Acad. Sci. U.S.A.* **2009**, *106*, 5546.
- (269) Crew, E.; Rahman, S.; Razzak-Jaffar, A.; Mott, D.; Kamundi, M.; Yu, G.; Tchah, N.; Lee, J.; Bellavia, M.; Zhong, C.-J. *Anal. Chem.* **2012**, *84*, 26.
- (270) Guo, S.; Huang, Y.; Jiang, Q.; Sun, Y.; Deng, L.; Liang, Z.; Du, Q.; Xing, J.; Zhao, Y.; Wang, P. C.; Dong, A.; Liang, X.-J. *ACS Nano* **2010**, *4*, 5505.
- (271) Ghosh, R.; Singh, L. C.; Shohet, J. M.; Gunaratne, P. H. *Biomaterials* **2013**, *24*, 807.
- (272) Braun, G. B.; Pallaoro, A.; Wu, G.; Missirlis, D.; Zasadzinski, J. A.; Tirrell, M.; Reich, N. O. *ACS Nano* **2009**, *3*, 2007.
- (273) Song, W. J.; Du, J. Z.; Sun, T. M.; Zhang, P. Z.; Wang, J. *Small* **2009**, *6*, 239.
- (274) Tian, H.; Guo, Z.; Chen, J.; Lin, L.; Xia, J.; Dong, X.; Chen, X. *Adv. Healthcare Mater.* **2012**, *1*, 337.
- (275) Sandhu, K. K.; McIntosh, C. M.; Simard, J. M.; Smith, S. W.; Rotello, V. M. *Bioconjug. Chem.* **2002**, *13*, 3.
- (276) Sée, V.; Free, P.; Cesbron, Y.; Nativo, P.; Shaheen, U.; Rigden, D. J.; Spiller, D. G.; Fernig, D. G.; White, M. R.; Prior, I. A.; Brust, M.; Lounis, B.; Lévy, R. *ACS Nano* **2009**, *3*, 2461.
- (277) Yan, X.; Blacklock, J.; Li, J.; Möhwald, H. *ACS Nano* **2012**, *6*, 111.
- (278) Lee, M.-Y.; Park, S.-J.; Park, K.; Kim, K. S.; Lee, H.; Hahn, S. K. *ACS Nano* **2011**, *5*, 6138.
- (279) Durán, M. C.; Willenbrock, S.; Barchanski, A.; Müller, J.-M. V.; Maiolini, A.; Soller, J. T.; Barcikowski, S.; Nolte, I.; Feige, K.; Escobar, H. M. *J. Nanobiotechnol.* **2011**, *9*, 47.
- (280) Elbakry, A.; Wurster, E.-C.; Zaky, A.; Liebl, R.; Schindler, E.; Bauer-Kreisel, P.; Blunk, T.; Rachel, R.; Goepferich, A.; Breunig, M. *Small* **2012**, *8*, 3847.

- (281) Lukianova-Hleb, E. Y.; Ren, X.; Constantinou, P. E.; Danysh, B. P.; Shenefelt, D. L.; Carson, D. D.; Farach-Carson, M. C.; Kulchitsky, V. A.; Wu, X.; Wagner, D. S.; Lapotko, D. O. *PLoS ONE* **2012**, *7*, e34537.
- (282) Szlachcic, A.; Pala, K.; Zakrzewska, M.; Jakimowicz, P.; Wiedlocha, A.; Otlewski, J. *Int. J. Nanomed.* **2012**, *7*, 5915.
- (283) Tsai, S.-W.; Liaw, J.-W.; Hsu, F.-Y.; Chen, Y.-Y.; Lyu, M.-J.; Yeh, M.-H. *Sensors* **2008**, *8*, 6660.
- (284) Dixit, V.; Van den Bossche, J.; Sherman, D. M.; Thompson, D. H.; Andres, R. P. *Bioconjug. Chem.* **2006**, *17*, 603.
- (285) Li, G.; Li, D.; Zhang, L.; Zhai, J.; Wang, E. *Chem.—Eur. J.* **2009**, *15*, 9868.
- (286) Tong, L.; Zhao, Y.; Huff, T. B.; Hansen, M. N.; Wei, A.; Cheng, J.-X. *Adv. Mater.* **2007**, *19*, 3136.
- (287) Bhattacharya, R.; Patra, C. R.; Earl, A.; Wang, S. F.; Katarya, A.; Lu, L.; Kizhakkedathu, J. N.; Yaszemski, M. J.; Greipp, P. R.; Mukhopadhyay, D.; Mukherjee, P. *Nanomed. Nanotechnol. Biol. Med.* **2007**, *3*, 224.
- (288) Park, J.; Jeon, W. I.; Lee, S. Y.; Ock, K.-S.; Seo, J. H.; Park, J.; Ganbold, E.-O.; Cho, K.; Song, N. W.; Joo, S.-W. *J. Biomed. Mater. Res. A* **2012**, *100A*, 1221.
- (289) Paciotti, G. F.; Kingston, D. G. I.; Tamarkin, L. *Drug Dev. Res.* **2006**, *67*, 47.
- (290) Shao, J.; Griffin, R. J.; Galanzha, E. I.; Kim, J.-W.; Koonce, N.; Webber, J.; Mustafa, T.; Biris, A. S.; Nedosekin, D. A.; Zharov, V. P. *Sci. Rep.* **2013**, *3*, 1293.
- (291) Dam, D. H. M.; Lee, J. H.; Sisco, P. N.; Co, D. T.; Zhang, M.; Wasielewski, M. R.; Odom, T. W. *ACS Nano* **2012**, *6*, 3318.
- (292) Dam, D. H. M.; Culver, K. S. V.; Sisco, P. N.; Odom, T. W. *Ther. Delivery* **2012**, *3*, 1263.
- (293) Kumar, S.; Harrison, N.; Richards-Kortum, R.; Sokolov, K. *Nano Lett.* **2007**, *7*, 1338.
- (294) Kumar, S.; Aaron, J.; Sokolov, K. *Nat. Protocols* **2008**, *3*, 314.
- (295) Lukianova-Hleb, E. Y.; Belyanin, A.; Kashinath, S.; Wu, X.; Lapotko, D. O. *Biomaterials* **2012**, *33*, 1821.
- (296) Mukherjee, P.; Bhattacharya, R.; Bone, N.; Lee, Y. K.; Patra, C. R.; Wang, S.; Lu, L.; Secreto, C.; Banerjee, P. C.; Yaszemski, M. J.; Kay, N. E.; Mukhopadhyay, D. J. *Nanobiotechnol.* **2007**, *5*, 4.
- (297) Kalishwaralal, K.; Sheikpranbabu, S.; BarathManiKanth, S.; Haribalaganesh, R.; RamkumarPandian, S.; Gurunathan, S. *Angiogenesis* **2011**, *14*, 29.
- (298) Wang, Y.; Xu, J.; Xia, X.; Yang, M.; Vangveravong, S.; Chen, J.; Mach, R. H.; Xia, Y. *Nanoscale* **2012**, *4*, 421.
- (299) Krpetić, Ž.; Porta, F.; Scari, G. *Gold Bull.* **2006**, *39*, 66.
- (300) Kasten, B. B.; Liu, T.; Nedrow-Byers, J. R.; Benny, P. D.; Berkman, C. E. *Bioorg. Med. Chem. Lett.* **2013**, *23*, 565.
- (301) Huang, X.; Peng, X.; Wang, Y.; Wang, Y.; Shin, D. M.; El-Sayed, M. A.; Nie, S. *ACS Nano* **2010**, *4*, 5887.
- (302) Song, K.; Xu, P.; Meng, Y.; Geng, F.; Li, J.; Li, Z.; Xing, J.; Chen, J.; Kong, B. *Int. J. Oncol.* **2013**, *42*, 597.
- (303) Li, X.; Zhou, H.; Yang, L.; Du, G.; Pai-Panandiker, A. S.; Huang, X.; Yan, B. *Biomaterials* **2011**, *32*, 2540.
- (304) Bhattacharyya, S.; Khan, J. A.; Curran, G. L.; Robertson, J. D.; Bhattacharya, R.; Mukherjee, P. *Adv. Mater.* **2011**, *23*, 5034.
- (305) Bhattacharyya, S.; Bhattacharya, R.; Curley, S.; McNiven, M. A.; Mukherjee, P. *Proc. Natl. Acad. Sci. U.S.A.* **2010**, *107*, 14541.
- (306) Bhattacharyya, S.; Singh, R. D.; Pagano, R.; Robertson, J. D.; Bhattacharya, R.; Mukherjee, P. *Angew. Chem., Int. Ed.* **2012**, *51*, 1563.
- (307) Hosta-Rigau, L.; Olmedo, I.; Arbiol, J.; Cruz, L. J.; Kogan, M. J.; Albericio, F. *Bioconjug. Chem.* **2010**, *21*, 1070.
- (308) Kumar, A.; Ma, H.; Zhang, X.; Huang, K.; Jin, S.; Liu, J.; Wei, T.; Cao, W.; Zou, G.; Liang, X.-J. *Biomaterials* **2012**, *33*, 1180.
- (309) Heo, D. N.; Yang, D. H.; Moon, H.-J.; Lee, J. B.; Bae, M. S.; Lee, S. C.; Lee, W. J.; Sun, I.-C.; Kwon, I. K. *Biomaterials* **2012**, *33*, 856.
- (310) Song, M.; Wang, X.; Li, J.; Zhang, R.; Chen, B.; Fu, D. J. *Biomed. Mater. Res. A* **2008**, *86A*, 942.
- (311) Egbedare, M.; Liopo, A. V.; Copland, J. A.; Oraevsky, A. A.; Motamedi, M. *Nano Lett.* **2009**, *9*, 287.
- (312) Dreaden, E. C.; Mwakwari, S. C.; Sodji, Q. H.; Oyelere, A. K.; El-Sayed, M. A. *Bioconjug. Chem.* **2009**, *20*, 2247.
- (313) Kim, B.; Han, G.; Toley, B.; Kim, C.-k.; Rotello, V. M.; Forbes, N. S. *Nat. Nanotechnol.* **2010**, *5*, 465.
- (314) Wang, F.; Wang, Y. C.; Dou, S.; Xiong, M. H.; Sun, T. M.; Wang, J. *ACS Nano* **2011**, *5*, 3679.
- (315) Bibikova, O. A.; Staroverov, S. A.; Sokolov, O. I.; Dykman, L. A.; Bogatyrev, V. A. *Proc. Saratov Univ. Ser. Physics* **2011**, *11*, 58 (in Russian).
- (316) Joshi, P.; Chakraborti, S.; Ramirez-Vick, J. E.; Ansari, Z. A.; Shanker, V.; Chakrabarti, P.; Singh, S. P. *Colloids Surf., B* **2012**, *95*, 195.
- (317) Kim, M.; Ock, K.; Cho, K.; Joo, S.-W.; Lee, S. Y. *Chem. Commun.* **2012**, *48*, 4205.
- (318) Zhao, P.; Astruc, D. *ChemMedChem* **2012**, *7*, 952.
- (319) Comenge, J.; Sotelo, C.; Romero, F.; Gallego, O.; Barnadas, A.; Parada, T. G.-C.; Dominguez, F.; Puntes, V. F. *PLoS ONE* **2012**, *7*, e47562.
- (320) Zhang, X.; Chibli, H.; Mielke, R.; Nadeau, J. *Bioconjug. Chem.* **2011**, *22*, 235.
- (321) Jang, H.; Ryoo, S.-R.; Kostarelos, K.; Han, S. W.; Min, D.-H. *Biomaterials* **2013**, *34*, 3503.
- (322) Shukla, R.; Bansal, V.; Chaudhary, M.; Basu, A.; Bhonde, R. R.; Sastry, M. *Langmuir* **2005**, *21*, 10644.
- (323) Lim, Y. T.; Cho, M. Y.; Choi, B. S.; Noh, Y.-W.; Chung, B. H. *Nanotechnology* **2008**, *19*, 375105.
- (324) Zhang, Q.; Hitchins, V. M.; Schrand, A. M.; Hussain, S. M.; Goering, P. L. *Nanotoxicology* **2011**, *5*, 284.
- (325) Choi, M.-R.; Stanton-Maxey, K. J.; Stanley, J. K.; Levin, C. S.; Bardhan, R.; Akin, D.; Badve, S.; Sturgis, J.; Robinson, J. P.; Bashir, R.; Halas, N. J.; Clare, S. E. *Nano Lett.* **2007**, *7*, 3759.
- (326) Dreaden, E. C.; Mwakwari, S. C.; Austin, L. A.; Kieffer, M. J.; Oyelere, A. K.; El-Sayed, M. A. *Small* **2012**, *8*, 2819.
- (327) Bastús, N. G.; Sánchez-Tilló, E.; Pujals, S.; Farrera, C.; Kogan, M. J.; Giralt, E.; Celada, A.; Lloberas, J.; Puntes, V. *Mol. Immunol.* **2009**, *46*, 743.
- (328) Bastús, N. G.; Sánchez-Tilló, E.; Pujals, S.; Farrera, C.; López, C.; Kogan, M. J.; Giralt, E.; Celada, A.; Lloberas, J.; Puntes, V. *ACS Nano* **2009**, *3*, 1335.
- (329) Staroverov, S. A.; Aksinenko, N. M.; Gabalov, K. P.; Vasilenko, O. A.; Vidyasheva, I. V.; Shchyogolev, S. Y.; Dykman, L. A. *Gold Bull.* **2009**, *42*, 153.
- (330) Lee, J. Y.; Park, W.; Yi, D. K. *Toxicol. Lett.* **2012**, *209*, 51.
- (331) Dykman, L. A.; Staroverov, S. A.; Bogatyrev, V. A.; Shchyogolev, S. Y. *Gold nanoparticles as an antigen carrier and an adjuvant*; Nova Science Publishers: New York, 2010.
- (332) Xu, L.; Liu, Y.; Chen, Z.; Li, W.; Liu, Y.; Wang, L.; Liu, Y.; Wu, X.; Ji, Y.; Zhao, Y.; Ma, L.; Shao, Y.; Chen, C. *Nano Lett.* **2012**, *12*, 2003.
- (333) Fallarini, S.; Paoletti, T.; Battaglini, C. O.; Ronchi, P.; Lay, L.; Bonomi, R.; Jha, S.; Mancin, F.; Scrimin, P.; Lombardi, G. *Nanoscale* **2013**, *5*, 392.
- (334) Wei, M.; Chen, N.; Li, J.; Yin, M.; Liang, L.; He, Y.; Song, H.; Fan, C.; Huang, Q. *Angew. Chem., Int. Ed.* **2012**, *51*, 1202.
- (335) Rothenfusser, S.; Tuma, E.; Wagner, M.; Endres, S.; Hartmann, G. *Curr. Opin. Mol. Ther.* **2003**, *5*, 98.
- (336) Tsai, C.-Y.; Lu, S.-L.; Hu, C.-W.; Yeh, C.-S.; Lee, G.-B.; Lei, H.-Y. *J. Immunol.* **2012**, *188*, 68.
- (337) Massich, M. D.; Giljohann, D. A.; Seferos, D. S.; Ludlow, L. E.; Horvath, C. M.; Mirkin, C. A. *Mol. Pharmaceutics* **2009**, *6*, 1934.
- (338) Kim, E.-Y.; Schulz, R.; Swantek, P.; Kunstman, K.; Malim, M. H.; Wolinsky, S. M. *Gene Ther.* **2012**, *19*, 347.
- (339) Walkey, C. D.; Olsen, J. B.; Guo, H.; Emili, A.; Chan, W. C. W. *J. Am. Chem. Soc.* **2012**, *134*, 2139.
- (340) Liu, Z.; Li, W.; Wang, F.; Sun, C.; Wang, L.; Wang, J.; Sun, F. *Nanoscale* **2012**, *4*, 7135.
- (341) García, C. P.; Sumbayev, V.; Gilliland, D.; Yasinska, I. M.; Gibbs, B. F.; Mehn, D.; Calzolai, L.; Rossi, F. *Sci. Rep.* **2013**, *3*, 1326.
- (342) Ueno, H.; Klechovsky, E.; Morita, R.; Aspord, C.; Cao, T.; Matsui, T.; Di Pucchio, T.; Connolly, J.; Fay, J. W.; Pascual, V.; Palucka, A. K.; Banchereau, J. *Immunol. Rev.* **2007**, *219*, 118.

- (343) Cheung, W.-H.; Chan, V. S.-F.; Pang, H.-W.; Wong, M.-K.; Guo, Z.-H.; Tam, P. K.-H.; Che, C.-M.; Lin, C.-L.; Yu, W.-Y. *Bioconjug. Chem.* **2009**, *20*, 24.
- (344) Cruz, L. J.; Rueda, F.; Cordobilla, B.; Simón, L.; Hosta, L.; Albericio, F.; Domingo, J. C. *Mol. Pharm.* **2011**, *8*, 104.
- (345) Villiers, C. L.; Freitas, H.; Couderc, R.; Villiers, M.-B.; Marche, P. *N. J. Nanopart. Res.* **2010**, *12*, 55.
- (346) Ye, F.; Vallhov, H.; Qin, J.; Daskalaki, E.; Sugunan, A.; Toprak, M. S.; Fornara, A.; Gabrielsson, S.; Scheynius, A.; Muhammed, M. *Int. J. Nanotechnol.* **2011**, *8*, 631.
- (347) Lin, A. Y.; Lunsford, J.; Bear, A. S.; Young, J. K.; Eckels, P.; Luo, L.; Foster, A. E.; Drezek, R. A. *Nanoscale Res. Lett.* **2013**, *8*, 72.
- (348) Sharma, M.; Salisbury, R. L.; Maurer, E. I.; Hussain, S. M.; Sulentic, C. E. W. *Nanoscale* **2013**, *5*, 3747.
- (349) Bartneck, M.; Keul, H. A.; Singh, S.; Czaja, K.; Bornemann, J.; Bockstaller, M.; Möller, M.; Zwadlo-Klarwasser, G.; Groll, J. *ACS Nano* **2010**, *4*, 3073.
- (350) Bartneck, M.; Keul, H. A.; Zwadlo-Klarwasser, G.; Groll, J. *Nano Lett.* **2010**, *10*, 59.
- (351) Bartneck, M.; Keul, H. A.; Wambach, M.; Bornemann, J.; Gbureck, U.; Chatain, N.; Neuss, S.; Tacke, F.; Groll, J.; Zwadlo-Klarwasser, G. *Nanomedicine* **2012**, *8*, 1282.
- (352) DeFranco, A. L.; Locksley, R. M.; Robertson, M. *Immunity: The Immune Response to Infection*; Oxford University Press: Oxford, 2007.
- (353) Blander, J. M.; Medzhitov, R. *Nat. Immunol.* **2006**, *7*, 1029.
- (354) Deng, Z. J.; Liang, M.; Monteiro, M.; Toth, I.; Minchin, R. F. *Nat. Nanotechnol.* **2011**, *6*, 39.
- (355) Arnáiz, B.; Martínez-Ávila, O.; Falcon-Perez, J. M.; Penadés, S. *Bioconjug. Chem.* **2012**, *23*, 814.
- (356) Dobrovolskaia, M. A.; McNeil, S. E. *Nat. Nanotechnol.* **2007**, *2*, 469.
- (357) Dobrovolskaia, M. A.; Aggarwal, P.; Hall, J. B.; McNeil, S. E. *Mol. Pharm.* **2008**, *5*, 487.
- (358) Patel, P. C.; Giljohann, D. A.; Daniel, W. L.; Zheng, D.; Prigodich, A. E.; Mirkin, C. A. *Bioconjug. Chem.* **2010**, *21*, 2250.
- (359) França, A.; Aggarwal, P.; Barsov, E. V.; Kozlov, S. V.; Dobrovolskaia, M. A.; González-Fernández, Á. *Nanomedicine (Lond.)* **2011**, *6*, 1175.
- (360) Soenen, S. J.; Manshian, B.; Montenegro, J. M.; Amin, F.; Meermann, B.; Thiron, T.; Cornelissen, M.; Vanhaecke, F.; Doak, S.; Parak, W. J.; De Smedt, S.; Braeckmans, K. *ACS Nano* **2012**, *6*, 5767.
- (361) Zhu, Z.-J.; Posati, T.; Moyano, D. F.; Tang, R.; Yan, B.; Vachet, R. W.; Rotello, V. M. *Small* **2012**, *8*, 2659.